Physics – Uspekhi **58** (1) 3 – 32 (2015)

REVIEWS OF TOPICAL PROBLEMS PACS numbers: 03.65.Sq, 32.80.Fb, 32.80.Rm, 32.80.Wr, 34.80.Qb

Current progress in developing the nonlinear ionization theory of atoms and ions

B M Karnakov, V D Mur, S V Popruzhenko, V S Popov

DOI: 10.3367/UFNe.0185.201501b.0003

Contents

Abstract. We review the status of the theory of ionization of atoms and ions by intense laser radiation (Keldysh's theory). We discuss the applicability of the theory, its relation to the Landau–Dykhne method, and its application to the ionization of atoms by ultrashort nonmonochromatic laser pulses of an arbitrary shape. The semiclassical imaginary time method is applied to describe electron sub-barrier motion using classical equations of motion with an imaginary time $t \to it$ for an electron in the field of an electromagnetic wave. We also discuss tunneling interference of transition amplitudes, a phenomenon occurring due to the existence of several saddle points in the complex time plane and leading to fast oscillations in the momentum distribution of photoelectrons. Nonperturbatively taking the Coulomb interaction between an outgoing electron and the atomic residual into account causes significant changes in the photoelectron momentum distribution and in the level ionization rates, the latter usually increasing by orders of magnitude for both tunneling and multiquantum ionization. The effect of a static magnetic field on the ionization rate and the magnetic cumulation process is examined. The theory of relativistic tunneling is discussed, relativistic and spin corrections to the ionization rate are calculated, and the applicability limits of the nonrelativistic Keldysh theory are determined. Finally, the application of the Fock method to the covariant description of nonlinear ionization in the relativistic regime is discussed.

Keywords: tunnel and multiquantum ionization, relativistic ionization, intense laser radiation, superstrong magnetic field, Keldysh theory, imaginary time method

B M Karnakov, V D Mur, S V Popruzhenko National Research Nuclear University 'MEPhI',
Kashirskoe shosse 31, 115409 Moscow, Russian Federation
E-mail: karnak@theor.mephi.ru, sergey.popruzhenko@gmail.com
V S Popov Russian Federation State Scientific Center
'Alikhanov Institute of Theoretical and Experimental Physics',
ul. B. Cheremushkinskaya 25, 117218 Moscow, Russian Federation

Received 11 July 2014, revised 4 October 2014
Uspekhi Fizicheskikh Nauk **185** (1) 3 – 34 (2015)
DOI: 10.3367/UFNr.0185.201501b.0003
Translated by E N Ragozin; edited by A M Semikhatov

1. Introduction

Half a century has passed since the publication of the pivotal work of Keldysh [1], which laid the foundation of our understanding of the ionization of atomic systems and solids by high-intensity laser irradiation. In Ref. [1], it was shown

for the first time that the tunnel and multiquantum ionizations of atoms are two limit cases of nonlinear photoionization: the tunnel ionization occurs for the adiabaticity parameter, or the Keldysh parameter [see formula (1.1) below] $\gamma \ll 1$, while the ionization is a multiquantum process for $\gamma \gg 1$.

Soon after the publication of Ref. [1], Nikishov and Ritus [2] and Perelomov, Popov, and Terent'ev [3–5] obtained explicit analytic expressions for the energy and momentum photoelectron spectra and for the pre-exponential factor in the Keldysh formula for the ionization probability w (under the condition that the atomic electron is bound by short-range forces and its Coulomb interaction with the atomic core can be neglected, i.e., in fact, for the ionization of singly charged negative ions like H^- and Na^-).

The importance of including the Coulomb interaction was recognized even in the early papers [6, 7]; in particular, a Coulomb correction to the atomic ionization rate was obtained in [7] in the tunnel regime $\gamma \ll 1$ and was often used in subsequent work.[1] In succeeding years, the nonperturbative method for calculating the amplitudes of multiquantum processes in the field of a strong electromagnetic wave, which was proposed in Ref. [1], received wide recognition. At present, it enjoys wide use for calculating nonlinear effects observed in the interaction of intense laser fields with atoms, molecules, and free electrons. In the modern literature, this method is also referred to as the strong-field approximation [11, 12]. The elaboration of the Keldysh ionization theory and its application to the description of experiments are discussed in several hundred papers (see, e.g., monographs and reviews [13–18] and the references therein). Because 10 years have passed since the publication of review [15] — a period during which a wealth of experimental and theoretical material has been accumulated — it is very timely to review the present-day state of the Keldysh theory. The objective of this review is to outline the new results obtained by our group after the publication of [15], to which we refer the reader for the formulation and history of the problem.

We begin with a brief description of modern achievements in the physics of superhigh-power lasers and future prospects in this area, because the experimental observation of many of the effects discussed below (ionization of multiply charged ions, effect of the magnetic field on ionization, electron–positron pair production in a vacuum, etc.) calls for a further increase in electric intensity and a change to shorter (femto- and attosecond) laser pulses. In Section 3, we formulate the basic equations of the Keldysh ionization theory and discuss its applicability conditions and its relation to other methods for calculating the probabilities of other nonlinear effects in strong laser fields, including the Landau–Dykhne method and the imaginary time method (ITM). Outlined next are results relating to the ionization by ultrashort laser pulses (Section 4) and the inclusion of the effect of Coulomb interaction on nonlinear atomic ionization (Section 5). Section 6 is concerned with the effect of a magnetic field on atomic ionization. We discuss the methods for obtaining ultrahigh magnetic fields and the effect of Lorentz ionization. In Section 7, we consider the relativistic version of the Keldysh theory and discuss the use of the Fock method in relativistic mechanics for solving the electron equations of motion in a laser field and for a relativistically covariant calculation of the tunneling probability. Formulated in Section 8 are the applicability conditions for the nonrelativistic approximation in the theory of ionization. Technical details are discussed in the Appendices.

We make several remarks about the notation in use. Throughout the review, the electric and magnetic fields are respectively denoted as $\boldsymbol{\mathcal{E}}(\mathbf{r}, t)$ and $\boldsymbol{\mathcal{H}}(\mathbf{r}, t)$, and the vector potential as $\mathbf{A}(\mathbf{r}, t)$. The frequency and wavelength are denoted as ω and $\lambda = 2\pi c/\omega$; intensity values $\mathcal{I} = c\langle \mathcal{E}^2 + \mathcal{B}^2 \rangle/(8\pi)$ are given in units of W cm^{-2}. Sections 3–6 are devoted to nonrelativistic problems, and therefore the atomic system of units, in which $e = \hbar = m_e = 1$, is used there; the speed of light is then $c = \alpha^{-1} = 137$. In Section 7, we use the relativistic system of units, $\hbar = c = m_e = 1$; accordingly, $\alpha = e^2 = 1/137$.

We define the main dimensionless parameters that characterize the interaction of an electromagnetic field with atoms and free electrons. Most often used in high-field atomic physics are the Keldysh adiabaticity parameter [1]

$$\gamma = \frac{\sqrt{2Im_e}\,\omega}{e\mathcal{E}} = \frac{\omega}{\omega_t}\,, \tag{1.1}$$

and the multiquantum parameter

$$K_0 = \frac{I}{\hbar\omega} = \frac{1}{2F\gamma}\,, \tag{1.2}$$

where $I = \hbar^2\kappa^2/(2m_e)$ is the ionization potential of an atomic system and F is the reduced field,

$$F = \frac{\mathcal{E}}{\mathcal{E}_{ch}}\,, \qquad \mathcal{E}_{ch} = \frac{\hbar^2\kappa^3}{m_e e} = (\kappa a_B)^3 \mathcal{E}_a\,. \tag{1.3}$$

Here, $a_B = \hbar^2/m_e e^2$ is the Bohr radius, $\mathcal{E}_{ch}$ is the characteristic electric field for a level with the ionization potential I, and $\mathcal{E}_a = m^2 e^5/\hbar^4 = e/a_B^2 = 5.14 \times 10^9$ V cm^{-1} is the atomic unit of the electric field (the field in the first Bohr orbit in the hydrogen atom).

According to its physical meaning, the Keldysh parameter is the ratio between the characteristic momentum $\hbar\kappa = \sqrt{2m_e I}$ of an atomic electron and the momentum $e\mathcal{E}/\omega$ acquired by the electron in a laser field. This parameter can also be interpreted as the ratio between the laser wave frequency and the characteristic tunneling frequency $\omega_t = e\mathcal{E}/(\hbar\kappa)$. The quantity $[K_0] + 1$ is the minimal number of laser wave photons whose absorption allows the ionization of the atomic level.

In the literature, the strong-field parameter [12]

$$z_f = \frac{e^2\mathcal{E}^2}{m_e\hbar\omega^3} = \frac{2K}{\gamma^2} \tag{1.4}$$

is quite frequently used, which is (up to a numerical factor) the ratio between the quiver nonrelativistic electron energy averaged over the period $T = 2\pi/\omega$ in the wave field

$$U_p = \left\langle \frac{m_e \mathbf{v}^2}{2} \right\rangle_T = \frac{1+\rho^2}{4}\,\frac{e^2\mathcal{E}^2}{m_e\omega^2}\,, \tag{1.5}$$

and the radiation photon energy. The averaging in formula (1.5) is performed in the reference frame in which the electron is on average at rest. The result of averaging is given for a monochromatic wave of ellipticity ρ, with $\rho = 0$ for a linear polarization and $\rho = \pm 1$ for a circular one.

[1] The Coulomb correction for arbitrary γ, including the multiphoton case $\gamma \gg 1$, was obtained only recently [8–10].

We also give some formulas that are helpful in making numerical estimates. If the laser wavelength λ is measured in nanometers (1 nm $= 10^{-7}$ cm), the photon energy $\hbar\omega$ and the ionization potential in electronvolts, and the radiation intensity $\mathcal{I}$ in units of 10^{15} W cm^{-2} (the output laser power 10^{15} W $\equiv$ 1 PW), then

$$\hbar\omega = \frac{1.24\times 10^3}{\lambda}\,, \qquad K_0 = \frac{0.011I}{I_{\rm H}}\,, \tag{1.6}$$

where $I_{\rm H} = m_{\rm e}e^4/(2\hbar^2) = 13.6$ eV is the ionization potential of the hydrogen atom. For a wave of ellipticity ρ, the field intensity in atomic units (au) is given by

$$\frac{\mathcal{E}}{\mathcal{E}_{\rm a}} = 0.169\left(\frac{\mathcal{I}}{1+\rho^2}\right)^{1/2}, \qquad -1 \leqslant \rho \leqslant 1\,. \tag{1.7}$$

In particular, $\mathcal{E} = \mathcal{E}_{\rm a}$ for $\mathcal{I} \approx 35(1+\rho^2)$ [PW cm^{-2}].

2. Current state of experiments

Since the advent of the first coherent sources of infrared and optical radiation — masers and lasers — more than 50 years ago, the physics of the interaction of high-intensity electromagnetic radiation with matter has remained one of the most rapidly advancing areas of modern natural science. The main factor that has been maintaining interest in this realm of research for several decades is the continual development of laser technology, which allows achieving increasingly higher intensity values, producing progressively shorter pulses, and generating high-power electromagnetic fields in new wavelength regions. The theoretical work whose results are outlined in this review has appeared largely because the achievements of laser-physics experiments during the last 10–15 years have led to the formulation of new problems. The following areas of modern laser technology hold the greatest interest for investigation of fundamental effects of the interaction of intense electromagnetic fields with matter:

- production of superintense laser pulses;
- development of high-power free-electron lasers (FELs);
- generation of ultrashort laser pulses, including femtosecond and attosecond pulses (1 fs $= 10^{-15}$ s, 1 as $= 10^{-18}$ s). To date, it has been possible to produce coherent radiation pulses with a duration of the order of 100 as [19].

A comprehensive review of these lines of research, including the physical principles of pulse production, the experimental techniques, and the most significant results, was given in Ref. [20] (ultrahigh intensities), Refs [17, 21, 22] (ultrashort pulses), and Refs [19, 23] (attosecond physics). Information about the capabilities of modern FELs and X-ray lasers, as well as about experiments performed with their use, can be extracted from Refs [24–28] (see also site [29]).

We enumerate the parameters of modern laser facilities that are most significant from the standpoint of experiments on nonlinear interaction of high-power laser radiation with atoms, elementary particles, and the vacuum. Superintense pulses are generated using solid-state lasers of the near-infrared (IR) and optical wavelength ranges. Employed most often are the neodymium (wavelength $\lambda = 1064$ nm) and titanium–sapphire ($\lambda \approx 800$ nm) lasers and, in particular, their second harmonics. Modern laser facilities permit obtaining pulses with an intensity up to $\mathcal{I} = c\mathcal{E}_0^2/(8\pi) \approx 2\times 10^{22}$ W cm^{-2} [30] (in this case, the electric field strength is $\mathcal{E}_0 \approx 10^{12}$ V cm^{-1}), which is approximately six orders of magnitude higher than the value $\mathcal{I}_{\rm a} = c\mathcal{E}_{\rm a}^2/(8\pi) \approx 3.51\times 10^{16}$ W cm^{-2} at which the electric field strength of the wave field is equal to the atomic one. The duration of pulses of such intensity is equal to several tens of femtoseconds. The nonlinear nature of electromagnetic radiation–matter interaction manifests itself even at substantially lower intensities. Specifically, the tunnel ionization of hydrogen atoms sets in at an intensity of the order of $\mathcal{I} \approx 10^{14}$ W cm$^{-2} \ll \mathcal{I}_{\rm a}$; for $\mathcal{I} \approx 10^{18}$ W cm^{-2}, the electron motion becomes relativistic (for a wavelength of about 1 μm); pulses of the intensity $10^{19}-10^{20}$ W cm^{-2} excite relativistic collective in-plasma motions, in particular, permitting the production of ultrarelativistic electron beams and protons with energies up to several GeV. Lastly, at intensities of the order of 10^{22} W cm^{-2}, multiple ionization of atoms occurs up to levels with relativistic binding energies comparable to $m_{\rm e}c^2$.

At present, there are technically substantiated projects [31–34] to make new lasers that show promise to increase the highest attainable field strength by several orders of magnitude more, to values close to the critical field $\mathcal{E}_{\rm cr}$ of quantum electrodynamics [35–37]:

$$\mathcal{E}_{\rm cr} = \frac{m_{\rm e}^2c^3}{e\hbar} = 1.32\times 10^{16}\ {\rm V\ cm^{-1}} = \alpha^{-3}\mathcal{E}_{\rm a}\,. \tag{2.1}$$

(The notation $\mathcal{E}_{\rm cr}$ follows Ref. [36]). The corresponding intensity is $\mathcal{I}_{\rm cr} = c\mathcal{E}_{\rm cr}^2/(8\pi) = \alpha^{-6}\mathcal{I}_{\rm a} = 4.65\times 10^{29}$ W cm^{-2}. We mention the relations

$$W_1 = e\mathcal{E}_{\rm cr}l_{\rm C} = m_{\rm e}c^2\,, \qquad W_2 = e\mathcal{E}_{\rm a}a_{\rm B} = \alpha^2W_1 = 2\ {\rm Ry}\,,$$

$$\mathcal{E}_{\rm cr}^2l_{\rm C}^3 = \frac{m_{\rm e}c^2}{\alpha}\,, \qquad \mathcal{E}_{\rm a}^2a_{\rm B}^3 = \alpha^2m_{\rm e}c^2\,, \tag{2.2}$$

where $l_{\rm C} = \hbar/(m_{\rm e}c) = \alpha a_{\rm B} = 3.86\times 10^{-11}$ cm is the Compton length and 1 Rydberg (Ry) = 13.6 eV.

For the investigation of basic effects in the interaction of superhigh electromagnetic fields with matter, of chief interest are experiments on multiple and relativistic nonlinear atomic ionization, as well as projected experiments on the search for nonlinear quantum electrodynamic effects, including vacuum pair production [20, 34, 38, 39].

Putting high-power FELs into operation has opened up fresh opportunities for experiments on the nonlinear interaction of laser radiation with matter in the ultraviolet and X-ray wavelength ranges [28]. Facilities of this type are presently operating in Germany [29], Japan [25], and the USA [26]. The record intensities of laser pulses attained at FELs to date are 10^{16} W cm^{-2} for $\lambda \approx 13$ nm (Deutsches Elektronen-Synchrotron (DESY) laboratory, Germany), 10^{14} W cm^{-2} for $\lambda \approx 50$ nm (Super Photon Ring-8 (SPring-8) facility, Japan), and 10^{18} W cm^{-2}, $\lambda \approx 1.2$ nm (FEL at the Stanford Linear Accelerator Center (SLAC), Stanford, USA). Beginning in 2002, numerous experiments on the nonlinear interaction of high-intensity high-frequency radiation with atoms, molecules, multiply charged ions, nanostructures, and solids have been carried out with the use of FELs.

Only 15–20 years ago, the production of high-intensity X-ray laser pulses was considered a matter of the distant future, and little emphasis was placed on research in this area. The experimental breakthrough in the physics of the interaction of high-power ultraviolet and X-ray radiation with

matter, which occurred about 10 years ago, turned out to be largely unexpected. As a consequence, with a wealth of new experimental data, theory seems to be in short supply today. In the ultraviolet and X-ray ranges, the nonlinear interaction of light with charged particles is qualitatively different from that in the case of low frequencies, which is realized with IR lasers. To be specific, for a close-to-atomic intensity 10^{16} W cm^{-2}, in the field of an IR laser with a wavelength of 1 μm, the average quiver electron energy [defined by Eqn (1.5)] is about 1 keV, and the excursion amplitude is about 30 nm (600 au), while for a wavelength of 10 nm and the same intensity, these quantities are approximately 0.2 eV and 0.1 au, respectively. That is, in the field of high-intensity X-ray lasers, the energy and spatial scales that characterize the electron motion turn out to be much smaller than the corresponding atomic quantities. For the same electromagnetic field strength, the values of the main dimensionless parameters are therefore different by several orders of magnitude. The interaction of atoms with intense laser pulses of the visible and IR ranges is usually characterized by the conditions $\gamma \lesssim 1$, $z_\mathrm{f} \gg 1$, while the opposite limit, $\gamma \gg 1$ and $z_\mathrm{f} \ll 1$, is realized in the field of high-power X-ray lasers. In Section 5, we outline the results in Refs [8, 9] on the multiquantum ionization of atoms for large values of the Keldysh parameter.

Lastly, in recent years it has become possible in experiments to use high-power pulses of visible and infrared radiation only several femtoseconds in duration, i.e., consisting of one or two wave cycles [17, 19]. It turns out to be possible to stabilize and control the short-pulse shape, i.e., to control the parameters that differentiate a short pulse from a monochromatic wave. Usually selected for this parameter is the carrier-envelope phase, with the electric vector represented as the product of a sinusoidal monochromatic oscillation by its envelope, whose shape and shift relative to the phase of the sine wave define the pulse shape. Accordingly, effects associated with the carrier-envelope phase are discussed in [17]. Observations of these effects furnishes additional possibilities for controlling the properties of ultrashort pulses. In particular, the experimentally observed dependence of the photoelectron spectrum shape on the carrier-envelope phase can be used for recovering the shape of the ionization-producing pulse [40]. By using the generation of higher-order harmonics of optical and infrared range lasers, it has been possible to obtain even shorter pulses of a duration below 1 fs. Such pulses, which are termed attosecond pulses, are obtained in the coherent summation of several high-order harmonics of the initial laser pulse. At present, attosecond optics is one of the most rapidly advancing areas in high-field physics (see review Refs [19, 23] and the references therein).

The wide use of ultrashort pulses, whose field is significantly different from the monochromatic one, in present-day experiments lends impetus to the further development of the theory. In early papers concerned with the theory of atomic, quantum-electrodynamic, and other processes in high fields, the laser wave field was considered to be monochromatic, which corresponded to the long duration of the pulses used at that time. At present, there is a large number of papers in which the theory of nonlinear processes in strong fields is generalized to the case of short pulses (see review Refs [15, 17] and the references therein). In Section 4, we briefly discuss the results in Refs [10, 41, 42], which appeared after the publication of reviews [15, 17].

3. Basic equations of the Keldysh theory

In Keldysh's paper [1], the expression for the nonlinear ionization amplitude was introduced by analogy with that in the time-dependent first-order perturbation theory. Below, we show how this expression results from the solution of the time-dependent Schrödinger equation. We also discuss the relation between the Keldysh theory and two other close approaches: the Landau–Dykhne method and the imaginary time method. The appropriateness of discussing these issues stems from the following fact: quite frequently in the modern literature, inexact statements are encountered, different meaning is assigned to the same formulas, and so on.

3.1 General expressions for the ionization probability in the Keldysh theory

In the nonrelativistic problem of electron detachment from a bound state in a short-range potential $U_\mathrm{sr}(r)$ under the action of an external uniform electric field $\boldsymbol{\mathcal{E}}(t)$ of finite duration, $\boldsymbol{\mathcal{E}}(t \to \pm\infty) \to 0$, it is required to solve the Schrödinger equation

$$\mathrm{i}\,\frac{\partial}{\partial t}\,\psi(\mathbf{r},t) = \left(-\frac{1}{2}\,\Delta + U_\mathrm{sr}(r) + \boldsymbol{\mathcal{E}}(t)\mathbf{r}\right)\psi(\mathbf{r},t) \tag{3.1}$$

with the initial condition

$$\psi(\mathbf{r}, t \to -\infty) \to \psi_0(\mathbf{r}) \exp\left(\frac{\mathrm{i}\kappa^2 t}{2}\right), \tag{3.2}$$

where $\psi_0(\mathbf{r})$ is the wave function of the unperturbed level, $I = \kappa^2/2$ is the binding energy (the ionization potential), and κ is the characteristic electron momentum in the bound state. To describe the interaction of the electron with the electric field of a laser wave, the dipole approximation and the so-called length gauge are used. Assuming that there are no other bound states, we write the wave function after field termination (for $t \to +\infty$) in the form

$$\psi(\mathbf{r},t) = a\psi_0(\mathbf{r}) \exp\left(\frac{\mathrm{i}\kappa^2 t}{2}\right) + \psi_\mathrm{out}(\mathbf{r},t)\,, \tag{3.3}$$

where the second term in the right-hand side describes the outgoing electron that moves a large distance away from the atom. For $r \to \infty$, this term is therefore an outgoing spherical wave, whose expansion coefficients in terms of plane waves define the photoelectron momentum distribution. The total ionization probability is expressed as

$$w = 1 - |a|^2 = \int |\psi_\mathrm{out}|^2\,\mathrm{d}^3 r\,. \tag{3.4}$$

We use the integral form of Eqn (3.1) with initial condition (3.2):

$$\psi(\mathbf{r},t) = \int_{-\infty}^{+\infty} \mathrm{d}t_1 \int \mathrm{d}^3 r_1\, G(\mathbf{r},t;\mathbf{r}_1,t_1)\, U_\mathrm{sr}(r_1)\,\psi(\mathbf{r}_1,t_1)\,, \tag{3.5}$$

where G is the retarded temporal Green's function of the electron in an electric field, which obeys the equation

$$\left(\mathrm{i}\,\frac{\partial}{\partial t} + \frac{1}{2}\,\Delta - \boldsymbol{\mathcal{E}}(t)\mathbf{r}\right) G(\mathbf{r},t;\mathbf{r}_1,t_1) = \delta(t-t_1)\,\delta(\mathbf{r}-\mathbf{r}_1) \tag{3.6}$$

and the condition $G(\mathbf{r}, t; \mathbf{r}_1, t_1) = 0$ for $t < t_1$:

$$G(\mathbf{r}, t; \mathbf{r}_1, t_1) = -\mathrm{i}\,\frac{\eta(t-t_1)}{(2\pi)^3}\int \mathrm{d}^3p\,\exp\left(\mathrm{i}S(\mathbf{r}, t; \mathbf{r}_1, t_1)\right), \quad (3.7)$$

where $\eta(z)$ is the Heaviside function, $S(\mathbf{r}, t; \mathbf{r}_1, t_1)$ is the classical action function for the electron in a uniform electric field,

$$S(\mathbf{r}, t; \mathbf{r}_1, t_1) = \mathbf{v}_\mathbf{p}(t)\mathbf{r} - \mathbf{v}_\mathbf{p}(t_1)\mathbf{r}_1 - \frac{1}{2}\int_{t_1}^{t} \mathbf{v}_\mathbf{p}^2(t')\,\mathrm{d}t', \quad (3.8)$$

$\mathbf{v}_\mathbf{p}(t)$ is the time-dependent electron velocity in the field of the wave,

$$\mathbf{v}_\mathbf{p}(t) = \mathbf{p} + \frac{1}{c}\,\mathbf{A}(t), \qquad \frac{1}{c}\,\mathbf{A}(t) = -\int_{-\infty}^{t} \boldsymbol{\mathcal{E}}(t')\,\mathrm{d}t', \quad (3.9)$$

$\mathbf{p}$ is a constant vector equal to the electron momentum (velocity) at infinity, and $\mathbf{A}(t)$ is the vector potential corresponding to the field $\boldsymbol{\mathcal{E}}(t)$, with $\mathbf{A}(-\infty) = \mathbf{A}(+\infty) = 0$.

It is also possible to consider a more general case, where

$$\mathbf{A}(+\infty) \neq \mathbf{A}(-\infty) = 0\,. \quad (3.10)$$

Under condition (3.10), Eqns (3.5)–(3.7) retain their form, but the classical action is given by a more complex expression, which is obtained by the replacement

$$\mathbf{v}_\mathbf{p}(t_i) \to \mathbf{p} + \frac{1}{c}\left(\mathbf{A}(t_i) - \mathbf{A}(+\infty)\right), \qquad t_i = t, t_1\,,$$

in action (3.8). It is commonly assumed that the electric field of a laser pulse satisfies the condition [43]

$$\int_{-\infty}^{+\infty} \boldsymbol{\mathcal{E}}(t)\,\mathrm{d}t = 0\,, \quad (3.11)$$

which signifies that the pulse does not do work on the particle over the total time of its action: $\mathbf{p}(-\infty) = \mathbf{p}(\infty)$. For pulses propagating through a nonlinear medium, constraint (3.11) may supposedly be circumvented (see, e.g., Ref. [44], which discusses the generation of half-cycle IR laser pulses in the filamentation in nitrogen).

Assuming that the probability of ionization during the action of the pulse is low, we replace the wave function $\psi(\mathbf{r}_1, t_1)$ in the right-hand side of Eqn (3.5) with its unperturbed value (3.2). As a result, we obtain an approximate solution of the equation in the form

$$\psi(\mathbf{r}, t) = -\frac{\mathrm{i}}{(2\pi)^3}\int \mathrm{d}^3p\,\exp\left(\mathrm{i}\mathbf{v}_\mathbf{p}(t)\mathbf{r}\right) \times \int_{-\infty}^{t} \mathrm{d}t_1 \int \mathrm{d}^3r_1\,\exp\left[-\mathrm{i}\left(\mathbf{v}_\mathbf{p}(t_1)\mathbf{r}_1 + \frac{1}{2}\int_{t_1}^{t} \mathbf{v}_\mathbf{p}^2(t')\,\mathrm{d}t'\right)\right] \times U_{\mathrm{sr}}(r_1)\psi_0(\mathbf{r}_1)\exp\left(\frac{\mathrm{i}\kappa^2 t_1}{2}\right), \quad (3.12)$$

which describes an outgoing wave at a long distance as $t \to \infty$:

$$\psi(\mathbf{r}, t) = \lim_{t\to\infty} \frac{1}{(2\pi)^{3/2}}\int \mathrm{d}^3p\,\exp\left(\mathrm{i}\mathbf{p}\mathbf{r} - \frac{\mathrm{i}p^2 t}{2}\right) M(\mathbf{p}), \quad (3.13)$$

where the amplitude $M(\mathbf{p})$ defines the momentum distribution of outgoing electrons:

$$\mathrm{d}w(\mathbf{p}) = \left|M(\mathbf{p})\right|^2 \mathrm{d}^3p\,. \quad (3.14)$$

By comparing formulas (3.12) and (3.13), we obtain the photoionization amplitude in the form (up to an insignificant phase factor)

$$M(\mathbf{p}) = -\frac{\mathrm{i}}{(2\pi)^{3/2}}\int_{-\infty}^{\infty} \mathrm{d}t\,\exp\left(\mathrm{i}S_0(\mathbf{p}, t)\right) \times \int \mathrm{d}^3r\,\exp\left(-\mathrm{i}\mathbf{v}_\mathbf{p}(t)\mathbf{r}\right) U_{\mathrm{sr}}(r)\,\psi_0(\mathbf{r}), \quad (3.15)$$

where

$$S_0(\mathbf{p}, t) = \frac{1}{2}\,\kappa^2 t + \frac{1}{2}\int_{-\infty}^{t} \mathbf{v}_\mathbf{p}^2(t')\,\mathrm{d}t'\,. \quad (3.16)$$

In Keldysh's work [1], the photoionization amplitude was calculated by the formula

$$M_{\mathrm{K}}(\mathbf{p}) = -\mathrm{i}\int_{-\infty}^{\infty} \mathrm{d}t \int \psi_\mathbf{p}^*(\mathbf{r}, t)\,V_{\mathrm{int}}(\mathbf{r}, t)\,\psi_0(\mathbf{r}, t)\,\mathrm{d}^3r\,, \quad (3.17)$$

where $V_{\mathrm{int}}(\mathbf{r}, t) = \boldsymbol{\mathcal{E}}(t)\mathbf{r}$. In that case, the wave function of the initial state was replaced by the wave function of the electron bound state unperturbed by the electric field, as was done in the derivation of formula (3.13): for the wave function of the outgoing electron, the Volkov electron wave function of the ejected electron in an external electric field was used [45–47]:

$$\psi_\mathbf{p}(\mathbf{r}, t) = \frac{1}{(2\pi)^{3/2}}\exp\left[\mathrm{i}\left(\mathbf{v}_\mathbf{p}(t)\mathbf{r} - \frac{1}{2}\int_0^t \mathbf{v}_\mathbf{p}^2(t')\,\mathrm{d}t'\right)\right], \quad (3.18)$$

where the velocity $\mathbf{v}_\mathbf{p}(t)$ is given by formula (3.9).

Amplitude (3.17) coincides with the one in (3.15). To show this, we make the following transformations in formula (3.15). From the Schrödinger equation for the unperturbed wave function, it follows that

$$U_{\mathrm{sr}}(r)\,\psi_0(\mathbf{r})\exp\left(\frac{\mathrm{i}\kappa^2 t}{2}\right) = \left(\frac{1}{2}\,\Delta + \mathrm{i}\,\frac{\partial}{\partial t}\right)\psi_0(\mathbf{r})\exp\left(\frac{\mathrm{i}\kappa^2 t}{2}\right),$$

where we transfer the action of operators Δ and $\partial/\partial t$ to the left. Then formula (3.15) assumes the form

$$M(\mathbf{p}) = -\frac{\mathrm{i}}{(2\pi)^{3/2}}\int_{-\infty}^{\infty} \mathrm{d}t\left\{\left(\frac{1}{2}\,\Delta - \mathrm{i}\,\frac{\partial}{\partial t}\right) \times \exp\left[-\mathrm{i}\left(\mathbf{v}_\mathbf{p}(t)\mathbf{r} - \frac{1}{2}\int_0^t \mathbf{v}_\mathbf{p}^2(t')\,\mathrm{d}t'\right)\right]\right\}\psi_0(\mathbf{r})\exp\left(\frac{\mathrm{i}\kappa^2 t}{2}\right)$$

and passes into formula (3.17) upon performing the differentiation.

Formulas (3.15) and (3.17) are of a general character [assuming that the ionization probability is low and that the forces are short-range and characterized by the potential $U_{\mathrm{sr}}(r)$] and uniquely describe both the case of applicability of the perturbation theory in its lowest orders and the case of a nonperturbative process under consideration (tunnel and multiquantum ionization in a time-dependent field).

Formulas (3.15) and (3.17) are significantly simplified for s states, when the asymptotic form of the initial wave function is

$$\psi_0(\mathbf{r}) = C_\kappa\sqrt{\frac{\kappa}{\pi}}\,\frac{\exp(-\kappa r)}{r}, \qquad r \gg \frac{1}{\kappa}\,, \quad (3.19)$$

where C_κ is a dimensionless asymptotic coefficient.[2] As a result, formula (3.15) assumes an especially simple form:

$$M(\mathbf{p}) = \mathrm{i}\,\frac{C_\kappa}{\pi}\sqrt{\frac{\kappa}{2}}\int_{-\infty}^{\infty}\exp\left(\mathrm{i}S_0(\mathbf{p},t)\right)\mathrm{d}t\,, \tag{3.20}$$

where the phase $S_0(\mathbf{p},t)$ is defined by (3.16).

Under the conditions of applicability of the perturbation theory to the interaction of the electron with an external field, in the expansion of the exponent in expression (3.20), we retain the term linear in the field and perform double integration by parts to obtain

$$M(\mathbf{p}) = -\frac{2\sqrt{\kappa}}{\pi(\kappa^2+p^2)^2}\int_{-\infty}^{\infty}\mathbf{p}\boldsymbol{\mathcal{E}}(t)\exp\left[\frac{\mathrm{i}(\kappa^2+p^2)t}{2}\right]\mathrm{d}t \tag{3.21}$$

for the potential of zero radius, which coincides with the expression for the amplitude calculated in the first-order time-dependent perturbation theory [48].

3.2 Keldysh theory and the Landau–Dykhne method

To calculate the probabilities of multiquantum processes in intense laser fields, in several papers (see, e.g., Refs [49, 50]) the Landau–Dykhne method [48, 51, 52] is used, which was initially proposed for describing bound–bound transitions under adiabatic perturbations. We discuss the relation between the Keldysh theory and the Landau–Dykhne method as applied to the ionization problem.

In the case of an adiabatically varying electric field (subject to the condition $I \gg \omega$ required for multiquantum ionization), the phase in the exponent in (3.20) is large, the integrand oscillates rapidly, and the saddle point method can be used to calculate the integral in the transition amplitude. The saddle-point positions $t_\mathrm{s}(\mathbf{p})$ in the upper half-plane of the complex time t such that $\partial S_0(\mathbf{p},t)/\partial t = 0$ are defined by the equation

$$E_1(t_\mathrm{s}) \equiv -\frac{1}{2}\,\kappa^2 = \frac{1}{2}\left(\mathbf{p}+\frac{1}{c}\,\mathbf{A}(t_\mathrm{s})\right)^2 \equiv E_2(\mathbf{p},t_\mathrm{s})\,. \tag{3.22}$$

Then the contribution of an individual saddle point $t_{\mathrm{s}\alpha}$, $\alpha = 1, 2, \ldots$, to amplitude (3.20) is given by the expression

$$M_\alpha(\mathbf{p}) = \mathrm{i}C_\kappa\sqrt{\frac{\mathrm{i}\kappa}{\pi S_0''(\mathbf{p},t_{\mathrm{s}\alpha})}}\exp\left(\mathrm{i}S_0(\mathbf{p},t_{\mathrm{s}\alpha})\right). \tag{3.23}$$

When the contribution of only one point prevails,[3] the differential ionization probability takes the form

$$\frac{\mathrm{d}w}{\mathrm{d}^3p} = \left|M(\mathbf{p})\right|^2 = \frac{\kappa C_\kappa^2}{\pi\left|\boldsymbol{\mathcal{E}}(t_\mathrm{s})\mathbf{v}_\mathbf{p}(t_\mathrm{s})\right|} \times\exp\left(-2\,\mathrm{Im}\int_{\tilde{t}_1}^{t_\mathrm{s}(\mathbf{p})}\left[E_2(\mathbf{p},t)-E_1(t)\right]\mathrm{d}t\right), \tag{3.24}$$

where $\tilde{t}_1$ is an arbitrary point on the real time axis.

[2] $C_\kappa = 1/\sqrt{2}$ for the state in a zero-range potential.

[3] The existence of several solutions of Eqn (3.22) with comparable contributions to the ionization amplitude gives rise to an interference structure in the photoelectron spectrum (see Section 4.1). The interference is most significant for a linearly polarized field [3]. In the limit of short pulses or in the case of considerable field ellipticity, the dominant contribution to the amplitude is made by one stationary point, and the interference effects are insignificant.

Formula (3.24) is similar in form to the transition probability between states 1 and 2 of a discrete spectrum under an adiabatic perturbation in the time-semiclassical Landau–Dykhne method and is its generalization in the case of transitions into the continuum. In this case, the role of state 1 is played by the bound electron state unperturbed by the electric field, and state 2 is the state of the ejected electron corresponding to its infinite motion in the external field $\boldsymbol{\mathcal{E}}(t)$. The value of $t_\mathrm{s}(\mathbf{p})$ determined from Eqn (3.22) defines the complex 'instant of transition' between the states under consideration.

We discuss the relation between formula (3.24) and formula (53.9) in Ref. [48]:

$$|M_{1\to2}|^2 \propto \exp\left(2\,\mathrm{Im}\int_C E(t)\,\mathrm{d}t\right), \tag{3.25}$$

as well as its kindred formula (52.1) in Ref. [48], which is applicable in the case of a time-independent Hamiltonian.

According to the central idea of the Landau–Dykhne method [48, §§ 52, 53], the squared modulus of the transition amplitude is defined (generally speaking, up to an exponential factor) by the imaginary part of the action acquired in the semiclassical (in time or in coordinates) motion of the system in the vicinity of the instant of transition $t_\mathrm{s} = t_0 + \mathrm{i}\tau_0$ or the complex 'transition point' q_0. In this case, it is necessary to refine the meaning of the action $S(t)$ in the time-semiclassical method, because the discrete spectrum states 1 and 2 between which the transition is considered are by no means assumed to be semiclassical in general. Because the Hamiltonian changes in time adiabatically, the wave functions of the states are of the form

$$\psi_n(q,t) \approx \tilde{\psi}_n(q,t)\exp\left(-\mathrm{i}\int^t E_n(t')\,\mathrm{d}t'\right), \tag{3.26}$$

where q is the set of coordinates of the particles of the system under consideration and $\tilde{\psi}_n(q,t)$ and $E_n(t)$ are the eigenfunctions and eigenvalues of the 'instantaneous' system Hamiltonian $\hat{H}(q,t)$, which depend on time as a parameter and are determined from the solution of the Schrödinger equation $\hat{H}(q,t)\tilde{\psi}_n(q,t) = E_n(t)\tilde{\psi}_n(q,t)$. The functions $\tilde{\psi}_n(q,t)$ and $E_n(t)$ vary slowly relative to the characteristic time of the finite motion of the system. In classical mechanics, in the case of a time-independent Hamiltonian function, the action is $S(q,t) = W(q) - Et$, where $W(q)$ is the reduced action [53]. For a slow time variation of the Hamilton function $H(\lambda(t),q)$ we have $S(q,t) \approx W(\lambda(t),q) - \int^t E(\lambda(t'))\,\mathrm{d}t'$ for states of finite motion [54], and the explicitly time-dependent part of the action is therefore given by the integral

$$S(t) = -\int^t E_n(t')\,\mathrm{d}t'\,. \tag{3.27}$$

In the ionization problem, the role of state 1 is played by the bound electron state unperturbed by the electric field, and hence $S_1(t) = \kappa^2 t/2$. At $t = t_\mathrm{s}$ (i.e., at $\tau = \tau_0$), the electron transits into a new 'orbit' corresponding to its infinite motion in the external electric field $\boldsymbol{\mathcal{E}}(t)$. In this case, formulas (3.26) and (3.27) for the wave function and the action are inapplicable directly because they pertain to the case of finite motion. Nevertheless, the exact wave function (3.18), which describes the ejected electron motion, is known in this case. The wave function is of the same form as expression (3.26)

and is the product of a slowly varying coordinate wave function $\exp(\mathrm{i}\mathbf{p}(t)\mathbf{r})$ and an exponential temporal factor $\exp(\mathrm{i}S_2(\mathbf{p},t))$, where

$$S_2(\mathbf{p},t) = -\int^t E_2(\mathbf{p},t')\,\mathrm{d}t'\,, \qquad E_2(\mathbf{p},t) = \frac{1}{2}\,\mathbf{v}_\mathbf{p}^2(t)\,. \quad (3.28)$$

Therefore, the formula for the ionization probability obtained by the Landau–Dykhne method coincides, with exponential accuracy, with the result of the Keldysh theory under the condition that the saddle-point method can be used for calculating the time integral in expression (3.17). This is possible in the multiquantum mode, i.e., when at least one of the conditions $K_0 \gg 1$ or $z_\mathrm{f} \gg 1$ is satisfied. On the other hand, the applicability of expressions (3.15) and (3.17) for the ionization amplitude is not limited to these conditions, which is clear, in particular, from the passage to the limit of the first-order perturbation theory. Furthermore, in the case of a short-range potential, calculations by the Keldysh theory provide the correct expression for the pre-exponential factor in the ionization probability.

To summarize, it is valid to say that in the ionization problem, Landau–Dykhne formula (3.25) is applicable in a narrower parameter range and is less accurate than the formulas that follow from the Keldysh theory. Furthermore, calculation by the Landau–Dykhne formula offers no advantages from the computational standpoint, because its result completely coincides with the result of calculation by the Keldysh theory with the use of the saddle-point method. On the other hand, the Landau–Dykhne method applies to the treatment of problems that are beyond the scope of the Keldysh theory, including adiabatic bound–bound transitions.

3.3 Imaginary-time method

The imaginary time method (ITM) is conveniently used in calculating the particle tunneling probability through a time-dependent barrier [4, 5, 15, 55]. Here, we outline the basic points of the ITM, referring the reader to the indicated papers.

We consider the ionization of a bound level of the energy $E_0 = -\kappa^2/2$ in a time-dependent uniform electric field of linear polarization:

$$\mathcal{E}(\theta) = \mathcal{E}_0\varphi(\theta)\,, \quad \varphi(-\theta) = \varphi(\theta)\,, \quad -\infty < \theta \equiv \omega t < +\infty\,, \quad (3.29)$$

assuming that $\varphi(\theta)$ is an even analytic function of t (θ is the dimensionless time). In the semiclassical approximation, the tunneling probability w is determined by the extremal sub-barrier trajectory, which is one-dimensional and is aligned with the electric field and minimizes the imaginary part of the reduced action function:

$$\dot{x} = \frac{\mathcal{E}_0}{\omega}\int_0^\theta \varphi(\theta')\,\mathrm{d}\theta' = \frac{\mathrm{i}\kappa}{\gamma}\,h(\tau)\,, \qquad \tau = -\mathrm{i}\theta\,, \quad (3.30)$$

where τ is the imaginary time. The 'initial instant' of sub-barrier motion $\tau_\mathrm{s}(\gamma)$ is determined from the condition $\dot{x}^2 + \kappa^2 = 0$ or $\dot{x}(\tau_\mathrm{s}) = \mathrm{i}\kappa$,

$$\tau_\mathrm{s}(\gamma) = h^{-1}(\gamma)\,, \qquad h(\tau) = \int_0^\tau \varphi(\mathrm{i}\theta)\,\mathrm{d}\theta\,, \quad (3.31)$$

where $h^{-1}(\tau)$ is the inverse function of $h(\tau)$. By calculating the imaginary part of the reduced action function W acquired in the particle motion along the sub-barrier trajectory, we obtain

$$W = \frac{1}{2}\int_{t_\mathrm{s}}^0 (\dot{x}^2 + \kappa^2)\,\mathrm{d}t = \mathrm{i}\,\frac{\kappa^3}{\mathcal{E}_0}\int_0^1 \chi(\gamma u)(1-u^2)\,\mathrm{d}u\,, \qquad \chi(u) \equiv \tau_\mathrm{s}'(u)\,. \quad (3.32)$$

To calculate the momentum spectrum of outgoing electrons, we must consider the beam of classical close-to-extremal trajectories defined by momenta $\mathbf{p} = (p_\parallel, p_\perp)$ at the end of the barrier, and find a quadratic correction $\sim \mathbf{p}^2$ to $\mathrm{Im}\,W$. This procedure is described at length in Ref. [15]. Omitting the details, we give the final result up to a pre-exponential factor:

$$w(\mathbf{p}) \sim \exp\left\{-\frac{\kappa^3}{\mathcal{E}_0}\left[\frac{2}{3}\,g(\gamma) + b_\parallel\,\frac{(p_\parallel - p_0)^2}{\kappa^2} + b_\perp\,\frac{p_\perp^2}{\kappa^2}\right]\right\}, \quad (3.33)$$

where $p_\parallel$ and $p_\perp$ are the longitudinal and transverse projections (relative to the polarization direction) of the photoelectron momentum,

$$g(\gamma) = \frac{3}{2}\int_0^1 \chi(\gamma u)(1-u^2)\,\mathrm{d}u\,, \qquad b_\perp(\gamma) = \gamma^{-1}\tau_\mathrm{s}(\gamma)\,, \quad b_\parallel(\gamma) = -\gamma b_\perp'(\gamma)\,, \quad (3.34)$$

the function $\chi(u)$ is defined in (3.32), and the most probable momentum is found from the condition

$$p_0 = \frac{\mathcal{E}_0}{\omega}\int_0^\infty \varphi(\theta)\,\mathrm{d}\theta\,. \quad (3.35)$$

Formulas (3.33) and (3.34), which were obtained using the ITM, define the probability of ionization by an even pulse of an arbitrary shape; they are convenient in the low-frequency domain $\gamma \ll 1$ and for passing to the limit of a constant field [15]. When $\gamma \gtrsim 1$, it is expedient to represent formulas (3.33) and (3.34) in a somewhat different (although equivalent) form

$$w(\mathbf{p}) \sim \exp\left\{-2K_0\left[f(\gamma) + c_\parallel\,\frac{(p_\parallel - p_0)^2}{\kappa^2} + c_\perp\,\frac{p_\perp^2}{\kappa^2}\right]\right\}, \quad (3.36)$$

where $K_0 = I/\omega$ (1.2),

$$f(\gamma) = \frac{2\gamma}{3}\,g(\gamma) = \int_0^\gamma \chi(u)\left(1 - \frac{u^2}{\gamma^2}\right)\mathrm{d}u\,, \quad c_\parallel = \gamma b_\parallel\,, \quad c_\perp = \gamma b_\perp\,. \quad (3.37)$$

It is assumed that the applicability conditions are fulfilled for the semiclassical approximation and a saddle point $t_\mathrm{s} = \mathrm{i}\omega^{-1}\tau_\mathrm{s}(\gamma)$ that makes the main contribution to the tunneling amplitude exists in the upper half-plane of complex time. The ionization probability and the electron momentum spectrum are defined in terms of the $\chi(u)$ function, whose computational procedure reliant on the pulse shape $\varphi(\omega t)$ is outlined above (see also Ref. [15] and Appendices A and B). Rather often, $\chi(u)$ can be calculated analytically (see Table 2 in Ref. [15]), and then the problem reduces to quadratures.

We consider the adiabatic case $\gamma \ll 1$ in greater detail, when only the behavior of the electric field near the maximum is of significance. For $\theta \to 0$, we write

$$\varphi(\theta) = 1 - \frac{a_2}{2!}\,\theta^2 + \frac{a_4}{4!}\,\theta^4 - \frac{a_6}{6!}\,\theta^6 + \ldots\,, \quad a_2 > 0 \quad (3.38)$$

and find

$$\chi(u) = 1 - \frac{a_2}{4}\,u^2 + \ldots, \qquad \tau_s(\gamma) = \gamma - \frac{a_2}{6}\,\gamma^3 + \mathcal{O}(\gamma^5)\,,$$
$$g(\gamma) = 1 - \frac{a_2}{10}\,\gamma^2 - \frac{1}{280}(a_4 - 10a_2^2)\gamma^4 - \frac{1}{15120}(a_6 - 56a_2a_4 + 280a_2^3)\gamma^6 + \ldots, \tag{3.39}$$
$$b_{\|}(\gamma) = \frac{a_2}{3}\,\gamma^2 + \ldots, \qquad b_{\perp}(\gamma) = 1 - \frac{a_2}{6}\,\gamma^2 + \ldots\,.$$

Expressions (3.39) define corrections to the ionization rate in the tunneling regime.

Specific models of pulses whose shape is given by (3.29), which allow analytic solutions of the ionization problem, are discussed in Appendices A and B. To summarize this section, we make several remarks.

(1) In Ref. [56], the ITM was generalized to the relativistic case and a relativistic tunneling theory was constructed.

(2) In Refs [57, 58], the dependence of the tunneling probability on the particle spin ($s = 0, 1/2$) was investigated (see also Section 7.5).

(3) The general case of an elliptically polarized wave has been considered: the extremal sub-barrier trajectory is found analytically in the ITM framework (neglecting the atomic-core–electron Coulomb interaction), and the saddle point is determined from the equation [4]

$$\sinh^2\tau_s - \rho^2(\cosh\tau_s - \tau_s^{-1}\sinh\tau_s)^2 = \gamma^2\,, \tag{3.40}$$

where ρ is the ellipticity of light, $-1 \leqslant \rho \leqslant 1$. Equation (3.40) is easily solved by numerical techniques. We have, up to a pre-exponential factor,

$$w \approx \exp\left(-2K_0 f(\gamma,\rho)\right),$$
$$f(\gamma,\rho) = \left(1 + \frac{1+\rho^2}{2\gamma^2}\right)\tau_s - \frac{1}{\gamma^2}\left(\rho^2\,\frac{\sinh^2\tau_s}{\tau_s} + \frac{1-\rho^2}{4}\,\sinh(2\tau_s)\right). \tag{3.41}$$

For a given field strength and frequency, the ionization probability decreases monotonically with an increase in ellipticity.

(4) The behavior of the ionization probability $w(\gamma)$ as $\gamma \to \infty$ is related to the analytic properties of the field in the complex plane. When $\varphi(\theta)$ has a singularity (a pole) at a point $\theta = i\tau_*$, then $w \sim \exp(-2K_0\tau_*)$ is virtually independent of γ for $\gamma \gg 1$.

(5) The application of the ITM is limited to the case of analytic functions of t^2 [i.e., even pulses of form (3.29)]. Under this condition, however, the ITM algorithm permits solving the ionization problem for virtually any pulse shape.

4. Ionization in the field of ultrashort laser pulses

Experimental investigations of the interaction of atoms and molecules with ultrashort few-cycle pulses of infrared and optical-range laser radiation, as well as the corresponding theoretical work, are discussed in comprehensive review [17].

In this section, we consider several model examples, which are simpler than those analyzed in Ref. [17] and permit us to derive analytic formulas for the ionization rate of atomic levels and the photoelectron spectrum, as well as to qualitatively investigate the behavior of these quantities in relation to the pulse shape. The content of this section is based on the results in Refs [41, 42, 59–61].

4.1 Tunneling interference

We restrict ourselves to the case of a zero-range potential, where the photoionization amplitude is given up to pre-exponential accuracy by formula (3.20) with $C_\kappa = 1/\sqrt{2}$. In the multiquantum regime $K_0 \gg 1$, the time integral in formula (3.20) can be calculated by the saddle-point method and the photoelectron momentum distribution is expressed as [10, 41]

$$\mathrm{d}w(\mathbf{q}) = \frac{2}{\pi}\,K_0\left|\sum_s \left[\Phi''(\mathbf{q},\theta_s)\right]^{-1/2}\exp\left(iK_0\Phi(\mathbf{q},\theta_s)\right)\right|^2 \mathrm{d}^3q\,, \tag{4.1}$$

where we introduce the notation

$$S_0(\mathbf{p},t) = K_0\Phi(\mathbf{q},\theta)\,,$$
$$\Phi(\mathbf{q},\theta) = \theta + \frac{1}{\gamma^2}\int_0^\theta \left(\mathbf{a}(\theta') - \mathbf{a}(\infty) + \gamma\mathbf{q}\right)^2 \mathrm{d}\theta', \quad \theta = \omega t\,, \tag{4.2}$$
$$\mathbf{p} = \kappa\mathbf{q}\,, \quad \boldsymbol{\mathcal{E}}(t) \equiv \mathcal{E}_0\boldsymbol{\varphi}(\theta) = -\mathcal{E}_0\mathbf{a}'(\theta)\,, \quad \mathbf{A}(t) = \frac{c}{\omega}\,\mathcal{E}_0\mathbf{a}(\theta)\,.$$

The result in (4.1) is valid for a pulse of arbitrary shape and polarization under the condition

$$\frac{\left|\Phi^{(\mathrm{IV})}(\theta_s)\right|}{\left|\Phi''(\theta_s)\right|^2} \ll K_0\,, \tag{4.3}$$

which ensures the applicability of the saddle-point method (see, e.g., Ref. [62]). The following treatment is restricted to the case of a linearly polarized field. The computationally simplest case of an even laser pulse, $\varphi(-\theta) = \varphi(\theta)$, is readily considered using the ITM (see Refs [59, 60] and Section 3.3). The results obtained in Refs [59, 60] are minutely discussed in review Ref. [15]. In a short even pulse, the dominating contribution is made by a single stationary point, and therefore the interference effect does not occur. For an odd pulse, $\varphi(-\theta) = -\varphi(\theta)$, there are at least two saddle points, which make equal contributions to the ionization amplitude, resulting in interference effects in the outgoing-electron momentum distribution. Oscillations in the photoelectron energy spectrum were supposedly first noticed in Ref. [3] for linearly polarized monochromatic radiation, and their existence for ultrashort laser pulses was pointed out in Ref. [63]. This effect, which received the name of tunneling interference, was observed experimentally (see, e.g., Refs [64, 65] and Ref. [15, Section 4]).

We consider the effect of tunneling interference in the model example of an odd pulse[4]

$$\varphi(\theta) = \theta\exp\left(\frac{1-\theta^2}{2}\right), \qquad a(\theta) = \exp\left(\frac{1-\theta^2}{2}\right). \tag{4.4}$$

[4] The ionization of an atomic level by a pulse of the form (4.4) was also considered in Ref. [49], but the contribution to the photoionization amplitude made by only one of the saddle points was taken into account there. Not only was the tunneling interference effect lost in the expressions for ionization probability obtained in Ref. [49], but also the total ionization probability of the level was underestimated by many orders of magnitude, especially in the domain $\gamma \ll 1$. For instance, formula (21) in Ref. [49] for $\omega \to 0$ takes the form $w \sim \exp(-\mathrm{const}\,K_0/\sqrt{|\ln\gamma|})$, which contradicts the well-known expression [48, 66] $w \sim \exp[-2/(3F)]$ for the ionization probability in a constant electric field $\mathcal{E}$.

The electric field reaches amplitude values for $\theta_m = \pm 1$, $|\varphi(\theta_m)| = 1$. The corresponding saddle points are located symmetrically with respect to the imaginary axis in the complex θ plane:

$$\theta_+ = \left\{1 - 2\ln\left[1 - i\gamma\sqrt{1+q_\perp^2} - \gamma(q_\parallel - q_0)\right]\right\}^{1/2}, \qquad \theta_- = -\theta_+^* . \tag{4.5}$$

Here, $q_\parallel$ and $q_\perp$ are the longitudinal and transverse components of the dimensionless momentum relative to the polarization direction and q_0 is its most probable value, i.e., the value that minimizes the imaginary part of action (4.2) [42]:

$$\int_0^{\theta_s(q_0)} \left(a(\theta) - a(+\infty) + \gamma q_0\right) d\theta = 0 . \tag{4.6}$$

In the tunneling limit, an approximate solution of Eqn (4.6) has the form [42]

$$q_0 = \frac{1}{\gamma}\left[a(+\infty) - a(\theta_m)\right], \tag{4.7}$$

where θ_m is the point of the maximum of the electric field. For pulse (4.4), for both saddle points [10],

$$q_0 = -\frac{1}{\gamma} . \tag{4.8}$$

The phases $\Phi(\theta_{s,\pm})$ are complex even for extremal values of the momentum ($q_\perp = 0$ and $q_\parallel = q_0$):

$$\Phi(\theta_\pm) = \chi_\pm(\gamma) + i f(\gamma) = \theta_\pm\left\{1 + \frac{1}{\gamma^2}\left[1 - 2e^{1/2}\,{}_1F_1\left(\frac{1}{2};\frac{3}{2};-\frac{\theta_\pm^2}{2}\right) + e\,{}_1F_1\left(\frac{1}{2};\frac{3}{2};-\theta_\pm^2\right)\right]\right\}, \tag{4.9}$$

where $e = 2.718\ldots$ and ${}_1F_1(\ldots)$ is the degenerate hypergeometric function; the function $f(\gamma)$ — a generalization of the Keldysh function to the case of ultrashort pulses — is the same for both saddle points $\theta_\pm$, the values $\chi_\pm(\gamma)$ being different only in sign.

4.2 Photoelectron momentum spectra

In the tunneling limit $\gamma \ll 1$, distribution (4.1) takes the form ($\chi_+(0) = 0.209$)

$$dw(\mathbf{q}) = \frac{8}{\pi}\gamma K_0 \cos^2\left(\chi_+(0)\,\frac{K_0}{\gamma^2}\right) \times \exp\left\{-\frac{2}{3F}\left[1 - \frac{1}{5}\gamma^2 + \frac{3}{2}q_\perp^2 + \gamma^2(q_\parallel - q_0)^2\right]\right\} d^2q_\perp\, dq_\parallel . \tag{4.10}$$

In the pre-exponential factor, fast oscillations caused by the interference of the contributions made by two extremal trajectories, along which the imaginary parts of action function (4.2) are equal (and minimal), emerge. Upon integration over the momentum space, we obtain the total ionization probability

$$w = (96\pi)^{1/2} K_0 F^{3/2} \cos^2\left(\frac{0.209 K_0}{\gamma^2}\right) \exp\left[-\frac{2}{3F}\left(1 - \frac{1}{5}\gamma^2\right)\right] . \tag{4.11}$$

When the averaging is performed over fast pre-exponential oscillations in expressions (4.10) and (4.11), we obtain expressions that differ by only a factor of 2 from the corresponding formulas for symmetric unipolar pulses for $\gamma \ll 1$ [15], as would be expected.

In the multiquantum limit $\gamma \gg 1$, the momentum distribution is given by [10]

$$dw(\mathbf{q}) = \frac{8}{\pi^2} K_0^2 \cos^2\left(\frac{\pi K_0}{2\sqrt{2\ln\gamma}}\right) \times \exp\left[-2K_0\sqrt{2\ln\gamma}\,(1+q^2)\right] d^3q . \tag{4.12}$$

As in the case of even pulses, the distribution becomes isotropic in this limit. The interference oscillations in expression (4.12) are not as fast as in (4.10); their frequency decreases with increasing γ, although only logarithmically. The oscillation period has the form

$$\Delta\gamma \approx \gamma(2\ln\gamma)^{3/2}K_0^{-1} < \gamma \quad \text{for} \quad \gamma < \exp\frac{K_0^{2/3}}{2} . \tag{4.13}$$

An analytic solution is also possible for a pulse with

$$\varphi(\theta) = 2\,\frac{\sinh\theta}{\cosh^2\theta}, \qquad a(\theta) = \frac{2}{\cosh\theta}, \tag{4.14}$$

for which $\theta_m = \pm\ln(1+\sqrt{2})$ and the saddle points $\theta_\pm$ do not go to infinity as $\gamma \to \infty$ but tend to a constant limit $i\pi/2$:

$$\theta_\pm = i\,\frac{\pi}{2} \pm 2\gamma^{-1} - i2^{3/2}\gamma^{-2} \mp 12\gamma^{-3} + \ldots . \tag{4.15}$$

In this case, the ionization probability depends only slightly on γ (for a fixed K_0) (see Refs [41, 42]). Figure 1 shows the dependences of the Keldysh function, the phase difference for extremal trajectories, and the most probable momentum on the adiabaticity parameter, which were calculated in Refs [41, 42] for a pulse of form (4.4) and (4.14).

4.3 Results of numerical simulations

Momentum distributions (4.10) and (4.12) were obtained by quadratic expansion of the action in terms of momenta about the most probable momentum q_0, while the phase difference was taken to be equal to that for extremal trajectories. That is why the factor $\cos^2(\ldots)$ in these distributions describes the interference of contributions of the two most probable trajectories depending on the parameters K_0 and γ but not on the photoelectron momentum. Investigating the interference structure of the momentum distribution requires a more precise calculation, the result of which is not representable in a closed analytic form even for the simplest symmetric and antisymmetric pulse shapes. In this case, it is easiest to use expression (4.1) for the probability, which was obtained by the saddle-point technique, by substituting the numerical solution for the saddle point into it. The thus calculated photoelectron momentum distributions along the radiation polarization direction (i.e., for $q_\perp = 0$) are plotted in Fig. 2.

The spectra shown in Fig. 2 are essentially asymmetric and exhibit an evident interference structure. The degree of asymmetry and the number of interference oscillations decrease with an increase in γ. We emphasize that the spacing between the neighboring interference maxima (minima) is by no means equal to the photon energy, and hence the spectrum, unlike that for a quasimonochromatic field, does not consist of separate peaks, each corresponding to the

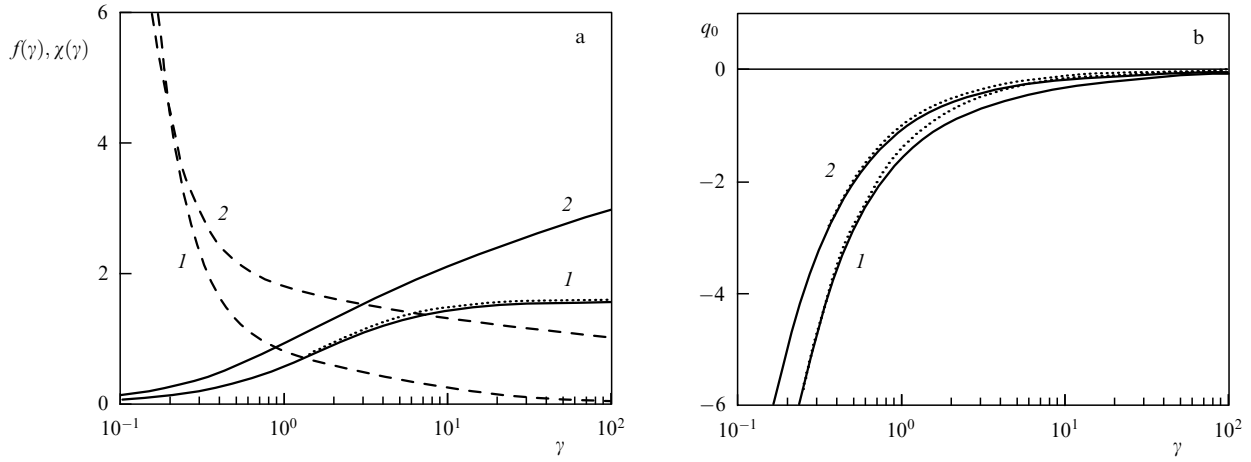

Figure 1. (a) Keldysh function $f(\gamma) = \mathrm{Im}\,\Phi(q_0, \theta_s)$ (solid curves); dashed curves show the phase $\chi(\gamma) = \mathrm{Re}\,\Phi(q_0, \theta_s)$. (b) Most probable momentum $q_0(\gamma)$. The calculations were performed for pulses (4.14) (curves *1*) and (4.4) (curves *2*). Dotted curves show the functions $q_0(\gamma)$ and $f(\gamma)$ calculated using approximate expression (4.7). (From Ref. [42].)

absorption of a definite number of photons of the laser wave. The absence of isolated above-threshold peaks in the spectrum comes as no surprise, because the spread of photon energies in few-cycle pulses is comparable to the energy itself. By and large, the shape of the spectra depends markedly on all parameters of the problem, including the intensity of laser radiation and the pulse shape. This permits using measurements of photoelectron momentum distributions to monitor the shape of short pulses, including the absolute phase [67]. At present, the interference structure of above-threshold ionization spectra is being observed experimentally, including experiments with ultrashort pulses [64, 65].

5. Coulomb effects in photoionization

The basic approximation employed in the Keldysh theory is that the state of a photoelectron in a continuum in the presence of an intense laser field is described by a plane Volkov wave [45–47], while the atomic-core–photoelectron interaction can be neglected. This permits obtaining analytic expressions for photoelectron momentum distributions and, for more intricate processes (harmonic generation, double ionization, etc.), restricting numerical calculations to those amenable to personal computers of average power. The Volkov wave approximation for the continuum is well justified and provides a quantitative description of the multiquantum ionization of the negative ions $H^-, F^-, \ldots$, which has been confirmed by comparing theoretical data with experimental data [68–73], with the results of calculations performed in the framework of the method of complex quasienergy states [74, 75] and the results of numerical integration of the time-dependent Schrödinger equation [76, 77].

For atoms and positively charged ions, there is the Coulomb interaction between the photoelectron and the atomic core, the continuum states are significantly different from plane waves, and amplitude (3.17) is not a good approximation. Neglecting the Coulomb interaction leads to significant discordance between theoretical predictions and experimental data, as well as to internal contradictions in the theory, such as the dependence of the momentum distribution shape and the total ionization probability on the gauge chosen for electromagnetic field potentials (see, e.g., Ref. [18]).

The data of numerical calculations suggest that the Keldysh theory with neglect of the Coulomb interaction in the final state provides only a qualitative description of nonlinear ionization, even in the simplest case of the hydrogen atom. The main factor responsible for the disagreement between the theory and experiment is the long-range Coulomb attraction force between the photoelectron and the nucleus, which is not taken into account in amplitude (3.17).

The importance of including the Coulomb interaction was already recognized in the first studies on the atomic physics of strong fields. As noted by Keldysh [1], his formula for the ionization rate is correct only up to exponential accuracy. However, the problem of including the Coulomb interaction turned out to be intricate and defied solution for a long time. The first attempt to find the pre-exponential factor in the ionization probability of a bound state was made by Nikishov and Ritus [6]; however, their result did not provide the passage to the constant-field limit in the case of linearly polarized radiation, and it therefore remains unclear to what extent it is correct. Perelomov and Popov [7] calculated the Coulomb correction to the atomic ionization rate in the tunneling limit $\gamma \ll 1$. In this case, the ionization rate w of the s state of an atom differs from the similar quantity w_{sr} for a level in a short-range well [15, 48, 66] (with the same ionization potential $I = \kappa^2/2$) by a factor Q_{C}:

$$w = Q_{\mathrm{C}} w_{\mathrm{sr}}\,,$$
$$Q_{\mathrm{C}}(\mathcal{E}_0) = \frac{w(\mathcal{E}_0, \gamma)}{w_{\mathrm{sr}}(\mathcal{E}_0, \gamma)} = \left(\frac{2\hbar^2\kappa^3}{m_{\mathrm{e}} e \mathcal{E}_0}\right)^{2n^*} = \left(\frac{2}{F}\right)^{2n^*} \gg 1\,. \tag{5.1}$$

Here, $\mathcal{E}_0$ is the amplitude of a linearly polarized electric wave field, $F = \mathcal{E}_0/\mathcal{E}_{\mathrm{ch}}$ is the reduced field (1.3), $\kappa = \sqrt{2m_{\mathrm{e}}I}/\hbar$ is the characteristic atomic momentum, $\mathcal{E}_{\mathrm{ch}} = \hbar^2\kappa^3/m_{\mathrm{e}}e$ is the characteristic electric field (for the ground state of atomic hydrogen, $\mathcal{E}_{\mathrm{ch}} \equiv \mathcal{E}_{\mathrm{a}} = m_{\mathrm{e}}^2 e^5/\hbar^4 = 5.14 \times 10^9$ V cm^{-1}), and $n^* = \mathcal{Z}e^2 m_{\mathrm{e}}/\hbar^2\kappa$ is the effective principal quantum number of the level, where $\mathcal{Z}$ is the atomic core charge ($\mathcal{Z} = 1$ for neutral atoms and $\mathcal{Z} = 0$ for singly charged negative ions),

$$w_{\mathrm{sr}}(\mathcal{E}_0, \gamma) = C_\kappa^2 \frac{\kappa^2\hbar}{m_{\mathrm{e}}} \sqrt{\frac{3F^3}{\pi}} \exp\left[-\frac{2}{3F}\left(1 - \frac{\gamma^2}{10}\right)\right], \tag{5.2}$$

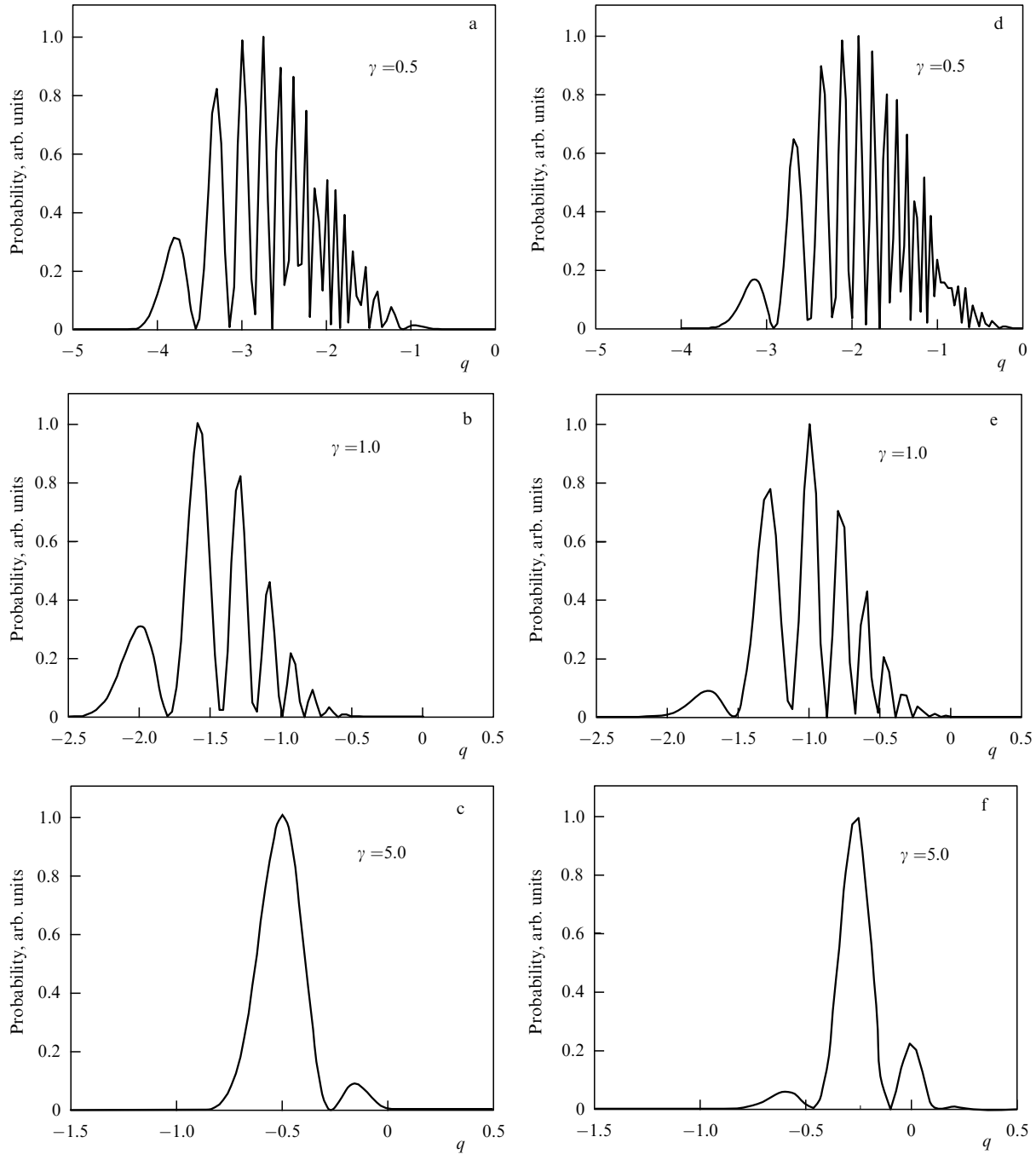

Figure 2. Photoelectron spectra along the polarization direction calculated using expression (4.1) in the case of xenon ionization ($I = 12.1$ eV) by the field of a titanium–sapphire laser ($\hbar\omega \approx 1.55$ eV) for $K_0 \approx 7.8$ and different values of the Keldysh parameters γ indicated in the plots of (a–c) soliton-like (4.14) and (d–f) exponential (4.4) pulse shapes. The peak intensity is 4×10^{14} W cm^{-2} in Figs a and d, 1×10^{14} W cm^{-2} in Figs b and e, and 4×10^{12} W cm^{-2} in Figs c and f. (From Ref. [42].)

where C_κ is a dimensionless asymptotic coefficient of the atomic wave function at distances $r \gg \hbar\kappa^{-1}$ from the nucleus, which is typically not much different from unity [15]. We emphasize that the ionization potential I and the asymptotic coefficient C_κ in formula (5.2) pertain not to a state in a short-range potential but to the atomic state whose ionization probability is calculated.

Correction (5.1) increases the tunnel ionization probability by several orders of magnitude, which is an experimentally determined effect [78]. At present, the expression for the tunnel ionization rate with the inclusion of Coulomb correction [7] is widely used for calibrating the intensity of laser pulses.[5]

[5] The analytic formulas in Refs [2–7] for atomic ionization probabilities and photoelectron momentum spectra in a low-frequency electromagnetic field have also come to be known in the literature as the Ammosov–Delone–Krainov (ADK) formulas [79]. The ADK formulas are a particular case (for $\gamma \ll 1$) of the expressions derived earlier in Refs [2–7]. It is pertinent to note that in Refs [79, 80] and other studies by these authors, the contribution of earlier investigations, which have not lost their significance to date, is ignored (see Refs [15, 81] for remarks concerning the so-called ADK theory).

However, formula (5.1) does not provide the complete solution of the problem and leaves two questions open:

• What is the form of the Coulomb correction $Q_C(\mathcal{E}_0, \omega)$ in the entire frequency range, including the multiquantum domain $\gamma \gg 1$?

• The Coulomb interaction affects not only the total ionization probability but also the photoelectron momentum distribution. Can this effect be described in the framework of the same approach that was used to obtain correction (5.1)?

These problems were solved in Refs [8, 9, 82–87]. The main idea is to use the semiclassical perturbation theory for the action [7]. This theory was generalized in order to calculate the Coulomb correction to the action for an arbitrary value of the final photoelectron momentum and an arbitrary frequency of the laser field. The ITM [55] outlined in Section 3.3 is used in calculations. The ITM was used to describe several effects occurring in the photoionization of atoms and positively charged ions in an intense laser field. The results are strongly different from those obtained under the Keldysh approximation with the Coulomb interaction neglected and agree nicely with the data of numerical integration of the time-dependent Schrödinger equation. Wherever comparison with experiment was possible, a satisfactory agreement was observed.

With the inclusion of the Coulomb interaction between the outgoing electron and the atomic core, corrections of two types emerge. First, the Coulomb potential $U_C = -\mathcal{Z}/r$ gives rise to an addition to the reduced action [7–9]

$$W_C^{(1)} = -\int_{t_s}^{+\infty} U_C\big(\mathbf{r}_0(t)\big)\,\mathrm{d}t = \mathcal{Z}\int_{t_s}^{+\infty} \frac{\mathrm{d}t}{\sqrt{\mathbf{r}_0^2(t)}}\,, \tag{5.3}$$

which explicitly contains the 'weak' Coulomb interaction, and the integral can therefore be calculated along the trajectory $\mathbf{r}_0(t)$ unperturbed by the Coulomb field.

Second, the Coulomb field distorts the electron trajectory. With the correction $\mathbf{r}_1(t)$ to the trajectory found from the solution of the Newton equation

$$\ddot{\mathbf{r}}_1 = -\frac{\mathcal{Z}(\mathbf{r}_0 + \mathbf{r}_1)}{|\mathbf{r}_0 + \mathbf{r}_1|^3}\,, \tag{5.4}$$

the corresponding correction to the action is of the form [8, 9]

$$W_C^{(2)} = \int_{t_s}^{+\infty} \left(\mathbf{v}_0\mathbf{v}_1 + \frac{1}{2}\,\mathbf{v}_1^2 - \mathcal{E}(t)\mathbf{r}_1\right)\mathrm{d}t - \left(\mathbf{v}_0\mathbf{r}_1 + \mathbf{v}_1\mathbf{r}_0 + \mathbf{v}_1\mathbf{r}_1\right)\Big|_{t=t_s}^{t\to+\infty}. \tag{5.5}$$

Furthermore, the instant of the onset of sub-barrier motion in the imaginary time $t_s(\mathbf{p})$ may also contain a Coulomb correction.

When these corrections are small in comparison with action (3.16) in the laser field, their substitution in the exponent gives the nonlinear ionization amplitude with the Coulomb interaction included. Accordingly, the Coulomb correction to the ionization probability is defined by the formula

$$Q_C = \exp\left[-2\,\mathrm{Im}\,(W_C^{(1)} + W_C^{(2)})\right]. \tag{5.6}$$

Corrections (5.3) and (5.5) can be large in magnitude in comparison with unity; in this case, the change in the photoelectron momentum distribution and the total ionization probability is significant.

In Sections 5.1–5.4, we give examples of calculating the Coulomb corrections to the spectra of the multiquantum ionization of atoms in intense laser fields. The results of calculations are compared with the data obtained by numerically solving the time-dependent one-electron Schrödinger equation with the use of two substantially different methods, [88] and [89]. A comparison is also made with available experimental data in the case of ionization in the field of elliptically polarized radiation.

5.1 Angular distributions in elliptically polarized fields

It is instructive to consider the *qualitative* effects whose very existence is a consequence of the Coulomb interaction. An effect of this kind is, for instance, the violation of the fourfold symmetry of photoelectron angular distributions in an elliptically polarized field. For sufficiently long laser pulses, in which the carrier-envelope phase effects are insignificant, the Keldysh approximation results in angular distributions that are symmetric about the major and minor axes of the polarization ellipse. At the same time, experimental data show clearly that this symmetry is not even approximately present in an elliptically polarized field [90, 91]. At intermediate values of the ellipticity ρ, $0.2 < \rho < 0.8$, the most probable photoelectron momentum is directed along the minor axis of the polarization ellipse [4]. This is evident because the electron emerges at the output of the barrier with a zero velocity (for simplicity, we restrict ourselves to the tunneling limit $\gamma \ll 1$). The tunneling probability is highest at the instant the electric field attains its maximum. The vector potential is then minimal in magnitude and is directed along the minor axis of the polarization ellipse. The momentum $\mathbf{p} = \mathbf{v} - \mathbf{A}/c$ measured by detectors has the same direction.

A characteristic example is given in Fig. 3, which also shows the data obtained by exactly solving the time-dependent Schrödinger equation and the data calculated by the ITM with the inclusion of Coulomb corrections [84]. In the latter case, as we can see in Fig. 3, the distribution has no four-fold symmetry of the polarization ellipse and is practically identical to the exact result. A comparison of the calculated data with experimental data [91] reveals a quantitative agreement [84].

5.2 Interference structure of the spectrum

In a linearly polarized field, there are two trajectories in every optical cycle whose contributions to the ionization amplitude are comparable in magnitude (and equal in the case of a strictly monochromatic field). The existence of several trajectories that make contributions to the amplitude with close weights leads to the interference effect in momentum distributions, which was first considered in the problem of multiquantum ionization in Ref. [3]. In ultrashort pulses, the character of interference depends on the carrier-envelope phase, which may be employed for its measurement [64]. As a rule, the observation of interference in the spectra of multiquantum ionization is hampered by the fact that the averaging over the at-focus laser intensity distribution, which inevitably takes place in experiments, results in a partial or complete blurring of the interference structure. It was not until recently that experimenters found ways to overcome this difficulty and measure the spectra showing subtle features of the interference structure [64, 65].

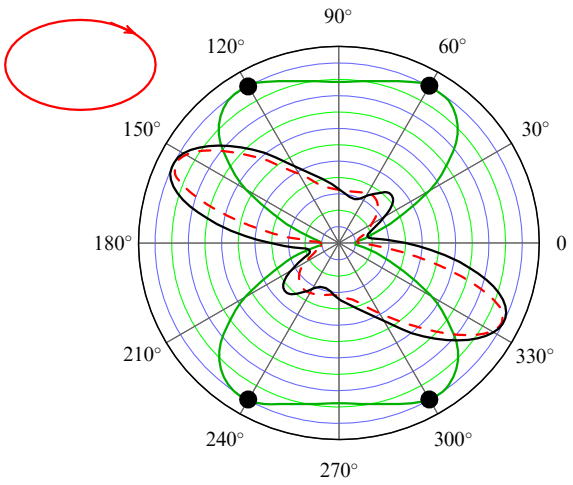

Figure 3. Angular distributions of the photoelectrons of energy $\epsilon = 7.9$ eV in the ionization of the ground state of atomic hydrogen by the field of a titanium–sapphire laser ($\hbar\omega = 1.55$ eV, $J \simeq 10^{14}$ W cm^{-2}, ellipticity $\rho = 0.5$). The results of calculations performed in the framework of the Keldysh model are shown with a solid grey curve; the dashed curve stands for the angular distribution determined by the ITM with the inclusion of Coulomb corrections. The solid black curve represents a numerical solution of the time-dependent Schrödinger equation. The circles denote the photoelectron escape directions for which the Keldysh model yields the same values of the ionization probability. Shown in the upper left part is the orientation of the polarization ellipse with an arrow indicating the rotation direction of the electric field vector.

The interference is clearly seen in the spectra obtained by numerically integrating the Schrödinger equation, and these data are in quantitative agreement with experimental data [64, 65]. At the same time, the interference pattern of the spectrum calculated in the framework of the Keldysh model shows only a qualitative agreement with the data of experiments and numerical calculations. Hence, the Coulomb field of the atomic core makes a significant contribution to the phase difference between the trajectories leading to the same final state, and this contribution must be taken into account in calculating the interference pattern of the spectrum. In this case, the most significant part of the Coulomb correction to the phase difference is due to action (5.3), which diverges logarithmically at the upper integration limit, $\mathbf{r}(t) = \mathbf{p}t + \mathcal{O}(1)$, $W_C^{(1)} \sim (\mathcal{Z}/p)\ln t$. Because different trajectories correspond to the same value of the electron momentum at infinity, the logarithmically diverging parts of the correction are segregated in the form of a common (inessential) phase factor and the finite contributions form the correction to the phase difference [85, 92].

5.3 Multiquantum ionization of atoms in the field of an arbitrary frequency

Popruzhenko et al. [8, 9] obtained the Coulomb correction $Q_C(\mathcal{E}, \omega)$ for a high-frequency field, $\gamma \gg 1$, when the formulas for the tunnel ionization probability are inapplicable even for qualitative estimates. In the multiquantum mode, correction (5.3) is of the same form as in the tunneling regime [7], but correction (5.5), related to the trajectory distortion by the Coulomb field, becomes significant. To calculate this correction, the relation between the momentum $p_{||}$ at the barrier exit and the electron momentum $\mathbf{p}$ at infinity should be taken into account (using the ITM), $p_{||} = \sqrt{p^2 + 2\mathcal{Z}/b}$, where b is the barrier width ($b = \kappa/\omega$ for $\gamma \gg 1$). The condition $p = 0$ corresponds to the most probable trajectory, and the nonzero longitudinal momentum at the barrier exit is [8, 9, 83]

$$p_{||} = \sqrt{\frac{2\mathcal{Z}}{b}} = \sqrt{2n^*\omega} = \kappa\sqrt{2\mu}\,, \qquad \mu = \frac{n^*}{2K_0}\,. \tag{5.7}$$

The small parameter μ defines the contribution of the Coulomb field to the distortion of the electron trajectory.

The Coulomb correction can be written in the form [8, 9]

$$Q_C(\mathcal{E}_0, \omega) = Q_0\, Q_1 \approx \left(\frac{2}{F}\right)^{2n^*} (1 + 2\mathrm{e}^{-1}\gamma)^{-2n^*}\,, \tag{5.8}$$

where e is the natural logarithm base, this form being applicable for arbitrary values of the adiabaticity parameter γ.

In the low-frequency limit, $Q_1 \to 1$ and expression (5.8) passes into formula (5.1) for the tunnel ionization rate of an s level in a low-frequency field. In the opposite limit $\gamma \gg 1$, correction (5.8) is independent of the field strength and is numerically large. The expression for the ionization rate takes the form

$$\begin{aligned} w &\simeq \frac{I}{\hbar}\, A(K_0, n^*) F^{\,2N_{\min}}\,, \\ A(K_0, n^*) &\simeq 2^{2n^*} C_\kappa^2 \exp\left(N_{\min} + 2n^*\right) K_0^{2N_{\min}+2n^*-3/2}\,, \end{aligned} \tag{5.9}$$

where $N_{\min} = [K_0] + 1$ is the minimal number of photons required for ionization. The power-law nature of the perturbation theory of a high order $N_{\min}$ is therefore reproduced, which would be expected in the multiquantum regime [1, 15].

To estimate the accuracy of formula (5.8), the ionization rate determined using this formula has to be compared with the data of numerical calculations [8, 9]. The ionization rates of the 1s state of atomic hydrogen exposed to the field of a second titan–sapphire laser harmonic with the photon energy $\hbar\omega = 3.10$ eV and to the field of a somewhat lower frequency $\hbar\omega = 2.94$ eV are plotted in Figs 4a and 4b. The value of the parameter μ in formula (5.7) is then about 0.11. The ionization rate calculated by the complex quasienergy method (the Floquet method) is shown by circles. The results of a numerical solution of the time-dependent Schrödinger equation in the field of a short 10-cycle pulse are shown by triangles. The coincidence of the results of independent numerical calculations is indicative of their reliability.

Figure 5 shows the ionization rate of the $4p_0$ Xe^{17+} ion state calculated by formulas (5.8), (5.2), and (5.1), as well as by numerical integration of the Schrödinger equation for the electron in the effective potential in the presence of the electric field of the wave. In this case, the Coulomb correction increases the ionization probability by many orders of magnitude: $Q_C \approx 9 \times 10^8$. A comparison of the analytic and numerical results shows a good quantitative agreement even for xenon, although the parameter $\mu = 0.34$ is not very small and the bound state has the angular momentum 1, while the analytic results were obtained for s states. The departure of analytic results from the numerically found ionization rates is primarily due to the resonances not included in this theory. A comparison of the curves in Figs 4a and 4b confirms that it is precisely the resonances that are responsible for these departures. In the former case, observed in the intensity range $\mathcal{I} \simeq (2-3) \times 10^{13}$ W cm^{-2} is a four-photon resonance with one of the Rydberg levels, whose position depends on the

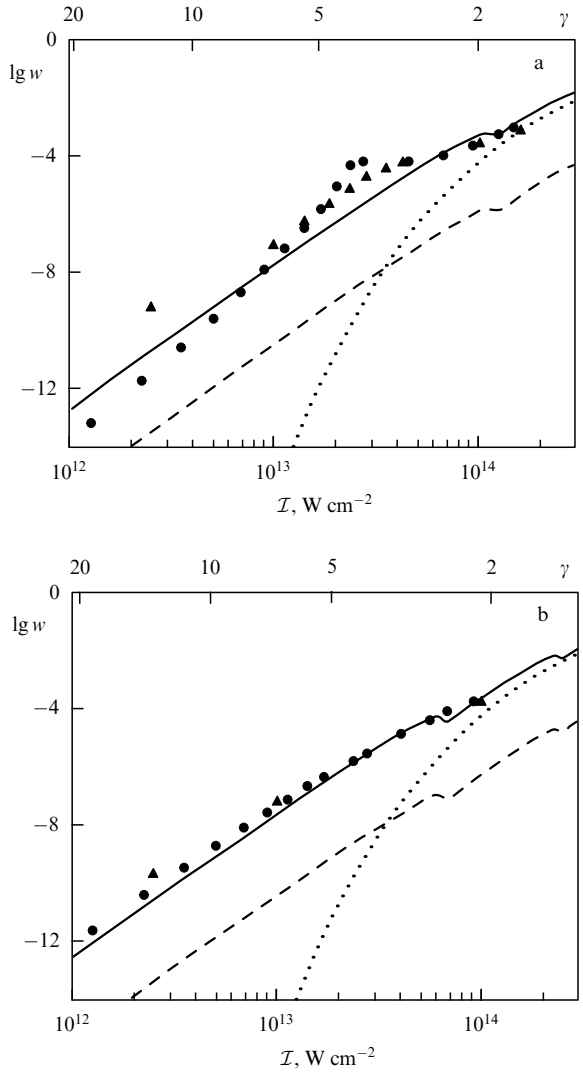

Figure 4. Ionization rate (in the units 1 au $= 4.13 \times 10^{16}$ s^{-1}) calculated by formulas (5.8) (solid curve), (5.2) (dashed curve), and tunneling formula (5.1) (dotted line), as well as calculated numerically by the Floquet method (circles) and by solving the time-dependent Schrödinger equation (triangles), as a function of intensity for the 1s state of atomic hydrogen in the field of a linearly polarized wave with wavelengths (a) 400 nm and (b) 422 nm. The parameter K_0 is respectively equal to 4.39 and 4.63. The field amplitude $\mathcal{E}_0 = 0.053\mathcal{E}_a$ corresponds to the intensity $\mathcal{I} = 10^{14}$ W cm^{-2} and the amplitude $\mathcal{E}_0 = 0.0169\mathcal{E}_a$ corresponds to the intensity $\mathcal{I} = 10^{13}$ W cm^{-2}. The Coulomb correction is $Q_C \approx 6 \times 10^2$.

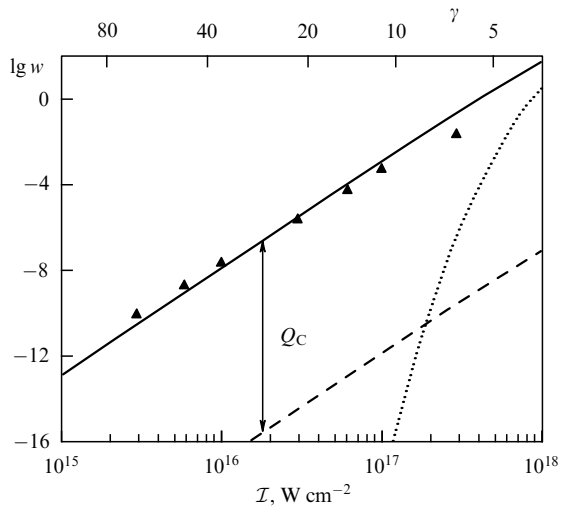

Figure 5. The same as in Fig. 4 for the Xe^{17+} ion ($I = 434$ eV, $4p_0$ shell) in the field of an X-ray laser with the wavelength $\lambda = 13.3$ nm ($\hbar\omega \approx 93$ eV) [93]. Parameters K_0, n^*, and μ are respectively equal to 4.67, 3.19, and 0.34; the Coulomb correction is $Q_C \approx 9 \times 10^8$.

intensity due to the dynamic Stark shift. The wavelength in Fig. 4b is selected such that this resonance is nonexistent, and the analytic and numerical data agree nicely in this case.

5.4 Other applications of the Coulomb correction method

Currently, the ITM and the associated calculation of the photoionization amplitude with the inclusion of Coulomb interaction are rather widely used in the physics of strong laser fields. The authors of Refs [86, 87] developed an approach (independently of Refs [8, 9, 83–85]) to the calculation of the Coulomb correction to the photoelectron action in a strong laser field, which involves using the eikonal approximation and the R-matrix method. For the most probable photoelectron trajectory, the expressions for the Coulomb correction obtained in Refs [86, 87] reproduce the result in (5.1) [7]. Calculation of the correction for the trajectories close to the extremal one, which is also performed analytically, permits finding the angular photoelectron distributions in an elliptically polarized field with the inclusion of Coulomb asymmetry (see Section 5.1) [94, 95]. The method developed in Refs [86, 87] also allows a generalization to the case of multielectron atoms [96].

The authors of Refs [97, 98] proposed and experimentally realized the method of photoelectron holography. The idea of the method is to use the interference structure for reconstructing the form of the electron–ion interaction potential. For atoms, this problem is of merely methodical interest, because the interaction potential is purely Coulombic at long distances. An important result in Refs [97, 98] is that the interference pattern is actually defined by the Coulomb interaction: without it, there is no way of reproducing experimental data even at a qualitative level. The measured photoelectron momentum distributions produced in the multiquantum ionization of xenon by an infrared laser field were compared with the data obtained by numerical integration of the time-dependent Schrödinger equation and with the data of an ITM-based approximate calculation.

In Ref. [99], the ITM was used to solve the problem of the decay of a quasistationary state in the presence of a strong laser field. In distorting a quasistationary level, the effect of the laser field on the sub-barrier motion can typically be taken into account perturbatively (by contrast, in ionization, the role of perturbation is played by the Coulomb field). Upon escape from the barrier, the laser field prevails and, for a system bound by Coulomb forces, the residual Coulomb interaction can be taken into account by the method outlined above. Also, two interaction modes were shown to be possible: in a relatively weak and in a relatively strong field. In the relatively weak field, which does not do appreciable work on a particle over the barrier length, the total level decay rate remains invariable. But if the field frequency is low, such that the inequality

$$e\mathcal{E}_0\sqrt{\frac{E_0}{m}} \gg \omega^2 \tag{5.10}$$

is satisfied, where E_0 is the quasistationary level and m and e are the mass and charge of the particle (not necessarily an electron), then the outgoing particle spectrum becomes broad and consists of many peaks, which correspond to the absorption or emission of a certain number of laser photons. In this mode, the laser field affects only the after-decay particle kinematics. A significant change in the sub-barrier action is possible in a stronger field, leading to an increase in the decay rate. The strong-field criterion depends on the specific system. For a short-range barrier of width b, the strong-field mode is realized when

$$\frac{e\mathcal{E}_0 b^2}{\sqrt{E_0/m}} \geqslant 1\,. \tag{5.11}$$

The conclusion that two decay regimes of a quasistationary level exist in the presence of a laser field coincides with the result of earlier work concerned with the possible effect of a laser field on β decay.

The influence of a strong laser field on β decay is the subject of many studies (see, e.g., review Ref. [38] and the references therein). Only a very strong field can have a significant effect on the decay rate, while the production of much weaker electromagnetic fields, close to the critical field of quantum electrodynamics, is probably unachievable in principle [100]. That is why the effect of the laser field on the decay of quasistationary states in atomic systems or nanosystems is of practical interest. Specifically, the effect of a laser field on the current arising on application of a potential difference between a nanometer-size electrode and a metal surface was studied in a recent experiment [101]. The results obtained in Ref. [99] can be used to describe experiments of this type.

6. Effect of the magnetic field on the atomic ionization rate. Lorentz ionization

6.1 Imaginary-time method in the presence of a magnetic field

Electrons experience the Lorentz force in a magnetic field, with the result that the extremal sub-barrier trajectory becomes twisted and is no longer one-dimensional. To apply the ITM, we must solve the equation of motion

$$\ddot{\mathbf{r}} = -\boldsymbol{\mathcal{E}} - \frac{1}{c}[\dot{\mathbf{r}}\boldsymbol{\mathcal{H}}] - \frac{Z\mathbf{r}}{r^3} \tag{6.1}$$

with a complex 'time' t (in the atomic system of units $c = \alpha^{-1} = 137$), which can be done analytically only for $Z = 0$. With the boundary conditions of the ITM for a short-range potential [4, 5]

$$\mathbf{r}(t_0) = 0\,, \quad \dot{\mathbf{r}}^2(t_0) = -\kappa^2 = -2I\,, \quad \operatorname{Im}\mathbf{r}(t=0) = 0\,, \tag{6.2}$$

we find this trajectory (for constant fields $\boldsymbol{\mathcal{E}}$ and $\boldsymbol{\mathcal{H}}$):

$$\begin{aligned} x &= \mathrm{i}\,\frac{\mathcal{E}}{\omega_\mathrm{c}^2}\left(\tau - \tau_0\,\frac{\sinh\tau}{\sinh\tau_0}\right)\sin\theta\,,\\ y &= \frac{\mathcal{E}}{\omega_\mathrm{c}^2}\,\frac{\tau_0}{\sinh\tau_0}\,(\cosh\tau - \cosh\tau_0)\sin\theta\,,\\ z &= \frac{\mathcal{E}}{2\omega_\mathrm{c}^2}\,(\tau_0^2 - \tau^2)\cos\theta\,. \end{aligned} \tag{6.3}$$

Here, $I = \kappa^2/2$ is the ionization potential of the atomic level, $\tau = \mathrm{i}\omega_\mathrm{c} t$, where

$$\omega_\mathrm{c} = \frac{\mathcal{H}}{c} \tag{6.4}$$

is the cyclotron, or Larmor, frequency, the y axis is aligned with $\boldsymbol{\mathcal{E}}$, the x axis is perpendicular to the plane $(\boldsymbol{\mathcal{E}}, \boldsymbol{\mathcal{H}})$, and θ is the angle between these fields. The initial (purely imaginary) instant $t_0 = \mathrm{i}\omega_\mathrm{c}^{-1}\tau_0$ of sub-barrier motion is determined from the equation [15, 102]

$$\tau_0^2\left[1 - \sin^2\theta\left(\coth\tau_0 - \frac{1}{\tau_0}\right)^2\right] = \gamma_\mathrm{c}^2\,, \tag{6.5}$$

which follows from the condition $\operatorname{Im}\mathbf{r}(0) = 0$ for the electron escape from the barrier. Here, γ_c is an analogue of the Keldysh adiabaticity parameter (1.1),

$$\gamma_\mathrm{c} = \frac{\kappa\mathcal{H}}{c\mathcal{E}} = \frac{\mathcal{H}}{\mathcal{H}_0}\,\frac{\mathcal{E}_\mathrm{ch}}{\mathcal{E}} = \frac{\omega_\mathrm{c}}{\omega_\mathrm{t}}\,, \tag{6.6}$$

where $\mathcal{E}_\mathrm{ch}$ is the characteristic electric field (1.3), $\mathcal{H}_0 = c\kappa^2$, and $\omega_\mathrm{t} = \mathcal{E}/\kappa$ is the tunneling time in a constant field. The physical meaning of γ_c is evident from the equality $\gamma_\mathrm{c} = 2b/R_\mathrm{L}$, where $b = \kappa^2/(2\mathcal{E})$ is the barrier width in a constant electric field and $R_\mathrm{L} = \kappa/\mathcal{H}$ is the Larmor radius. For the hydrogen atom in the ground state, $\kappa = 1$ and $\mathcal{H}_0 = m^2e^3c/\hbar^3 = 2.35\times10^9$ G, with $\mathcal{E}_\mathrm{ch}/\mathcal{H}_0 = \alpha = 1/137$.[6] The level ionization rate depends on the parameter $\gamma_\mathrm{c} > 1$, i.e., is defined by the ratio between the Larmor frequency and the tunneling frequency. The values $\gamma_\mathrm{c} > 1$ can be realized, for instance, for $\mathcal{E} \sim 10^5$ V cm^{-1} and $\mathcal{H} \sim 10^5$ G, which is realistic for semiconductors.

With an exponential accuracy, the ionization probability is

$$w \propto \exp\left(-2\operatorname{Im} W\right), \tag{6.7}$$

where W is the reduced action,

$$W = \int_{t_0}^{0}\left[\mathcal{L} + E_0 - \frac{\mathrm{d}}{\mathrm{d}t}(\mathbf{r}\dot{\mathbf{r}})\right]\mathrm{d}t\,, \qquad \mathcal{L} = \frac{1}{2}\,\dot{\mathbf{r}}^2 - \frac{1}{c}(\mathbf{A}\dot{\mathbf{r}}) + \varphi\,, \tag{6.8}$$

and the potentials are $\mathbf{A} = (1/2)[\boldsymbol{\mathcal{H}}\mathbf{r}]$ and $\varphi = -\boldsymbol{\mathcal{E}}\mathbf{r}$. We calculate action (6.8) along trajectory (6.3) to obtain [15, 104]

$$w(\boldsymbol{\mathcal{E}}, \boldsymbol{\mathcal{H}}) \propto \exp\left(-\frac{2}{3F}\,g(\gamma_\mathrm{c}, \theta)\right), \tag{6.9}$$

where $F = \mathcal{E}/\mathcal{E}_\mathrm{ch}$ is the reduced electric field (1.3) and

$$g(\gamma_\mathrm{c}, \theta) = \frac{3\tau_0}{2\gamma_\mathrm{c}}\left(1 - \frac{\sqrt{\tau_0^2 - \gamma_\mathrm{c}^2}}{\gamma_\mathrm{c}^2}\,\sin\theta - \frac{\tau_0^2}{3\gamma_\mathrm{c}^2}\,\cos^2\theta\right). \tag{6.10}$$

We give the asymptotic expansions of function (6.10): in the domain $\gamma_\mathrm{c} \ll 1$ ('weak' magnetic fields),

$$\begin{aligned} \tau_0(\gamma_\mathrm{c}, \theta) &= \gamma_\mathrm{c} + \frac{1}{18}\,\gamma_\mathrm{c}^3\sin^2\theta + \ldots\,,\\ g(\gamma_\mathrm{c}, \theta) &= 1 + \frac{1}{30}\,\gamma_\mathrm{c}^2\sin^2\theta + \ldots\,, \end{aligned} \tag{6.11}$$

[6] It is possible to introduce $\mathcal{H}_\mathrm{cr} = m_\mathrm{e}^2c^3/(e\hbar) = 4.41\times10^{13}$ G [to be compared with expression (2.1)]. We note that $\mathcal{E}$ [V cm^{-1}] $= \mathcal{H}$ [G].

and for $\gamma_c \gg 1$ and $\theta = \pi/2$,

$$g(\gamma_c) = \frac{3}{8}\,\gamma_c(1 + 2\gamma_c^{-2} + \ldots)\,. \tag{6.12}$$

For $\theta = 0$, i.e., for parallel fields, $\tau_0 = \gamma_c$, $g(\gamma_c, 0) \equiv 1$, and the exponent in expression (6.9) is the same as in the case of a purely electric field. With an increase in γ_c, the function g increases monotonically and the ionization probability decreases. Therefore, the application of a magnetic field stabilizes the atomic level. This is attributable to the fact that the sub-barrier trajectory in the ITM twists, and the barrier width and the imaginary part of the action in expression (6.8) increase under the influence of the Lorentz force.

Further details, including the calculation of the Coulomb correction and the pre-exponential factor in (6.9) (which is analytically possible but leads to cumbersome expressions), can be found in Refs [102–104]. We note that the ionization probability for $\gamma_c > 1$ is exponentially small but does not vanish identically.

6.2 Lorentz ionization of atoms and ions

When an atom or ion flies in a magnetic field $\boldsymbol{\mathcal{H}}$, an electric field $\boldsymbol{\mathcal{E}}_0$ appears in their rest frames owing to the Lorentz transformation, which may lead to ionization. This process is referred to as Lorentz ionization. We restrict ourselves to the case where the atom velocity $\mathbf{v}$ is perpendicular to the field $\boldsymbol{\mathcal{H}}$. Then the fields acting in the atom rest frame have the form [7]

$$\mathcal{E}_0 = \frac{v}{\sqrt{1-v^2}}\,\mathcal{H}\,, \qquad \mathcal{H}_0 = \frac{1}{\sqrt{1-v^2}}\,\mathcal{H}\,, \qquad \boldsymbol{\mathcal{E}}_0 \perp \boldsymbol{\mathcal{H}}_0\,, \tag{6.13}$$

and adiabaticity parameter (6.6) is

$$\gamma_L = \frac{\kappa\mathcal{H}_0}{c\mathcal{E}_0} = \frac{\kappa}{v}\,, \tag{6.14}$$

where the velocity v is expressed in atomic units (1 au $= e^2/\hbar = 2.19 \times 10^8$ cm s$^{-1} \approx 0.007c$). For the ground states of neutral atoms, the parameter κ is close to unity (see, e.g., Table 1 in Ref. [15]). The function $g(\gamma_c)$, which appears in the exponent, is obtained directly from expression (6.10) with $\gamma_c = \gamma_L$ and $\theta = \pi/2$. All functions that enter in the pre-exponential factors are also calculated in [105, 106].

The Lorentz ionization rate is conveniently represented as

$$w_L = (1 - v^2)^{1/2} S w(\mathcal{E}_0)\,, \tag{6.15}$$

where $w(\mathcal{E}_0)$ is the atomic ionization rate under the action of only the electric field $\mathcal{E}_0$ and S is the stabilization factor, which takes the suppression of atomic level decay due to the magnetic field into account. For fast particles ($v \gtrsim 10\kappa$), $S \to 1$, i.e., the ionization of the atomic level occurs at virtually the same rate as in the purely electric field $\mathcal{E}_0$ (the factor $\sqrt{1-v^2}$ in formula (6.15) accounts for the effect of time dilation for the moving atom). When $v \ll \kappa$, the stabilization factor S becomes exponentially small.

We give several estimates. For $\mathcal{H} \lesssim 1$ MG, the atom is essentially stable because the electric field $\mathcal{E}_0$ is too low. In the domain $\mathcal{H} \sim 10$ MG, the Lorentz ionization may already be observed if the atomic velocity is not too low. Specifically, for $\mathcal{H} = 25$ MG (see Table 1) in the velocity interval from $v = 0.5$ au to $v = 10$ au, the situation changes from the complete stability of the atom to its ionization in a time comparable with the atomic time $\tau_a = \hbar^3/(me^4)$ ($w_a = 1/\tau_a = 4.13 \times 10^{16}$ s^{-1}).

Table 1. Lorentz ionization probability for atomic hydrogen*.

v, au	$\mathcal{E}_0$, au	S	w_L, s^{-1}
0.5	5.32(−3)	3.7(−9)	0
1.0	1.06(−2)	0.119	1.03(−9)
1.25	1.33(−2)	0.345	6.41(−4)
1.67	1.77(−2)	0.645	2.40
2.0	2.13(−2)	0.779	1.55(5)
2.5	2.66(−2)	0.882	5.56(7)
5.0	5.32(−2)	0.984	6.24(12)
10	0.107	0.998	7.73(14)

* $v = 1$ au corresponds to an atom velocity of 2.19×10^8 cm s$^{-1} \approx 0.007c$. We assumed a value $\mathcal{H} = 25$ MG — the highest magnetic field achieved in Sakharov's experiments [108]; $\mathcal{E}_0$ is the electric intensity which acts in the atomic rest frame.

In the case of negative ions with a low binding energy,[8] $\kappa \ll 1$, the dependence of the ionization probability on v and $\mathcal{H}$ is qualitatively of the same form as for neutral atoms, but the transition region between the values $w_L \approx 0$ and $w_L \approx w(\mathcal{E}_0)$ lies at lower values of the parameters v and $\mathcal{H}$. In this case, the stabilization factor is smaller than unity:

$$S = 1 - \frac{1}{6}\,\gamma_L^2 + O(\gamma_L^3)\,, \qquad \gamma_L \ll 1\,, \tag{6.16}$$

and S is exponentially small for $\gamma_L \gg 1$. Weakly bound states are known not only in atomic physics but also in solid-state physics (for instance, Wannier–Mott excitons with $\kappa \sim 0.01$ for germanium crystals [107]). In these cases, the ionization occurs in substantially lower fields than for neutral hydrogen atoms.

6.3 Magnetic cumulation

Constant magnetic fields obtained in laboratory do not exceed 1 MG. Sakharov proposed the method of magnetic cumulation [108–110]: compression of a magnetic field enclosed in a shell (a cylindrical tube of a high-conductivity metal, for instance, copper) using the shock wave produced in the explosion of the substance that surrounds the shell. From the conservation of the magnetic flux $\Phi = \pi R^2 \mathcal{H}$, it follows that $\mathcal{H}/\mathcal{H}_0 \approx (R_0/R)^2 \gg 1$, where $R(t)$ is the shell radius. Record high fields $\mathcal{H} \sim 25$ MG ($\sim 10^{-5}$ s in duration) have already been attained [108], and further progress in this area is expected to continue [111].

A description of magnetic cumulation dynamics, which is a certain development of the estimates made by Sakharov, was obtained on the basis of the equation [9]

$$\ddot{\xi} = \frac{1}{K\xi^3}\left(1 + \frac{\mu}{\sqrt{-\xi\ddot{\xi}}}\right)^2, \qquad 0 < \tau < \tau_m\,, \tag{6.17}$$

[7] In the general case of an arbitrary angle between $\mathbf{v}$ and $\boldsymbol{\mathcal{H}}$, the formulas for the electric and magnetic fields are given in Refs [105, 106].

[8] For instance, the H^- ion with the binding energy $I = 0.754$ eV ($\kappa = 0.236$), Na^- with $I = 0.548$ eV ($\kappa = 0.201$), and Sr^- with $I = 0.11$ eV and $\kappa = 0.09$.

[9] See formulas (24) and (31) in Ref. [106] for plane and cylindrical geometries. It is pertinent to note that Eqn (6.17) applies only to the shell compression stage ($\dot{\xi} < 0$) and is inapplicable at the expansion stage.

with the initial conditions $\xi(0) = -\dot{\xi}(0) = 1$ and with $\xi(\tau)$ having a weak singularity of the form $\xi(\tau) = \xi_m + \text{const}\,(\tau_m - \tau)^{5/3}$ at the final point. Here, $\xi = R/R_0$, $\tau = v_0 t/R_0$, the dot denotes the derivative with respect to the dimensionless time τ, $K = 4Mv_0^2/\mathcal{H}_0^2 R_0^2$ is the ratio of the kinetic shell energy to the magnetic energy $\mathcal{H}_0^2 R_0^2/8$ contained in the shell at the initial instant $t = 0$, M is the shell mass, and $\mu = c/\sqrt{2\pi\sigma R_0 v_0}$ is the ohmic loss coefficient of the shell substance. In the ideal case ($\mu = 0$, $\sigma = \infty$, a superconductor), Eqn (6.17) has an energy integral and can be solved analytically:

$$\xi = \xi^{(0)}(t) = \sqrt{\xi_m^2 + (1 + K^{-1})(\tau - \tau_m)^2}\,. \tag{6.18}$$

At the instant of greatest shell compression and of the highest magnetic field, $\dot{\xi}(\tau_m) = 0$,

$$\xi_m^{(0)} = (K+1)^{-1/2} \approx K^{-1/2}\,, \qquad \tau_m^{(0)} = \frac{K}{K+1} \to 1\,, \quad \frac{\mathcal{H}_m^{(0)}}{\mathcal{H}_0} = K + 1 \tag{6.19}$$

(in real experiments, the parameter $K \gg 1$). Using the Maxwell equations[10] for a well-conducting medium [114],

$$\frac{\partial \boldsymbol{\mathcal{H}}}{\partial t} = \frac{c^2}{4\pi\sigma}\,\Delta\boldsymbol{\mathcal{H}}\,, \qquad \boldsymbol{\mathcal{E}} = \frac{c}{4\pi\sigma}\,\text{rot}\,\boldsymbol{\mathcal{H}}\,,$$

it is possible to calculate the electromagnetic energy flux flowing into the shell, $J = (1/2)cR\mathcal{E}_\varphi \mathcal{H}_z|_{r=R}$, and the Joule heat power released in it. This permits estimating the loss of the magnetic flux Φ during cumulation due to the finite shell conductivity. Taking the loss into account, in lieu of expressions (6.19), we obtain

$$\xi_m = \frac{R(\tau_m)}{R_0} = (K+1)^{-1/2} \times \left[1 - \frac{2}{K+1}\int_0^{\tau_m}\left(\mu^2 + 2\mu\sqrt{-\xi\dot{\xi}}\,\right)\xi^{-4}\,\mathrm{d}\tau\right]^{-1/2}, \tag{6.20}$$

$$\frac{\mathcal{H}_m}{\mathcal{H}_0} = (K+1)\left[1 + 2\mu\int_0^{\tau_m}\left(1 + \frac{2}{K\xi^2}\right)\sqrt{-\frac{\dot{\xi}}{\xi^3}}\,\mathrm{d}\tau\right]^{-1}. \tag{6.21}$$

Numerical calculations using Eqns (6.17), (6.21) give the curves plotted in Fig. 6 [106]. Referring the reader to Refs [108, 109] for details, we give some estimates: $\mu = 0.01$ and 0.037, respectively, for $\sigma = 6 \times 10^5\ \Omega^{-1}\ \text{cm}^{-1}$ (the conductivity of copper at room temperature $T = 300$ K) and $\sigma = 4 \times 10^4\ \Omega^{-1}\ \text{cm}^{-1}$ ($T = 1500\,^\circ$C; the metal is in a liquid state). Therefore, the parameter $\mu \ll 1$, but Eqn (6.17) must be solved exactly owing to its strong nonlinearity. Due to the loss (for Foucault currents), the peak magnetic field is 2–3 times lower than that in the ideal case in (6.18), (6.19). This estimate corresponds to the brief remarks contained in Refs [108, 109].

Therefore, the magnetic cumulation technique permits increasing the limit $\mathcal{H}$ values produced under stationary conditions in laboratories by at least two orders of magnitude. Unfortunately, this is a pulsed technique, and the lifetime of the peak field is quite short: $\Delta t \sim 2R_0(\sqrt{K}v_0)^{-1} \lesssim 10^{-6}$ s, which complicates the execution of physical experiments, including those in Lorentz ionization. Even higher magnetic fields (several hundred MGs in intensity) are generated in the interaction of dense plasmas with high-power laser pulses (see, e.g., Refs [115, 116] and the references therein). The durations of such pulsed fields are even shorter, no longer than about 10^{-11} s.

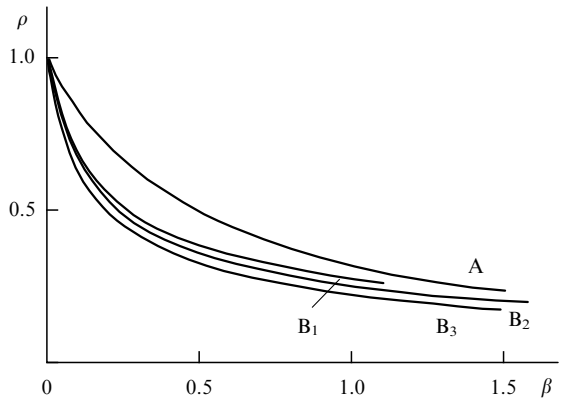

Figure 6. Loss in the peak magnetic field in the course of magnetic cumulation: $\rho = \mathcal{H}_m/\mathcal{H}_m^{(0)}$, $\beta = K^{1/4}\mu$ is the characteristic parameter of the process. Curve A corresponds to the conservation of magnetic flux Φ (i.e., $\mu = 0$), curves B_1, B_2, and B_3 were calculated using Eqn (6.21) for $K = 100$, 10^3, and 10^8, respectively. The last-mentioned K value corresponds to shell compression using an underground nuclear explosion of relatively small yield rather than an ordinary explosive charge (see Ref. [110, p. 85]) (borrowed from Ref. [106]).

6.4 Ultrahigh magnetic fields

Ultrahigh magnetic fields are encountered in astrophysics: in magnetic white dwarfs (up to $\mathcal{H} \sim 350$ MG on the stellar surface), in neutron stars ($\mathcal{H} \sim 10^{11} - 10^{14}$ G), and in magnetars ($\mathcal{H} \sim 10^{15}$ G). An advantage of white dwarfs is the possibility of investigating their optical spectra, which permits studying the effect of the fields $\mathcal{E}$ and $\mathcal{H}$ on atomic levels, primarily of atomic hydrogen and helium, which exist on the stellar surface. The Lorentz ionization of atoms can occur when a star transits the cloud of interstellar gas (neutral hydrogen). For $\mathcal{H} = 350$ MG, the probability w_L becomes appreciable for the stellar velocity $v \gtrsim 1000$ km s^{-1}, the dependence of w_L on v being extremely strong (see Table 1). However, ionization is possible even for a lower velocity of stellar motion relative to the interstellar gas cloud, because the atoms fall on the stellar surface at the velocity $v = \sqrt{2GM/R}$ in the gravitational field. Assuming the white dwarf mass $M \sim M_\odot = 2 \times 10^{33}$ g and radius $R \sim 10^4$ km, we obtain $v \sim 4 \times 10^3$ km s^{-1}. Outside the star, magnetic fields decrease with the distance r as $(r/R)^{-3}$, and therefore the Lorentz ionization of hydrogen atoms can occur at distances of the order of several radii R.

More detailed data about extreme magnetic fields obtained in terrestrial laboratories and encountered in space, as well as about the properties of atomic hydrogen in strong ($\mathcal{H} \simeq 10^{11}$ G) and superstrong ($\mathcal{H} \simeq 10^{14}$ G) fields, can be found in review [117].

7. Relativistic ionization theory

The record high intensities of laser radiation attained to date are $\mathcal{I} = c\mathcal{E}_0^2/(8\pi) \sim 2 \times 10^{22}$ W cm^{-2} [30] (in this case, the field strength is $\mathcal{E}_0 \sim 10^3 \mathcal{E}_a \sim 10^{12}$ V cm^{-1}), and they can be increased. Although the 'critical' field of quantum electro-

[10] The convoluted story of the discovery of Maxwell equations was set forth in Terent'ev's book [112], and the same for the Dirac equation, by Dirac himself in [113].

dynamics (2.1) [36] is unlikely to be attainable in experiments [100], raising the intensity of laser pulses to $10^{24}-10^{25}$ W cm^{-2} seems to be possible. The fields of such a high intensity, which far exceed the characteristic atomic field $\mathcal{E}_a$, are capable of 'stripping' a heavy atom of its electron shells and producing multiply charged ions with $Z \gtrsim 40-60$, for which the ionization potential of the ground state is comparable to the electron rest energy. In this case, describing the ionization requires using the relativistic generalization of the Keldysh theory, which was developed in Refs [57, 58, 118–121]. The main results obtained in these studies are discussed in review [15] and subsequent publications [58, 122].

In this section, we consider the method proposed by Fock for solving the equations of motion and the relativistic wave equation and its application to the covariant description of the particle tunneling effect in a strong electromagnetic field.

Hereafter, we use the relativistic system of units $\hbar = m = c = 1$, $\alpha = e^2 = 1/137$. In the Dirac equation and some other formulas, the electron mass is retained in explicit form.

7.1 General expression for the ionization probability in the relativistic case

We consider the ionization of an atomic level of energy ε_0 in a potential with a Coulomb 'tail', $U_C = -Z\alpha/r$. Away from the nucleus, the wave function corresponding to the quantum numbers j, l, and M has the form [47]

$$\psi^{(0)}_{jlM}(\mathbf{r}, t; \varepsilon_0) = C_{jlM}\lambda_0^{3/2}\begin{pmatrix}\sqrt{1+\varepsilon_0}\\ \mathrm{i}\sqrt{1-\varepsilon_0}\,\boldsymbol{\sigma}\mathbf{n}\end{pmatrix} \times R_0(r)\Omega_{jlM}(\mathbf{n})\exp(-\mathrm{i}\varepsilon_0 t)\,. \tag{7.1}$$

Here, $\lambda_0 = \sqrt{1-\varepsilon_0^2}$, $\boldsymbol{\sigma}$ are the Pauli matrices, $\mathbf{n} = \mathbf{r}/r$, $\Omega_{jlM}(\mathbf{n})$ is a spherical spinor, C_{jlM} is a dimensionless asymptotic coefficient, and

$$R_0(r) = (\lambda_0 r)^{\nu-1}\exp(-\lambda_0 r)\,, \qquad r \gg \frac{1}{\lambda_0}\,,$$

where $\nu = Ze^2\varepsilon_0/\lambda_0$ is the relativistic analogue of the effective principal quantum number. For the ground state of a hydrogen-like ion of charge Z, we have $j = M = 1/2$, $l = 0$, and

$$\varepsilon_0 = \nu = \sqrt{1-(\alpha Z)^2}\,, \quad \lambda_0 = \alpha Z\,, \quad C^2_{1/2,0,1/2} = \frac{2^{2\varepsilon_0}}{\Gamma(2\varepsilon_0+1)}\,, \tag{7.2}$$

with $\Gamma(\ldots)$ being the Euler gamma function. The values $Z < 137$ and $\varepsilon_0 > 0$ correspond to the presently known atoms; in this case, the approximation of a point-like nuclear charge applies.

As in the nonrelativistic problem, the ionization probability is defined by the imaginary part of the reduced action W calculated along the extremal sub-barrier trajectory:

$$w_R(\varepsilon_0; jlM) = w_0|C_{jlM}|^2 P_{jlM} Q\exp(-2\,\mathrm{Im}\,W)\,. \tag{7.3}$$

Here, Q is the Coulomb factor, the pre-exponential factor P_{jlM} includes a spinor factor [57] (see Section 7.5), and

$$W = \int(L-\varepsilon_0)\,\mathrm{d}t = S - \varepsilon_0 t\,, \tag{7.4}$$

$$w_0 = \frac{mc^2}{\hbar} = 0.776\times 10^{21}\ \mathrm{c}^{-1}\,. \tag{7.5}$$

We use Fock's method (see Appendix D) to write the action integral as

$$S = \int_{s_0}^{s} L\,\mathrm{d}s'\,, \qquad L = -\frac{1}{2}\,m\dot{x}^2 - \frac{1}{2}\,m + eA_\mu(x)\dot{x}^\mu\,, \tag{7.6}$$

where the dot denotes the derivative with respect to s, $\dot{x}^\mu \equiv \mathrm{d}x^\mu/\mathrm{d}s$. Action (7.6) is considered to be a function of the final, $x = x^\mu(s)$, and initial, $x_0 = x^\mu(s_0)$, electron coordinates. Then the ITM equations in Section 3.3 can be written in terms of s: the extremal trajectory, which corresponds to the variation of the proper time from $s = s_0$ to $s = 0$ at the instant of escape from the barrier, is determined from the equations

$$\dot{t}(s_0) - \frac{e}{m}\,A_0(s_0) = \varepsilon_0\,, \quad t(s_0) = t_0\,, \quad \mathbf{r}(s_0) = 0\,, \qquad \mathrm{Im}\,x^\mu(0) = \mathrm{Im}\,\dot{x}^\mu(0) = 0\,, \tag{7.7}$$

and the reduced action in expression (7.4) has the form

$$W = S(\varepsilon_0, s_0) - \varepsilon_0 m t_0\,, \qquad S(\varepsilon_0, s_0) = \int_0^{s_0}\mathrm{d}s\left\{m - e\dot{x}^\mu(s)\,A_\mu\big[x(s)\big]\right\}, \tag{7.8}$$

where s_0 is the total imaginary proper time of sub-barrier electron motion.

In the weak-field case $\mathcal{E} \ll \lambda_0^3\mathcal{E}_{cr}$, there is a broad range of distances in which the Coulomb field is small in comparison with the external one. The Coulomb contribution to the classical action integral can therefore be found using the perturbation theory, as was done in the nonrelativistic case in Section 5. The contribution to the Lagrange function corresponding to the atomic-core–electron Coulomb interaction is expressed in terms of the proper time, $L_C = -Ze^2\dot{t}(\tau)/r(\tau)$, which gives the Coulomb factor of the wave function in the form

$$\psi \propto \exp\left\{\nu\left[\ln(\lambda_0 m r) + \ln\left(\frac{s_0-\tilde{s}}{s_0-s}\right) + \mathrm{i}\lim_{s\to s_0}\int_s^{\tilde{s}}\left(\frac{\lambda_0\dot{t}(s')}{\varepsilon_0 r(s')} - \frac{\mathrm{i}}{s_0-s'}\right)\mathrm{d}s'\right]\right\}, \tag{7.9}$$

where $\tilde{s}$ is an arbitrary point on the real axis of proper time, whose position does not affect the Coulomb factor. We make the substitutions $s = \mathrm{i}\tau$ and $s_0 = \mathrm{i}\tau_0$ and take into consideration that $s_0 - s = \mathrm{i}r/\lambda_0$ at short distances from the nucleus; this gives the r-independent Coulomb factor

$$Q = \exp\left\{2\nu\left[\ln(\lambda_0^2 m\tau_0) + \int_0^{\tau_0}\mathrm{d}\tau\left(\frac{\lambda_0\dot{t}(\tau)}{\varepsilon_0 r(\tau)} - \frac{1}{\tau_0-\tau}\right)\right]\right\}. \tag{7.10}$$

Formulas (7.3)–(7.10) are the main equations of the semiclassical theory of relativistic ionization constructed in Refs [57, 58, 118, 120, 121] and written in the proper time representation. In Sections 7.2–7.4, the use of these equations is illustrated with several examples.

7.2 Ionization by the field of a plane wave

We consider a plane electromagnetic wave propagating along the x axis. We choose the gauge

$$A_\mu(x,t) = \frac{\mathcal{E}}{\omega}\left\{0, 0, a(\theta), -\rho b(\theta)\right\}, \quad \theta = \omega(t-x)\,, \tag{7.11}$$

where θ is the light-front variable, ω is the frequency, and ρ is the wave ellipticity, $-1 \leqslant \rho \leqslant 1$. We then obtain the electric and magnetic fields

$$\begin{aligned} \boldsymbol{\mathcal{E}} &= \mathcal{E}\{0, a'(\theta), -\rho b'(\theta)\}, \\ \boldsymbol{\mathcal{H}} &= \mathcal{H}\{0, \rho b'(\theta), a'(\theta)\}. \end{aligned} \tag{7.12}$$

By the Noether theorem, the integrals of motion are the generalized momenta p_y and p_z, and the gradient-invariant integral

$$J = \frac{p^0 - p^1}{m} = \frac{E_{\mathrm{kin}} - p_x}{m} = \frac{\dot{\theta}}{\omega}, \qquad \theta = J\omega s, \tag{7.13}$$

where E_{kin} is the electron kinetic energy. The light-front variable is linear in the proper time s. The classical equations of motion are therefore readily integrated. To find the extremal trajectory, on the strength of conditions (7.7), it is necessary to segregate the imaginary and real parts of the solution. This can be done explicitly when the pulse shape satisfies the equalities

$$a(\mathrm{i}\eta) = \mathrm{i}\alpha(\eta), \qquad b(\mathrm{i}\eta) = \mathrm{i}\beta(\eta), \qquad \theta = \mathrm{i}\eta, \tag{7.14}$$

where $\alpha(\eta)$ and $\beta(\eta)$ are real analytic functions of η. Without writing the cumbersome expressions for the sub-barrier electron trajectory, we give the final result for the exponential factor [57, 58]:

$$w_{\mathrm{R}} \sim \exp(-2\,\mathrm{Im}\,W) = \exp\left[-\frac{2m}{\omega}\,\eta_0(J - \varepsilon_0)\right], \tag{7.15}$$

where $\eta_0 = -\mathrm{i}\theta_0$, θ_0 is the total imaginary 'phase' time of sub-barrier electron motion, and the quantities η_0 and J are determined from the equations

$$\begin{aligned} &\alpha^2(\eta_0) - \rho^2\big(\beta(\eta_0) - I_\beta(\eta_0)\big)^2 = \gamma_{\mathrm{r}}^2(1 - 2\varepsilon_0 J + J^2), \\ &I_{\alpha^2}(\eta_0) - \rho^2\big(I_{\beta^2}(\eta_0) - I_\beta^2(\eta_0)\big) = \gamma_{\mathrm{r}}(1 - J^2). \end{aligned} \tag{7.16}$$

Here,

$$\gamma_{\mathrm{r}} = \frac{m\omega}{e\mathcal{E}} = \frac{\omega}{m}\,\frac{\mathcal{E}_{\mathrm{cr}}}{\mathcal{E}} \tag{7.17}$$

is the relativistic analogue of the Keldysh parameter, and

$$\begin{aligned} &I_{\alpha^2}(\eta_0) = \frac{1}{\eta_0}\int_0^{\eta_0} \alpha^2(\eta)\,\mathrm{d}\eta, \qquad I_\beta(\eta_0) = \frac{1}{\eta_0}\int_0^{\eta_0} \beta(\eta)\,\mathrm{d}\eta, \\ &I_{\beta^2}(\eta_0) = \frac{1}{\eta_0}\int_0^{\eta_0} \beta^2(\eta)\,\mathrm{d}\eta. \end{aligned} \tag{7.18}$$

For an elliptically polarized monochromatic wave, we have $a = \sin\theta$, $b = \cos\theta$, $\alpha(\eta) = \sinh\eta$, and $\beta(\eta) = \cosh\eta$, whence

$$\begin{aligned} &I_{\alpha^2} = \frac{1}{2}\left(\frac{\sinh(2\eta_0)}{2\eta_0} - 1\right), \qquad I_\beta = \frac{\sinh\eta_0}{\eta_0}, \\ &I_{\beta^2} = \frac{1}{2}\left(\frac{\sinh(2\eta_0)}{2\eta_0} + 1\right), \end{aligned}$$

and system (7.16) transforms into the equations in Ref. [58, Section 4] that are readily solved numerically (see Tables 1 and 2 in Ref. [58]).

The equations become significantly simpler as $\omega \to 0$, i.e., in passing to a low-frequency crossed field; calculated analytically in this case is not only the leading exponential factor in the probability but also the Coulomb one in (7.10):

$$\begin{aligned} &w_{\mathrm{R}} \propto Q_0 \exp\left(-\frac{2}{3F}\right), \\ &Q_0 = \left[\frac{2}{F}\left(1 - \frac{\xi}{3}\right)^2\right]^{2\nu} \exp\left(6\alpha Z \arcsin\frac{\xi}{\sqrt{3}}\right). \end{aligned} \tag{7.19}$$

Here, F is a relativistic generalization of reduced field (1.3),

$$F = \frac{\mathcal{E}}{\mathcal{E}_{\mathrm{ch}}}, \tag{7.20}$$

$$\mathcal{E}_{\mathrm{ch}} = \big(\sqrt{3}\xi_0\big)^3(1 + \xi_0^2)^{-1}\mathcal{E}_{\mathrm{cr}} = \begin{cases} \kappa^3\mathcal{E}_{\mathrm{a}}, & \varepsilon_0 = 1 - \dfrac{\kappa^2}{2}, \\ 2.60\,\mathcal{E}_{\mathrm{cr}}, & \varepsilon_0 = 0, \end{cases}$$

where ξ_0 is the convenient variable introduced in Ref. [120], related to the energy level as

$$\xi_0 = \left[1 - \frac{1}{2}\,\varepsilon_0\left(\sqrt{\varepsilon_0^2 + 8} - \varepsilon_0\right)\right]^{1/2}, \quad 0 < \xi_0 \leqslant 1. \tag{7.21}$$

In the nonrelativistic limit,

$$\varepsilon_0 = 1 - \frac{\kappa^2}{2m}, \qquad \xi_0 = \frac{\kappa}{\sqrt{3m}},$$

and $\mathcal{E}_{\mathrm{ch}}$ coincides with expression (1.3). In a constant crossed field, $J = (1 + \xi_0^2)^{-1/2}$ and the total imaginary proper time of the sub-barrier electron motion is proportional to ξ_0:

$$\tau_0 = \frac{\sqrt{3}\,\xi_0}{\omega_0} = \frac{\sqrt{3}\,\xi_0 m}{e\mathcal{E}}, \qquad t_0 = Js_0 = \frac{s_0}{\sqrt{1 + \xi^2}}, \tag{7.22}$$

which is the total laboratory time of the sub-barrier motion.

As shown in Ref. [58], for a characteristic tunneling time T_{t} in the relativistic generalization of the Keldysh parameter $\gamma_{\mathrm{R}} = \omega T_{\mathrm{t}}$, it is useful to take the absolute value of the laboratory time $|t_0|$, such that

$$\gamma_{\mathrm{R}} = \omega|t_0| = \sqrt{\frac{3\xi_0^2}{1 + \xi_0^2}}\,\gamma_{\mathrm{r}}. \tag{7.23}$$

Then the exponential in ionization rate (7.15) can be represented as

$$w_{\mathrm{R}} \propto \exp\left(-\frac{2\sqrt{3}\,\xi_0^2}{1 + \xi_0^2}\,\frac{\mathcal{E}_{\mathrm{cr}}}{\mathcal{E}_0}\right) = \exp\left(-\frac{2}{3F}\,g(\gamma_{\mathrm{R}}, \varepsilon_0, \rho)\right), \tag{7.24}$$

$$g(\gamma, \varepsilon, \rho) = 1 - \frac{1}{10}\,\frac{1 - \rho^2/3}{1 - \xi_0^2/3}\,\gamma^2 + \mathcal{O}(\gamma^4). \tag{7.25}$$

The results of numerical calculations of $g(\gamma_{\mathrm{R}}, \varepsilon_0, \rho)$ as a function of the adiabaticity parameter γ_{R}, the energy level ε_0, the charge Z, and the ellipticity ρ are given in Refs [58, 122].

For optical and infrared lasers, $\omega/m \leqslant 10^{-5}$, and the ionization of multiply charged ions therefore occurs in the tunneling regime, $\gamma_{\mathrm{R}} \ll 1$ and $\xi_0 \to 0$. Then

$$\begin{aligned} &w_{\mathrm{R}} \propto Q \exp\left\{-\frac{2}{3F}\left[1 - \frac{1}{10}\left(1 - \frac{\rho^2}{3}\right)\gamma_{\mathrm{R}}^2\right]\right\}, \\ &Q = Q_0 \exp\left(\frac{\alpha Z}{\sqrt{3}\,\xi_0}\,q(\xi_0, \rho)\gamma_{\mathrm{R}}^2\right), \\ &q(\xi_0, \rho) = q_I(\xi_0) - \rho^2 q_\rho(\xi_0). \end{aligned} \tag{7.26}$$

The functions $q_l(\xi_0)$ and $q_\rho(\xi_0)$ were defined in Ref. [58]. For a linearly polarized wave $\rho = 0$, the semiclassical exponent in (7.26) was obtained by Nikishov and Ritus [6], and for arbitrary ρ, in Refs [4, 58].

Therefore, the semiclassical exponential and the Coulomb factor in the ionization rate of a relativistic atomic level are known in analytic form for a plane wave of the general form in the weak-field approximation. Neglecting the Coulomb interaction in a constant uniform crossed field, it is possible to obtain a closed equation for the complex energy, which defines the energy level, its width, and the spin factor without assuming the field to be weak (see Section 7.4).

7.3 Pair production in a constant crossed field

We consider the production of an electron–positron pair in the vacuum by a perpendicular constant and uniform (electric and magnetic) fields. Assuming that the electric field is aligned with the y axis and the magnetic field with the z axis, we choose the 4-potential in the form

$$A_\mu = \{-\mathcal{E}y,\, \mathcal{H}y,\, 0,\, 0\}\,. \tag{7.27}$$

Let s_0 be the proper time instant that corresponds to the onset of the production of an electron in the vacuum, when its total energy is equal to zero, $m\varepsilon_0 = 0$. Because the energy of a real electron is $\geqslant m$, the production process is tunneling in character. The electron is assumed to escape from the effective barrier at $s = 0$. The probability of electron production in the vacuum is highest when it moves along the extreme trajectory that minimizes the imaginary part of the action function in the classically forbidden domain. By solving the equations of motion in proper time with the initial condition

$$\dot{t}(s_0) \equiv \varepsilon_0(s_0) = 0\,, \quad \mathbf{p}(s_0) = 0\,, \quad \operatorname{Im} x^\mu(0) = 0\,, \tag{7.28}$$

we obtain (see Appendix D)

$$\begin{aligned} &s = \mathrm{i}\,\frac{\omega_0}{\Omega^2}\sin\eta\,, \quad x = \mathrm{i}\,\frac{\omega_0}{\Omega^2}\,\beta\sin\eta = \beta s\,,\\ &y = -\frac{1}{\Omega}\cos\eta\,, \quad z = z_0\,, \quad 0 \leqslant \eta \leqslant \frac{\pi}{2}\,. \end{aligned} \tag{7.29}$$

Here, ω_0 is the proper acceleration of the electron in the constant electric field and β has the meaning of the velocity of the frame of reference in which the magnetic field is equal to zero,

$$\omega_0 = e\mathcal{E}\,, \quad \beta = \frac{\mathcal{H}}{\mathcal{E}}\,, \quad \Omega = \sqrt{1-\beta^2}\,\omega_0\,. \tag{7.30}$$

Condition (7.28) gives

$$\cos\eta_0 = 0\,, \quad \eta_0 = \frac{\pi}{2}\,, \quad s_0 = \frac{\mathrm{i}\pi}{2\Omega}\,,$$

where s_0 is the total imaginary proper time of the sub-barrier electron motion.

Action (7.6) calculated along extremal trajectory (7.29) is given by

$$S = \frac{1}{2}\,ms_0 = \mathrm{i}\,\frac{\pi}{4}\,\frac{m}{\Omega} = \mathrm{i}\,\frac{\pi}{4}\,\frac{m^2}{e\sqrt{\mathcal{E}^2-\mathcal{H}^2}}\,. \tag{7.31}$$

For the electron production probability in the vacuum, we then obtain (with exponential accuracy)

$$w_{\mathrm{e}^-} \propto \exp\left(-2\operatorname{Im} S\right) = \exp\left(-\frac{\pi}{2\sqrt{1-\beta^2}}\,\frac{\mathcal{E}_{\mathrm{cr}}}{\mathcal{E}}\right). \tag{7.32}$$

By the electrical charge conservation law, the probability of positron production in the vacuum is equal to the electron production probability, $w_{\mathrm{e}^+} = w_{\mathrm{e}^-}$, and hence the $\mathrm{e}^+\mathrm{e}^-$-pair production probability in the vacuum is [125]

$$w_{\mathrm{e}^+\mathrm{e}^-} = w_{\mathrm{e}^+}w_{\mathrm{e}^-} \propto \exp\left(-\frac{\pi\mathcal{E}_{\mathrm{cr}}}{\sqrt{\mathcal{E}^2-\mathcal{H}^2}}\right). \tag{7.33}$$

A more accurate formula, which comprises the pre-exponential factor, was obtained by Schwinger [37]. As would be expected, this probability is expressed only in terms of the field invariant $\mathcal{F} = \mathcal{E}^2 - \mathcal{H}^2$, because the second invariant vanishes in this case: $\mathcal{G} = \boldsymbol{\mathcal{E}}\boldsymbol{\mathcal{H}} = 0$.

As is evident from expression (7.33), the magnetic field decreases the pair production probability. In the crossed fields $\boldsymbol{\mathcal{E}} \perp \boldsymbol{\mathcal{H}}$, $\mathcal{E} = \mathcal{H}$, the pair production probability vanishes, because the (imaginary) proper tunneling time turns to infinity. For $\mathcal{H} > \mathcal{E}$, action (7.31) becomes real, and the pair production probability in the vacuum is equal to zero. For this field configuration, it is possible to find a reference frame in which the electric field is equal to zero, and a purely magnetic field does not produce $\mathrm{e}^+\mathrm{e}^-$ pairs.

7.4 Ionization from a state in a short-range potential by a constant crossed field

With the Coulomb interaction neglected, it is possible to obtain an equation that determines the ionization probability with a higher accuracy than the Keldysh theory and does not require, in particular, that the external field be low in comparison with the atomic one. Equations for the quasienergy[11] of a level of a nonrelativistic system bound by short-range forces were first obtained by Manakov and Rapoport [131] and Berson [132]. Currently, the method of quasistationary quasienergy states is widely used in atomic high-field physics (see review Refs [75, 133] and the references therein). Here, we consider a relativistic generalization of the quasienergy equation for constant crossed fields, i.e., for quasistationary states.

The solution of the Dirac equation $D_-\psi = 0$ in an external field $F_{\mu\nu} = \partial_\mu A_\nu - \partial_\nu A_\mu$ can be represented in the form

$$\psi = D_+\Psi\,, \qquad D_\pm = \gamma^\mu(\mathrm{i}\partial_\mu + eA_\mu) \pm m\,, \tag{7.34}$$

where Ψ is the solution of the squared equation

$$D_-D_+\Psi \equiv \mathcal{K} + \mathrm{i}e(\boldsymbol{\alpha}\boldsymbol{\mathcal{E}} + \boldsymbol{\sigma}\boldsymbol{\mathcal{H}})\Psi = 0\,. \tag{7.35}$$

Here, $\mathcal{K}$ is the differential operator of the Klein–Fock–Gordon equation [126–128],[12]

$$\mathcal{K} = (\mathrm{i}\partial + eA)^2 - m^2\,, \qquad A^2 = A^\mu A_\mu = A_0^2 - \mathbf{A}^2\,, \tag{7.36}$$

and $\boldsymbol{\alpha}$ and $\boldsymbol{\sigma}$ are the four-row matrices introduced by Dirac.

[11] The notion of quasienergy of a quantum system in a periodic external field was introduced by Zel'dovich and Ritus [129, 130].

[12] For the history of Fock's discovery of gauge symmetry and its related Klein–Fock–Gordon equation, see the paper by Okun' [134].

In a weak external field $\mathcal{E} \ll \lambda_0^3 \mathcal{E}_{\rm cr}$, the ionization has the character of penetration through a low-transmittance barrier; to calculate the current at a long distance from the atom, we can use the matching procedure of the solution ψ of the Dirac equation and the asymptotic form of atomic function (7.1) in the sub-barrier region

$$\frac{1}{\lambda_0} \ll r \ll (1-\varepsilon_0)\,\frac{1}{f}\,, \qquad f = \frac{\mathcal{E}}{\mathcal{E}_{\rm cr}}\,. \tag{7.37}$$

Here, we introduce the dimensionless field f by analogy with the reduced field in (1.3).

Using Fock's method, it is possible to write the solution of Eqn (7.34) as a contour integral with respect to s. In the semiclassical approximation,

$$\Psi^{(S)}(x,x_0) = \int_C {\rm d}s\, \Delta(x,x_0;s-s_0) \times \exp\left[{\rm i}S(x,x_0;s-s_0)\right] f_{jlM}^{(S)}\,. \tag{7.38}$$

Here, the action integral is given by expression (7.6),

$$\Delta = \frac{1}{m^2}\left[\det\left(-\frac{\partial^2 S}{\partial x\,\partial x_0}\right)\right]^{1/2},$$

and the bispinor $f^{(S)}$ satisfies the equation

$$\frac{{\rm d}f_{jlM}^{(S)}}{{\rm d}s} + \frac{e}{2m}(\boldsymbol{\alpha}\boldsymbol{\mathcal{E}} + \boldsymbol{\sigma}\boldsymbol{\mathcal{H}})\, f_{jlM}^{(S)} = 0\,, \quad \frac{\rm d}{{\rm d}s} = \frac{\partial}{\partial s} + \dot{x}^\mu\,\frac{\partial}{\partial x^\mu}\,, \tag{7.39}$$

and when the field is turned off,

$$f_{jlM}^{(S)} \to f_{jlM}^{(0)} = \begin{pmatrix} 1 \\ 0 \end{pmatrix} \Omega_{jlM}(\mathbf{n})\,.$$

Formulas (7.38), (7.39) define the solution of the Dirac equation for an electron in an electromagnetic field with a semiclassical accuracy. In the special case of a constant and uniform electromagnetic field, this solution is exact.

We obtain a closed equation for the complex energy $\varepsilon = \varepsilon_0 - {\rm i}\Gamma/2$ (where Γ is the level width) of quasistationary states in a short-range potential. In the weak-field case, this equation permits finding an analytic form of the quasistationary energy level and its width, i.e., the rate of level ionization. In accordance with Schwinger's work [37], as a path of integration C in expression (7.38), we choose the positive semiaxis τ in the complex plane; for the Green's function of the Dirac equation, we then have

$$G(x,x_0) = \frac{1}{m}\,D_+ \int_0^\infty \frac{{\rm d}s}{s^2}\left[1 - \frac{1}{2}\,\omega_0 s(\alpha_y + {\rm i}\sigma_z)\right] \times \exp\left[{\rm i}S_\perp(x,x_0;s-s_0)\right] \tag{7.40}$$

with the action

$$S_\perp(x,x_0;s-s_0) = S^{(0)}(x,x_0;s-s_0) - \frac{1}{24}\,m(\theta-\theta_0)^2(s-s_0) - \frac{1}{2}\,m(\theta-\theta_0)(y+y_0)\,, \tag{7.41}$$

where $\theta = \omega_0(t-x)$ and $S^{(0)}$ is the action of a free particle,

$$S^{(0)}(x,x_0;s-s_0) = -\frac{1}{2}\,m\left[\frac{(x-x_0)^2}{s-s_0} + s - s_0\right], \qquad \{x^\mu\} = \{t,\mathbf{r}\}\,. \tag{7.42}$$

Passing to a mixed representation,

$$G(\mathbf{r},t;\varepsilon) = \exp(-{\rm i}\varepsilon m t)\int_{-\infty}^{+\infty}\frac{{\rm d}t_0}{2\pi}\exp\left[-{\rm i}\varepsilon m(t_0-t)\right]G(\mathbf{r},t;0,t_0), \tag{7.43}$$

and calculating the integral over the difference $t_0 - t$, for the s state as $r \to 0$, we obtain

$$\frac{1}{1+\varepsilon}(1\;0)\,\chi_\sigma^+ G(\mathbf{r},0;\varepsilon)\chi_\sigma\begin{pmatrix}1\\0\end{pmatrix} \equiv g_\sigma(\mathbf{r},\varepsilon) = \frac{1}{mr} - \lambda + g_\sigma(\varepsilon) + \mathcal{O}(r)\,. \tag{7.44}$$

Here, χ_σ is an eigenfunction of the operator of spin projection onto the magnetic field direction, $\lambda = \sqrt{1-\varepsilon^2}$, $\sigma = 2M = \pm 1$ ($j = 1/2$, $l = 0$), and, after the change $\omega_0\tau \to 2\sqrt{3}u$, the function $g_\sigma(\varepsilon)$ assumes the form

$$g_\sigma(\varepsilon) = \sqrt{\frac{f}{4\pi{\rm i}\sqrt{3}}}\int_0^\infty \frac{{\rm d}u}{u^{3/2}}\left\{\frac{k_\sigma(u)}{\sqrt{1+u^2}} \times \exp\left[-{\rm i}\,\frac{\sqrt{3}u}{f}\left(1 - \frac{\varepsilon^2}{1+u^2}\right)\right] - \exp\left[-{\rm i}\,\frac{\sqrt{3}u}{f}(1-\varepsilon^2)\right]\right\}, \tag{7.45}$$

where

$$k_\sigma(u) = 1 - {\rm i}\sigma\sqrt{3}u - \frac{(3 - {\rm i}\sigma\sqrt{3}u)\varepsilon u^2}{(1+\varepsilon)(1+u^2)}\,. \tag{7.46}$$

As in the nonrelativistic limit, the quasienergy value ε is determined from the boundary condition as $r \to 0$:[13]

$$g_\sigma(\mathbf{r},\varepsilon) = \frac{1}{mr} - \lambda_0 + O(r)\,, \qquad \lambda_0 = \sqrt{1-\varepsilon_0^2}\,. \tag{7.47}$$

A comparison of expressions (7.44) and (7.47) leads to the equation

$$\sqrt{1-\varepsilon^2} - g_\sigma(\varepsilon) = \sqrt{1-\varepsilon_0^2}\,, \tag{7.48}$$

which defines the complex energy $\varepsilon = \varepsilon_0 - {\rm i}\Gamma/2$ of the quasistationary s level in a strong field and is the relativistic generalization (in the constant field case) of the quasienergy equation for a short-range potential [131, 132].

In the weak field limit $f \ll 1$, solving Eqn (7.48) approximately using the perturbation theory, we obtain the level shift $\Delta\varepsilon_0$ as

$$\Delta\varepsilon_0 = \sqrt{\varepsilon_0^2 + \sigma f} - \varepsilon_0\,, \qquad \sigma = \pm 1\,, \qquad \varepsilon_0^{1/2} > f. \tag{7.49}$$

Here, we took into consideration that

$$\mathrm{Re}\, g_\sigma(\varepsilon_0) = -{\rm i}\,\frac{1}{2}\,\frac{\sigma f}{\sqrt{{\rm i}\pi}\lambda_0}\int_0^\infty \frac{{\rm d}v}{v^{1/2}}\exp(-{\rm i}v) = -\frac{\sigma f}{2\lambda_0}\,. \tag{7.50}$$

At the same time, the imaginary part of $g_\sigma(\varepsilon_0)$ cannot be obtained from expression (7.45) by expansion into a series. We calculate it by the saddle-point method and take into

[13] The effective radius in the case of the Dirac equation can be taken into account in a standard way [135, 136].

account the saddle point

$$u_s = -i\xi\,, \quad \xi = \left[1 - \frac{1}{2}\,\varepsilon\left(\sqrt{\varepsilon^2+8} - \varepsilon\right)\right]^{1/2}, \quad \xi = \xi_0 + \Delta\xi\,, \tag{7.51}$$

to obtain the s-level ionization rate

$$w_R \equiv \Gamma = \frac{f k_\sigma(\xi_0)}{\sqrt{3}(1-\xi_0^2)}\sqrt{\frac{(1+\xi_0^2)(3-\xi_0^2)}{\xi_0^2(3+\xi_0^2)}} \times \exp\left[\frac{2\sqrt{3}\xi_0(1-\xi_0^2)}{(1+\xi_0^2)f}\left(\sqrt{1+\frac{\sigma f}{\varepsilon_0^2}} - 1\right)\right] \exp\left[-\frac{2\sqrt{3}\xi_0^3}{(1+\xi_0^2)f}\right], \tag{7.52}$$

where $k_\sigma(\xi_0) = k_\sigma(u = -i\xi_0)$ in formula (7.46).

7.5 Spin correction in the relativistic tunneling theory

The ionization rate of a relativistic s level by a linearly polarized low-frequency field ($\mathcal{E} = \mathcal{H}$, $\boldsymbol{\mathcal{E}}\boldsymbol{\mathcal{H}} = 0$, $\gamma \ll 1$) is given by formula (7.24) up to a pre-exponential factor. This expression is spin-independent and can be obtained from the solution of the Klein–Fock–Gordon equation in constant cross fields [2, 120, 121] or using the relativistic version of the ITM. Although the spin correction to formula (7.24) is numerically small (more precisely, is a factor of the order of unity), it leads to a difference between the tunneling of bosons and fermions and is therefore of interest. We calculated this correction in two independent ways.

(1) In formula (7.52), which was derived by the method for solving relativistic equations of motion proposed by Fock, it is possible to separate a factor containing the spin projection σ — the so-called spin factor, which determines the dependence of the tunneling probability on the particle spin:

$$S_\sigma = \frac{1+\sqrt{1+\xi_0^2} - \sigma\sqrt{3}\xi_0}{1+\sqrt{1+\xi_0^2} + \sigma\sqrt{3}\xi_0} \times \exp\left[\frac{2\sqrt{3}\xi_0}{(1-\xi_0^2)f}\left(\sqrt{1+\frac{\sigma f}{\varepsilon_0^2}} - 1\right)\right], \quad \sigma = \pm 1\,. \tag{7.53}$$

It is significant that formulas (7.50), (7.52), and (7.53) for the level shift, the level width, and the spin factor were obtained by an approximate solution of Eqn (7.48) with the additional condition (7.49). If

$$\sqrt{f} \ll \varepsilon_0\,, \tag{7.54}$$

then the expression for the spin factor (7.53) is simplified:

$$S_+ = \frac{1}{S_-} = \frac{1+\sqrt{1+\xi_0^2} - \sqrt{3}\xi_0}{1+\sqrt{1+\xi_0^2} + \sqrt{3}\xi_0}\exp\left(\frac{\sqrt{3}\xi_0}{1-\xi_0^2}\right). \tag{7.55}$$

(2) A different way of obtaining the spin factor was developed in Refs [57, 58, 122, 137]. Proceeding from the initial-state wave function $\Psi^{(0)}_{jlM}$ (7.1) and applying the semiclassical approximation, we find a wave $\Psi^{(+)}(r)$ that diverges at infinity and corresponds to a quasistationary state of the outgoing electron. By matching these solutions in overlap region (7.37), calculating the particle flux $\int \Psi^{(+)*}\alpha\Psi^{(+)}\,dS$, and taking the atomic level splitting in the strong magnetic field into account, we find the electron escape probability per unit time, i.e., the level ionization rate (see formulas (3.19) and (3.20) in Ref. [58]). For the spin factor, which we now denote by $\tilde{S}$, we obtain [14]

$$\tilde{S}_+ = \frac{1}{\tilde{S}_-} = \frac{1+\sqrt{1+\xi_0^2} + \sqrt{3}\xi_0}{1+\sqrt{1+\xi_0^2} - \sqrt{3}\xi_0}\exp\left(-\frac{\mu}{\mu_B}\,\frac{\sqrt{3}\xi_0}{\sqrt{1+\xi_0^2}}\right). \tag{7.56}$$

The values of $S_\pm$ and $\tilde{S}_\pm$ in expressions (7.53), (7.55), and (7.56) apply to states with the spin projection $s_z = \pm\hbar/2$ in the direction of magnetic field $\boldsymbol{\mathcal{H}}$, ξ_0 is defined by formula (7.21), and μ is the magnetic moment of the electron at distances $r \ll a_B/Z$ from the nucleus, which differs from the Bohr magneton μ_B (for a free electron) when $Z\alpha \simeq 1$. We use the model of a hydrogen-like atom (ion) in which, for the $1s_{1/2}$ state,

$$\varepsilon_0 = \sqrt{1-(Z\alpha)^2}\,, \quad 0 < Z\alpha < 1\,, \qquad \frac{\mu}{\mu_B} = \frac{1+2\varepsilon_0}{3} = \begin{cases} 1 - \dfrac{1}{3}(Z\alpha)^2\,, & Z \ll 137\,, \\ \dfrac{1}{3}\left[1 - 2^{3/2}(1-Z\alpha)\right], & Z \to 137\,. \end{cases} \tag{7.57}$$

(3) It follows from formulas (7.55) and (7.56) that the spin correction is negligible when $Z \ll 137$:

$$\tilde{S}_\pm = 1 \pm \frac{1}{3}(Z\alpha)^3 + \mathcal{O}\left((Z\alpha)^5\right). \tag{7.58}$$

This is attributable to the fact that the spatial and spin variables separate in the Pauli Hamiltonian for an electron in a uniform magnetic field, spin is not coupled to the orbital electron motion, and the terms of the order $Z\alpha$ and $(Z\alpha)^2$ are absent from expansion (7.58).

Table 2 gives numerical values of the spin factors for the $1s_{1/2}$ levels of hydrogen-like atoms with $Z \leqslant 137$. Although formulas (7.55) and (7.56) are different, this difference is insignificant even for $Z = 92$ (uranium); in this case, the values of S_+ and $\tilde{S}_+$ themselves do not exceed 1.2. Such a weak spin dependence of the tunneling probability leaves little hope for extracting the magnitude of the spin factor from experimental data, especially so in view of the sharp

Table 2. Spin factor for the $1s_{1/2}$ level of a hydrogen-like atom*.

Z	ε_0	ξ_0	$\mathcal{E}_{ch}$, V cm^{-1}	$\mathcal{E}_{ch}/\mathcal{E}_{cr}$	$\tilde{S}_+$	S_+
20	0.989	8.47(−2)	4.13(13)	3.13(−3)	1.00104	1.00106
40	0.956	0.172	3.38(14)	2.56(−2)	1.008564	1.00909
60	0.899	0.265	1.19(15)	9.0(−2)	1.0155	1.0350
80	0.812	0.368	3.00(15)	0.227	1.078	1.104
92	0.741	0.437	4.82(15)	0.365	1.127	1.195
100	0.684	0.489	6.47(15)	0.490	1.174	1.302
118	0.508	0.631	1.23(16)	0.936	1.354	—
137	0	1.0	3.42(16)	2.598	1.768	—

* The values of ε_0, ξ_0, and $\mathcal{E}_{ch}$ were calculated by formulas (7.2), (7.20), and (7.21). We give the values of the spin correction calculated by formulas (7.56) and (7.55); the — sign indicates that condition (7.54) is not satisfied.

[14] The details of the calculation are given in Refs [57, 58].

dependence of tunneling exponent (7.24) on the laser field strength. Expressions (7.55) and (7.56) are different because, in the derivation of expression (7.56), the level energy ε was assumed to be a given value, while in expression (7.55) the spin-projection-dependent energy shift (7.49) in an external magnetic field was taken into account.

(4) In quantum mechanics, self-adjoint operators correspond to physical quantities (the observables [138]).[15] As an example, we consider the model of a hydrogen-like atom with a (point-like) nuclear charge Z:

$$V(r) = -\frac{Z\alpha}{r}\,, \qquad 0 < r < \infty\,. \tag{7.59}$$

Following Ref. [140], we pass from the potential $V(r)$ in the Dirac equation to the effective potential $U(r, j, \varepsilon)$, which satisfies the Schrödinger equation and is expressed in terms of $V(r)$, although in a rather complicated way. As is easily shown [140], for model (7.59), the term in the potential U that is most singular at short distance from the center has the form

$$U(r, j, \varepsilon) = \frac{j(j+1) - (Z\alpha)^2}{2r^2} - \frac{Z\alpha\varepsilon}{r} + \ldots\,, \qquad r \to 0\,, \tag{7.60}$$

where $j = 1/2, 3/2, \ldots$ is the angular momentum of the electron and $\varepsilon = E/m_e$ is the level energy normalized to the electron rest energy. As long as $Z < Z_s = \sqrt{j(j+1)}\,\alpha^{-1}$, the potential $U(r, j, \varepsilon) > 0$ for $r \to 0$, and the Dirac Hamiltonian

$$H_D = \gamma^0(-i\gamma\nabla + m) - \frac{Z\alpha}{r} \tag{7.61}$$

uniquely defines the energy spectrum $\varepsilon_{nj}(Z)$, but this is not so when $Z > Z_s$. It can be shown [141, 142] that the uniqueness of the spectrum is restored by a self-adjoint extension of the H_D operator, which requires introducing additional parameters not contained in the initial potential $V(r)$; without them, however, the problem is not defined. In the case of Coulomb potential (7.59), this situation already occurs for

$$Z > Z_s\left(j = \frac{1}{2}\right) = \frac{\sqrt{3}}{2\alpha} = 118.7\,. \tag{7.62}$$

We recall that for $Z > \alpha^{-1} = 137$, the Dirac equation with a point-like Coulomb potential leads to the well-known 'fall to the center' [47]. In the interval $119 < Z < 137$, the potential is not a self-adjoint operator. As was first shown by Pomeranchuk and Smorodinskii [143], these mathematical subtleties[16] disappear when the finite dimensions of the nucleus are taken into account (for more details, see Refs [140, 145–148]).

8. Domain of applicability of the nonrelativistic Keldysh theory

We find under what conditions the nonrelativistic description of tunneling becomes inapplicable and the formulas in Section 7 should be used to calculate the ionization probability. The highest intensities have been achieved to date with IR lasers in the tunneling regime $\gamma \ll 1$ (see Sections 1 and 2). We compare the ionization probability in the nonrelativistic (w_{NR}) and relativistic (w_R) theory. For linearly polarized radiation, up to a pre-exponential factor, we have

$$w_{NR} \propto \exp\left[-\frac{2}{3F}\left(1 - \frac{1}{10}\,\gamma^2\right)\right], \tag{8.1}$$

$$w_R \propto \exp\left[-\frac{2}{3F}\left(1 - \frac{3\xi^2}{10(1+\xi^2)}\right)\gamma_r^2\right], \tag{8.2}$$

where F is reduced field (1.3), and γ and γ_r are adiabaticity parameters (1.1) and (7.17).[17] The dimensionless momentum κ of the bound state is expressed in terms of the level energy E_0:

$$\varepsilon_0 = \frac{E_0}{mc^2} = 1 - \frac{1}{2}\,\alpha^2\kappa^2 + \ldots\,, \tag{8.3}$$

and the characteristic electric field $\mathcal{E}_{ch}$ is expressed in terms of the critical field of quantum electrodynamics:

$$\mathcal{E}_{ch} = 3^{3/2}\xi^3(1+\xi^2)^{-1}\mathcal{E}_{cr}\,, \tag{8.4}$$

where the variable $\xi = \xi(\varepsilon_0)$ is defined by formula (7.21). The values $0 < \xi < 1$ correspond to level energies $\varepsilon > 0$.

For the model of a hydrogen-like atom with the potential $V(r) = -Z\alpha/r$, $0 < r < \infty$, in particular, the Dirac equation is solved analytically and the ground-state energy is [47]

$$\varepsilon_{1s_{1/2}} = \sqrt{1 - (Z\alpha)^2}\,, \quad \kappa = Z\,, \quad Z < \alpha^{-1} = 137\,. \tag{8.5}$$

In this case, $\mathcal{E}_{ch} = Z^3\mathcal{E}_a = (Z\alpha)^3\mathcal{E}_{cr}$ for $Z \ll 137$, $\mathcal{E}_{ch} = 0.365\mathcal{E}_{cr}$ for $Z = 92$, $\mathcal{E}_{ch} = \mathcal{E}_{cr}$ for $\varepsilon_0 = 0.485$, $Z = 120$, and $\mathcal{E}_{ch} = 2.6\mathcal{E}_{cr}$ for $Z = 137$, $\varepsilon_0 = 0$.

It follows from formulas (8.1) and (8.2) that

$$R \equiv \frac{w_{NR}}{w_R} \approx \exp\left[-\frac{1}{36}(Z\alpha)^5\,\frac{\mathcal{E}_{cr}}{\mathcal{E}_0}\right], \qquad Z \ll 137\,. \tag{8.6}$$

The difference between the nonrelativistic and relativistic formulas for the probability w becomes appreciable only when $Z \gtrsim Z_*$,

$$Z_* = \alpha^{-1}\left(36\,\frac{\mathcal{E}_0}{\mathcal{E}_{cr}}\right)^{1/5} \approx 45\left(\frac{\mathcal{I}}{10^{22}\ \mathrm{W\ cm^{-2}}}\right)^{1/10}, \tag{8.7}$$

where $\mathcal{I}$ is the radiation intensity. This simple estimate respectively gives $Z_* = 35$, 45, 60, and 75 for $\mathcal{I} = 10^{21}$, 10^{22}, 10^{23}, and 10^{24} W cm^{-2} [15].

Therefore, formula (8.1) significantly underestimates the atomic ionization probability of high-Z ions. Specifically, for $Z = 40$, 60, and 80 at $\mathcal{I} = 10^{23}$ W cm^{-2}, the values of w_{NR} and w_R differ by respective factors of 1.15, 3, and 65. Consequently, although the domain of applicability of the nonrelativistic Keldysh theory extends to rather high Z, the relativistic tunneling theory must be used for heavy ions with $Z \gtrsim 40$. We note that formula (7.21) implies relations

[15] On the difference between self-adjoint and Hermitian operators in the Hilbert space, see, e.g., Ref. [139].

[16] "... And now I have a profound respect for mathematics, whose subtleties I treated as a luxury owing to my narrow-mindedness." From A. Einstein's letter to A. Sommerfeld, Zurich, 29 October 1912 [144].

[17] In this case, $\gamma_r = \gamma/\alpha\kappa$. In the nonrelativistic limit $\varepsilon \to 1$, $3\xi^2(1+\xi^2)^{-1}\gamma_r^2 \to \gamma^2$, and formulas (8.1) and (8.2) coincide.

(for the ground state)

$$\xi_0 = \frac{1}{\sqrt{3}}\left[Z\alpha + \frac{2}{9}(Z\alpha)^3 + \mathcal{O}\big((Z\alpha)^5\big)\right],$$

$$1 - \xi_0^2 = \sqrt{2}\,\varepsilon_0 - \frac{1}{2}\,\varepsilon_0^2 + \ldots \quad \text{for} \quad \varepsilon_0 \to 0\,, \tag{8.8}$$

which we used in Section 7.

9. Conclusions

At present, the applicability domain of the Keldysh theory is extremely broad and is not limited to the description of nonlinear ionization of atoms and ions. We briefly list the areas in high-field physics where the method proposed in Ref. [1] is being widely used and which remain beyond the scope of this paper due to its limited length.

(1) The Keldysh theory is widely used to describe the ionization of not only atoms but also more complex systems — molecules, clusters, fullerenes, dielectrics, etc. The reader interested in this area of research is referred to book [149], reviews [150, 151], papers [152–157], and the references therein.

(2) The nonlinear ionization amplitude (3.17) enters a complex matrix element that describes more complicated processes induced in atomic and molecular systems by a high-intensity laser field. Among these processes are rescattering, which is responsible for the formation of the high-energy plateau in photoelectron spectra; the generation of high-order harmonics of laser radiation; and nonsequential multiple ionization. These effects were experimentally discovered about 20 years ago and are now under intensive investigation. Especially keen interest is aroused by the effect of high-order harmonic generation, which is used for producing coherent ultraviolet and soft X-ray radiation pulses (attosecond pulses in particular). The current status of this area of investigation is reviewed in Refs [14, 16, 19, 22, 23].

(3) In the tunneling regime, the Keldysh parameter admits a clear physical interpretation: the quantity $t_{\mathrm{K}} = \gamma/\omega$, which is the time an electron takes to transit a potential barrier, is referred to as the Keldysh tunneling time in the literature. The possibility of experimental measurement of this time with the use of attosecond technology has come under active discussion. Despite the large number of theoretical and experimental studies recently published on this subject [94, 95, 158–165], the question of the tunneling time in the context of nonlinear ionization is still open.

(4) In recent experiments on the tunnel ionization of atoms by IR laser pulses, a discovery was made of the effect of 'tunneling without ionization' [166], in which the Coulomb atomic field captures a photoelectron into a Rydberg level, and the apparently closely related formation of peaks in the photoelectron spectrum at very low energies [167–170]. These new properties of tunnel ionization turned out to be rather unexpected to researchers [171], and attempts are now being made to describe them theoretically (see, e.g., Refs [92, 172–174] and the references therein), including attempts involving the use of the Keldysh theory and its modifications.

(5) For systems with a high polarizability (for instance, for large molecules), the photoelectron spectra are significantly affected by the dipole interaction of the photoelectron with the core polarized by the field of the laser wave, and not only by the Coulomb interaction [175]. Supposedly, the inclusion of polarization interaction can be done using the ITM, as in the case of a purely Coulomb potential.

The applications of the Keldysh theory mentioned above and many other ones are discussed in the special issue of *Journal of Physics B* [176] dedicated to the 50th anniversary of the publication of Ref. [1].

By and large, it is hard to overestimate the significance of Keldysh's work [1]. Along with the Landau–Dykhne method and the ITM, it served as the basis for numerous investigations, theoretical and experimental, in the area of high-field atomic and laser physics and has remained topical. Suffice it to say that there are more than 2500 citations of Ref. [1], most of them falling in the last 10–15 years. The ideas expressed in Ref. [1] will undoubtedly affect the development of high-field laser physics for many years to come.

10. Appendices

A. Analytic models of laser pulses

(1) The equality $\varphi(\theta) = \cos\theta$ and the function $\chi(u) = (1+u^2)^{-1/2}$ correspond to linearly polarized monochromatic light.

Calculating the elementary integral in (3.34), we obtain

$$f(\gamma) = \frac{2\gamma}{3}\,g(\gamma) = \left(1 + \frac{1}{2\gamma^2}\right)\operatorname{arsinh}\gamma - \frac{\sqrt{1+\gamma^2}}{2\gamma}\,, \tag{A.1}$$

$$b_{\parallel}(\gamma) = \frac{\operatorname{arsinh}\gamma}{\gamma} - (1+\gamma^2)^{-1/2}\,, \quad b_{\perp}(\gamma) = \frac{\operatorname{arsinh}\gamma}{\gamma}\,.$$

Here, $f(\gamma)$ is the Keldysh function [1], which defines the exponential factor in the ionization probability, and $b_{\parallel}$ and $b_{\perp}$ are the coefficients of the momentum spectrum [3, 15]. As follows from formulas (3.33) and (3.34), with the function $\chi(u)$ found from the laser pulse shape $\varphi(\theta)$, the problem reduces to quadratures. Explicit expressions for $\chi(u)$ are given in Ref. [15]. We mention the expansions

$$g(\gamma) = 1 - \frac{1}{10}\,\gamma^2 + \frac{9}{280}\,\gamma^4 + \frac{5}{336}\,\gamma^6 + \ldots, \quad \gamma \ll 1\,,$$

$$f(\gamma) = \ln 2\gamma - \frac{1}{2} + \mathcal{O}\left(\frac{\ln\gamma}{\gamma^2}\right), \quad \gamma \gg 1\,. \tag{A.2}$$

ITM formulas permit determining the effective barrier width $b(\mathcal{E}_0, \omega)$ in the laser field. For the extremal sub-barrier electron trajectory,

$$z(t) = \frac{\mathcal{E}_0}{\omega^2}\,(\cosh\tau_{\mathrm{s}} - \cosh\tau)\,, \quad \mathbf{r}_{\perp} = 0\,, \quad \tau = -\mathrm{i}\omega t\,,$$

$$0 < \tau < \tau_{\mathrm{s}} = \ln\left(\gamma + \sqrt{1+\gamma^2}\right),$$

$$\dot{z}(\tau_{\mathrm{s}}) = \mathrm{i}\kappa\,, \quad \sinh\tau_{\mathrm{s}} = \frac{\omega\kappa}{\mathcal{E}_0} = \gamma\,,$$

whence

$$b = z(0) = \frac{\kappa^2}{2\mathcal{E}_0}\,l(\gamma)\,, \quad l(\gamma) = \frac{2}{1+\sqrt{1+\gamma^2}}\,. \tag{A.3}$$

For $\gamma \gg 1$, the barrier width b becomes smaller (than that in the case of a constant electric field, where $b = \kappa^2/2\mathcal{E}_0$), which clearly explains [3, 7] the fast growth of the ionization rate in

going from the adiabatic domain to the multiquantum ionization domain $\gamma \gg 1$. In this case, $b \sim \kappa^2/\gamma\mathcal{E}_0 \sim K_0\kappa^{-1} \gg \kappa^{-1}$, i.e., the barrier width is far greater than the atomic radius, which makes the ITM applicable for $K_0 \gg 1$ [see formula (B.3) in Appendix B].

(2) A soliton-like pulse [63]: $\varphi(\theta) = 1/\cosh^2\theta$, $\chi(u) = 1/(1+u^2)$. In this case,

$$g(\gamma) = 1 - \frac{1}{5}\,\gamma^2 + \frac{3}{35}\,\gamma^4 - \ldots, \quad \gamma \ll 1\,,$$

$$f(\gamma) = (1+\gamma^{-2})\arctan\gamma - \gamma^{-1} = \frac{\pi}{2} - \frac{1}{\gamma} + \frac{\pi}{2\gamma^2} - \ldots, \quad \gamma \gg 1\,, \tag{A.4}$$

$$b_{\|}(\gamma) = \frac{\arctan\gamma}{\gamma} - (1+\gamma^2)^{-1}, \quad b_{\perp} = \frac{\arctan\gamma}{\gamma}\,,$$

$$z(\tau) = \frac{\mathcal{E}_0}{\omega^2}\ln\frac{\cos\tau}{\cos\tau_s}\,, \quad \cos\tau_s = (1+\gamma^2)^{-1/2}\,, \tag{A.5}$$

$$l(\gamma) = \frac{\ln(1+\gamma^2)}{\gamma^2}\,.$$

(3) The next example

$$\varphi(\theta) = \frac{(1-\alpha)^2\cos\theta}{1+\alpha^2-2\alpha\cos(2\theta)} = (1-\alpha)\sum_{k=0}^{\infty}\alpha^k\cos\left[(2k+1)\theta\right], \quad 0<\alpha<1\,, \tag{A.6}$$

may serve as an illustration of the effect of higher harmonics of laser radiation on the ionization probability. In this case,

$$\tau_s = \operatorname{arsinh}\left(\frac{\tanh\beta\gamma}{\beta}\right), \quad \beta = \frac{2\sqrt{\alpha}}{1-\alpha}\,,$$

$$f(\gamma,\alpha) = \int_0^{\tau_s}\left\{1 - \left[\frac{\operatorname{arsinh}(\beta\sinh\tau)}{\beta\gamma}\right]^2\right\}\mathrm{d}\tau\,. \tag{A.7}$$

Owing to the presence of the higher harmonics in the spectrum, the ionization probability in this field always exceeds the ionization probability in a monochromatic wave of the same amplitude. As $\gamma \to \infty$, the function $f(\gamma)$ approaches a constant.

(4) An even pulse,

$$\varphi_e(\theta) = (1-\theta^2)(1+\alpha^{-1}\theta^2)^{-(\alpha+3)/2} \equiv \frac{\mathrm{d}}{\mathrm{d}\theta}\left[\theta(1+\alpha^{-1}\theta^2)^{-(\alpha+1)/2}\right], \tag{A.8}$$

may exemplify an ultrashort laser field less than a half-cycle in duration (Fig. 7). In this pulse, the field is maximum at $\theta_m = \pm\sqrt{3}$:

$$\varphi_m = -2\left(\frac{\alpha}{\alpha+3}\right)^{(\alpha+3)/2} = -\frac{1}{8}\,, -\frac{1}{4}\,, -0.305,\ -0.446$$

respectively for $\alpha = 1$, 3, 5, and ∞. Only one trajectory is extremal, which corresponds to the saddle point $\theta_s = \mathrm{i}\tau_s$ in the imaginary time axis; τ_s is determined from the equation

$$\tau_s(1-\alpha^{-1}\tau_s^2)^{-(\alpha+1)/2} = \gamma\,. \tag{A.9}$$

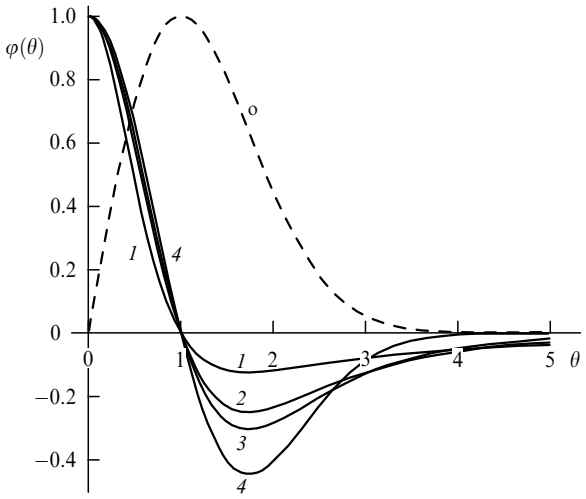

Figure 7. Pulse shapes (A.8). The curves correspond to the following α parameter values: $\alpha = 1$ (curve *1*), $\alpha = 3$ (curve *2*), $\alpha = 5$ (curve *3*), and $\alpha = \infty$ (curve *4*). The dashed curve o corresponds to odd pulse (A.18).

The functions $g(\gamma)$ are plotted in Fig. 8 for several pulses of form (A.8). We note that the proximity of curves K and o is attributable to the fact that an odd pulse is close to $\varphi = \cos\theta$ within one half-cycle. Because $g_e(\gamma) < g_o(\gamma)$, the probability of atomic ionization by an even pulse is higher than by the odd one for the same values of $\mathcal{E}_0$ and γ (see also Fig. 1 in Ref. [41]).

(5) In the limit case $\alpha \to \infty$, formula (A.8) takes the form

$$\varphi(\theta) = (1-\theta^2)\exp\left(-\frac{\theta^2}{2}\right) = \frac{\mathrm{d}}{\mathrm{d}\theta}\left[\theta\exp\left(-\frac{\theta^2}{2}\right)\right], \tag{A.10}$$

and for the saddle point, we obtain

$$\tau_s\exp\frac{\tau_s^2}{2} = \gamma\,, \tag{A.11}$$

$$\tau_s(\gamma) = \begin{cases} \gamma - \dfrac{1}{2}\,\gamma^3 + \dfrac{5}{8}\,\gamma^5 - \ldots, & \gamma \ll 1\,, \\ \sqrt{2\ln\gamma}\left[1 - \dfrac{\ln(2\ln\gamma)}{4\ln\gamma} + \ldots\right], & \gamma \gg 1\,, \end{cases}$$

and the function $f(\gamma)$ is of the form

$$f_e(\gamma) = \tau_s\left[1 - \frac{1}{3}\,{}_1F_1\left(1, \frac{5}{2}\,; -\tau_s^2\right)\right],$$

where ${}_1F_1$ is the degenerate hypergeometric function. Using the asymptotic forms

$$f_e(\gamma) = \frac{2}{3}\,\gamma g(\gamma) = \begin{cases} \dfrac{2}{3}\left(\tau_s + \dfrac{1}{5}\,\tau_s^3 - \dfrac{6}{35}\,\tau_s^5 + \ldots\right), & \gamma \ll 1\,, \\ \tau_s - \dfrac{1}{2\tau_s} + \dfrac{1}{4\tau_s^3} + \ldots, & \gamma \gg 1\,, \end{cases}$$

we obtain the expansions

$$g_e(\gamma) = 1 - \frac{3}{10}\,\gamma^2 + \frac{15}{56}\,\gamma^4 - \frac{49}{144}\,\gamma^6 + \ldots, \quad \gamma \to 0\,, \tag{A.12}$$

$$f_e(\gamma) = \sqrt{2\ln\gamma}\left(1 - \frac{\ln\ln\gamma + c_1}{4\ln\gamma} + \ldots\right), \quad \gamma \to \infty\,, \tag{A.13}$$

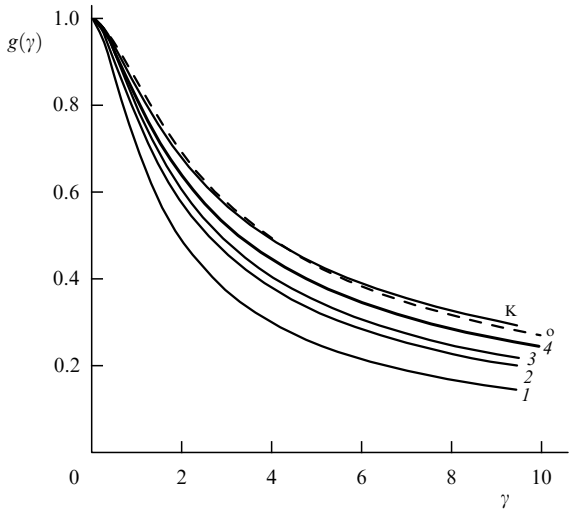

Figure 8. Function $g(\gamma)$ for the same pulses as in Fig. 7 as well as for the monochromatic field $\varphi(\theta) = \cos\theta$ (curve K) considered in Keldysh's work [1].

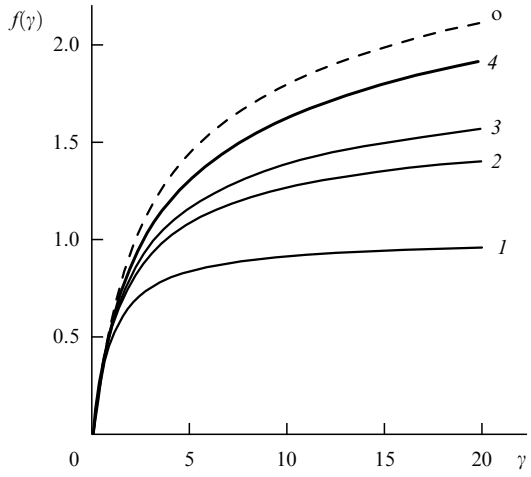

Figure 9. Function $f(\gamma)$. The notation is the same as in Figs 7 and 8.

where $c_1 = \ln 2 + 1/2$. In the more general case (A.8), we have

$$g(\gamma) = 1 - \frac{3}{10}(1+\alpha^{-1})\gamma^2 + \frac{15}{56}\left(1 + \frac{8}{5}\,\alpha^{-1} + \frac{3}{5}\,\alpha^{-2}\right)\gamma^4 + \ldots . \tag{A.14}$$

In Figs 8 and 9, we plot the functions $g(\gamma)$ and $f(\gamma)$ for various pulses of form (A.8). We note that for $\gamma \gg 1$, the ionization rate is higher for an odd pulse than for an even one (for the same values of $\mathcal{E}_0$ and γ).

(6) An analogue of pulse shape (A.8) is the odd pulse

$$\varphi(\theta) = \theta\left(\frac{1+\alpha}{\theta^2+\alpha}\right)^{(\alpha+1)/2} . \tag{A.15}$$

The electric field reaches extrema $\pm\mathcal{E}_0$ at $\theta_\mathrm{m} = \pm 1$:

$$\varphi(\theta) = \pm\left[1 - \frac{\alpha}{1+\alpha}(\Delta\theta)^2 + \mathcal{O}\big((\Delta\theta)^3\big)\right], \quad \Delta\theta = \theta - \theta_\mathrm{m} \to 0 . \tag{A.16}$$

Comparing with (3.38), we find

$$w(\gamma) \sim \exp\left[-\frac{2}{3F}\left(1 - \frac{\alpha}{5(1+\alpha)}\,\gamma^2 + \ldots\right)\right], \quad \gamma \ll 1 . \tag{A.17}$$

The next terms of this expansion cannot be calculated with the help of expression (3.39) because a cubic term is present in expressions (A.15), (A.16) which is absent from expression (3.38). In the limit $\alpha \to \infty$, formula (A.15) becomes

$$\varphi(\theta) = \theta\exp\frac{1-\theta^2}{2} = 1 - (\Delta\theta)^2 + \frac{1}{3}(\Delta\theta)^3 + \ldots, \quad \Delta\theta \to 0 . \tag{A.18}$$

(7) For the Gaussian $\varphi(\theta) = \exp(-\theta^2/2)$, we restrict ourselves to the expansion in the low-frequency domain:

$$g(\gamma) = 1 - \frac{1}{10}\,\gamma^2 + \frac{1}{40}\,\gamma^4 - 0.0084\gamma^6 + \ldots . \tag{A.19}$$

(8) The function $\chi(u)$ is sometimes calculated analytically [15]. In any case, it is easily calculated numerically, following which formulas (3.33)–(3.35) define the frequency dependence of atomic ionization and pair production in a compact form, without requiring preliminary calculation of the Green's function of the temporal Schrödinger equation.

(9) We note that the fields considered in items 1 and 4–6 satisfy the relation

$$J = \int_{-\infty}^{+\infty} \varphi(\omega t)\,\mathrm{d}t = 0 , \tag{A.20}$$

which is known in laser physics [43] and which signifies that the pulse does not do work on a particle over the total time of its action: $\mathbf{p}(-\infty) = \mathbf{p}(\infty)$. The other examples correspond to single-polarity pulses, for which $J \neq 0$. Thereon, we conclude discussing the ITM (also see reviews [15, 55] and books [177, Ch. V]).

B. Sub-barrier motion in an alternating field

In the model of an alternating and linearly polarized uniform field $\mathcal{E}(t)$, the extremal sub-barrier electron trajectory is one-dimensional and is expressed in quadratures. As an example, we consider the case of ionization of a nonrelativistic atomic level. Integrating the equation of motion $\mathrm{d}^2x/\mathrm{d}t^2 = \mathcal{E}_0\varphi(\omega t)$ with the ITM boundary conditions

$$E_0 = -I = -\frac{\kappa^2}{2} , \quad p(t_\mathrm{s}) = \mathrm{i}\kappa , \quad p(t=0) = 0 , \quad \mathrm{Im}\,x(0) = 0 , \tag{B.1}$$

in field (3.29) and passing to the dimensionless imaginary time $\tau = -\mathrm{i}\omega t$, we find this trajectory

$$x(\tau) = x(\tau_\mathrm{s}) + \frac{\mathcal{E}_0}{\omega^2}\int_\tau^{\tau_\mathrm{s}} h(\tau')\,\mathrm{d}\tau' , \quad \tau_\mathrm{s} = h^{-1}(\gamma) , \quad h(\tau) = \int_0^\tau \varphi(\mathrm{i}t)\,\mathrm{d}t , \tag{B.2}$$

and the barrier width

$$b = x(0) - x(\tau_\mathrm{s}) = \frac{\kappa^2}{2\mathcal{E}_0}\,l(\gamma) , \quad l(\gamma) = 2\gamma^{-2}\int_0^{\tau_\mathrm{s}} h(\tau)\,\mathrm{d}\tau , \quad l(0) = 1 . \tag{B.3}$$

Table 3. Asymptotic behavior of the functions $\chi(u)$, $f(\gamma)$, and $l(\gamma)$ as $\gamma \to \infty$ *.

Number	$\varphi(\theta)$	$\chi(u)$	$f(\gamma)$	$l(\gamma)$
1	$\cos\theta$	$(1+u^2)^{-1/2}$	$\ln(2\gamma) - 1/2$	$2/\gamma$
2	$(1-\theta^2)\exp(-\theta^2/2)$	$\chi = \begin{cases} 1 - \frac{3}{2}u^2, & u \to 0 \\ \left(u\sqrt{2\ln u}\right)^{-1}, & u \gg 1 \end{cases}$	$\sqrt{2\ln\gamma}$	$\left(\gamma\sqrt{\ln\gamma}\right)^{-1}$
3	$\exp(-\theta^2)$	—	$\sqrt{\ln\gamma}$	$\sim \left(\gamma\sqrt{\ln\gamma}\right)^{-1}$
4	$1/\cosh^2\theta$	$(1+u^2)^{-1}$	$\pi/2 - 2\gamma^{-1}$	$2\ln\gamma/\gamma^2$
5	$1/\cosh\theta$	$1/\cosh u$	$\pi/2$	$3{,}66\gamma^{-2}$
6	$(1+\theta^2)^{-3/2}$	$(1+u^2)^{-3/2}$	$1 - \ln\gamma/\gamma^2$	$2\gamma^{-2}$
7	$(1+\theta^2)^{-1}$	$1/\cosh^2 u$	$1 - \pi^2/12\gamma^2$	$2\gamma^{-2}\ln 2$
8	$(1-\theta^2)(1+\theta^2)^{-2}$	$2/v(1+v)$	$1 + \mathcal{O}(\gamma^{-1})$	—

* Function $\varphi(\theta)$ defines the pulse shape, $v = \sqrt{1+4u^2}$.

The initial instant of sub-barrier motion lies on the imaginary time axis:

$$t_s = i\omega^{-1}\tau_s(\gamma), \quad h(\tau_s) = \gamma, \tag{B.4}$$

t_s being the singular point for the action function $S(t)$; for $t = 0$, the electron escapes the barrier and its further trajectory is real.

Calculating the imaginary part of the action along the sub-barrier trajectory, we arrive at formulas (3.32) and (3.37). We note that these formulas relate to the case of even pulses, $\varphi(-t) = \varphi(t)$, when the 'time' varies along the imaginary axis in the course of tunneling and the factor $i = \sqrt{-1}$ can be removed from the formulas; this is the simplest version of the ITM. Furthermore, for convenience we choose the normalization condition

$$\varphi(0) = 1, \quad \varphi'(0) = 0, \quad \varphi''(0) < 0, \tag{B.5}$$

which signifies that the electric field has a maximum at $t = 0$, i.e., at the instant the electron escapes the barrier (in the final result, the peak position is insignificant). In the simplest cases of a monochromatic field and a soliton-like pulse, which were considered in Appendix A, we obtain (A.3) and (A.4). For an even pulse (A.10), we find

$$x(\tau) = \frac{\mathcal{E}_0}{\omega^2}\left(\exp\frac{\tau_s^2}{2} - \exp\frac{\tau^2}{2}\right), \quad 0 < \tau < \tau_s,$$
$$l(\gamma) = \frac{2}{\gamma^2}\left(\exp\frac{\tau_s^2}{2} - 1\right) = \begin{cases} 1 - \dfrac{3\gamma^2}{4}, & \gamma \ll 1, \\ \gamma^{-1}\sqrt{\dfrac{2}{\ln\gamma}}, & \gamma \to \infty, \end{cases} \tag{B.6}$$

with $\tau_s = \tau_s(\gamma)$ to be determined from Eqn (A.11).

As $\gamma \to 0$, it follows from (B.3) that

$$l(\gamma) = 1 - \frac{1}{4}a_2\gamma^2 + \ldots, \quad a_2 > 0, \tag{B.7}$$

and for an elliptically polarized wave,

$$l(\gamma, \rho) = 1 - \left(\frac{1}{4} - \frac{\rho^2}{9}\right)\gamma^2 + \ldots, \quad -1 \leqslant \rho \leqslant 1, \tag{B.8}$$

whence it is clear that the barrier begins to shrink with increasing the Keldysh parameter. The asymptotic behavior of functions $\chi(u)$, $f(\gamma)$, and $l(\gamma)$ as $\gamma \to \infty$ is described in Table 3.

C. Function $\chi(u)$ and adiabatic expansions

The calculation of the ionization rate in the ITM framework reduces to quadratures (3.33)–(3.37). These formulas involve the function $\chi(u)$, which is defined by the laser pulse shape $\varphi(\theta)$. The relation between φ and χ is conveniently specified in a parametric form:

$$\chi(u) = \frac{1}{\varphi(i\tau)}, \quad u(\tau) = \int_0^\tau \varphi(i\theta)\,d\theta, \quad \theta = \omega t, \tag{C.1}$$

where τ is an auxiliary variable. We consider several examples.

(1) Monochromatic radiation: $\varphi = \cos\theta$,

$$u = \sinh\theta, \quad \chi(u) = \frac{1}{\cosh\tau} = (1+u^2)^{-1/2}, \tag{C.2}$$

and calculating integral (3.37) gives Keldysh function (A.1).

(2) A pulse of the form $\varphi = 1/\cosh^2\theta$ (a 'soliton'):

$$u = \tan\theta, \quad \chi(u) = \cos^2\tau = (1+u^2)^{-1}, \tag{C.3}$$

and integral (3.37) leads to $f(\gamma)$ from expression (A.4).

(3) If $\varphi = 1/\cosh\theta$, then

$$u = \frac{1}{2}\ln\frac{1+\sin\tau}{1-\sin\tau}, \quad \tanh u = \sin\tau, \quad \chi(u) = \cos\tau = \frac{1}{\cosh u}, \tag{C.4}$$

$$f(\gamma) = \gamma\int_0^1 \frac{1-u^2}{\cosh(\gamma u)}\,du = \frac{2\gamma}{3}\begin{cases} 1 - \dfrac{1}{5}\gamma^2 + \dfrac{3}{35}\gamma^4 - \ldots, & \gamma \to 0, \\ \dfrac{3\pi}{4\gamma}, & \gamma \to \infty. \end{cases} \tag{C.5}$$

(4) For $\varphi(\theta) = (1+\theta^2)^{-\alpha}$ (a Lorentzian pulse for $\alpha = 1$), conditions (C.1) take the form

$$\chi = (1-\tau^2)^\alpha, \quad u = \tau\,{}_2F_1\left(\frac{1}{2}, \alpha; \frac{3}{2}; \tau^2\right), \tag{C.6}$$

where ${}_2F_1$ is the hypergeometric function. For $\alpha = 1/2$, 1, and 3/2, the result is expressed in terms of elementary functions.

For instance, for $\alpha = 3/2$, $u = \tau(1-\tau^2)^{-1/2}$,

$$\chi(u) = (1+u^2)^{-3/2}\,, \qquad f(\gamma) = \sqrt{1+\gamma^{-2}} - \gamma^{-2}\ln\left(\gamma + \sqrt{1+\gamma^2}\right). \tag{C.7}$$

(5) Generalizing expressions for $\chi(u)$ from the first, fourth, and sixth lines in Table 3, we set

$$\chi(u) = (1+u^2)^{-\sigma}\,, \quad \sigma > 0\,, \tag{C.8}$$

with

$$g(\gamma) = {}_2F_1\left(\frac{1}{2}\,,\,\sigma;\,\frac{5}{2}\,;\,-\gamma^2\right) = 1 - \frac{\sigma}{5}\,\gamma^2 + \frac{3}{70}\,\sigma(\sigma+1)\gamma^4 - \ldots, \quad \gamma \to 0\,. \tag{C.9}$$

In particular, $g(\gamma) = (1+\gamma^2)^{-1/2}$ for $\sigma = 5/2$.

(6) Adiabatic expansion: for an arbitrary even pulse $\chi(u) = \sum_0^\infty c_n u^{2n}$,

$$f(\gamma) = \frac{2\gamma}{3}\,g(\gamma) = \sum_0^\infty \frac{c_n}{(2n+1)(2n+3)}\,\gamma^{2n+1}, \quad \gamma \to 0\,. \tag{C.10}$$

Comparing expressions (C.10) and (3.39), we obtain

$$c_0 = 1\,, \quad c_1 = -\frac{1}{2}\,a_2\,, \quad c_2 = \frac{1}{24}(10a_2^2 - a_4)\,, \ldots\,, \tag{C.11}$$

where a_k are the coefficients in expression (3.38).

D. Fock method in relativistic mechanics

The relativistically covariant equations of motion of a charged particle in an external electromagnetic field defined by the tensor

$$F^{\mu\nu} = \frac{\partial A^\nu}{\partial x_\mu} - \frac{\partial A^\mu}{\partial x_\nu}\,, \quad \mu = 0,1,2,3, \tag{D.1}$$

where $A^\mu(x)$ is the 4-potential of the field, have the form (here, we restore the dimensional constants m, e, and c)

$$m\ddot{x}^\mu = \frac{e}{c}\,F^{\mu\nu}\dot{x}_\nu\,, \tag{D.2}$$

where $x \equiv x^\mu = (ct, \mathbf{r})$ are coordinates in the 4-dimensional pseudo-Euclidean space, and the dot denotes the derivative with respect to proper time,

$$\dot{x} = \frac{\mathrm{d}x}{\mathrm{d}s}\,, \quad s(t) = s_0 + \int_{t_0}^{t}\sqrt{1 - \frac{\mathbf{v}^2}{c^2}}\,\mathrm{d}t\,. \tag{D.3}$$

According to Fock [123], it is possible to introduce the action integral

$$S = \int_{s_0}^{s} L\,\mathrm{d}s'\,, \qquad L = -\frac{1}{2}\,m\dot{x}^\mu\dot{x}_\mu - \frac{e}{c}\,A^\mu(x)\dot{x}_\mu - \frac{1}{2}\,mc^2\,, \tag{D.4}$$

whose extremality condition leads to the Lagrange equations

$$\frac{\mathrm{d}}{\mathrm{d}s}\,\frac{\partial L}{\partial \dot{x}^\mu} - \frac{\partial L}{\partial x^\mu} = 0 \tag{D.5}$$

with s being considered an independent variable not necessarily coincident with the proper time.

Because the Lagrange function in expression (D.4) does not depend on s explicitly, there is an integral of motion

$$H = \dot{x}^\mu\,\frac{\partial L}{\partial \dot{x}^\mu} - L = \frac{1}{2}\,m(c^2 - \dot{x}^\mu\dot{x}_\mu) = \mathrm{const}\,. \tag{D.6}$$

Setting the constant in expression (D.6) equal to zero, we obtain the condition

$$\dot{x}^\mu\dot{x}_\mu = c^2\,, \tag{D.7}$$

which states that the independent variable s coincides with the proper time and Lagrange equations (D.5) coincide with equations of motion (D.2).

The equations given above permit finding the trajectory of a charged particle in parametric form. When the electromagnetic field configuration has a certain symmetry, it is possible to obtain the solution in closed form.

For example, we consider the electron motion in perpendicular constant and uniform electric and magnetic fields. Assuming that the electric field is aligned with the y axis and the magnetic field with the z axis, we select the 4-potential in the form of expression (7.27) to obtain Lagrange function (D.4) in the form

$$L = -\frac{1}{2}\,mc^2 + \frac{1}{2}\,m(\dot{\mathbf{r}}^2 - c^2\dot{t}^2) - m\omega_0(c\dot{t} - \beta\dot{x})y\,, \tag{D.8}$$

where ω_0 and β are defined in expressions (7.30). Four integrals of motion correspond to the translational invariance with respect to spatial and temporal coordinates:

$$c\dot{t} + \omega_0 y = cq_\mathrm{t}\,, \quad \dot{x} + \beta\omega_0 y = cq_x\,, \qquad \dot{z} = cq_z\,, \quad \dot{y} + \omega_0(ct - \beta x) = cq_y\,. \tag{D.9}$$

The generalized momenta $p_t = mcq_t$, $p_x = -mcq_x$, and $p_z = mcq_z$ correspond to the cyclic coordinates t, x, and z, while the conservation of the quantity mcq_y follows from the Noether theorem. Integrating these equations gives trajectory (7.29).

References

1. Keldysh L V *Sov. Phys. JETP* **20** 1307 (1965); *Zh. Eksp. Teor. Fiz.* **47** 1945 (1964)
2. Nikishov A I, Ritus V I *Sov. Phys. JETP* **23** 168 (1966); *Zh. Eksp. Teor. Fiz.* **50** 255 (1966)
3. Perelomov A M, Popov V S, Terent'ev M V *Sov. Phys. JETP* **23** 924 (1966); *Zh. Eksp. Teor. Fiz.* **50** 1393 (1966)
4. Perelomov A M, Popov V S, Terent'ev M V *Sov. Phys. JETP* **24** 207 (1967); *Zh. Eksp. Teor. Fiz.* **51** 309 (1966)
5. Popov V S, Kuznetsov V P, Perelomov A M *Sov. Phys. JETP* **26** 222 (1968); *Zh. Eksp. Teor. Fiz.* **53** 331 (1967)
6. Nikishov A I, Ritus V I *Sov. Phys. JETP* **25** 145 (1967); *Zh. Eksp. Teor. Fiz.* **52** 223 (1967)
7. Perelomov A M, Popov V S *Sov. Phys. JETP* **25** 336 (1967); *Zh. Eksp. Teor. Fiz.* **52** 514 (1967)
8. Popruzhenko S V, Mur V D, Popov V S, Bauer D *Phys. Rev. Lett.* **101** 193003 (2008)
9. Popruzhenko S V, Mur V D, Popov V S, Bauer D *JETP* **108** 947 (2009); *Zh. Eksp. Teor. Fiz.* **135** 1092 (2009)
10. Karnakov B M, Mur V D, Popov V S, Popruzhenko S V *JETP Lett.* **93** 238 (2011); *Pis'ma Zh. Eksp. Teor. Fiz.* **93** 256 (2011)
11. Faisal F H M *J. Phys. B At. Mol. Phys.* **6** L89 (1973)
12. Reiss H R *Phys. Rev. A* **22** 1786 (1980)
13. Delone N B, Krainov V P *Nelineinaya Ionizatsiya Atomov Lazernym Izlucheniem* (Nonlinear Ionization of Atoms by Laser Radiation) (Moscow: Fizmatlit, 2001)
14. Becker W et al. *Adv. At. Mol. Opt. Phys.* **48** 35 (2002)
15. Popov V S *Phys. Usp.* **47** 855 (2004); *Usp. Fiz. Nauk* **174** 921 (2004)

16. Becker A, Faisal F H M *J. Phys. B At. Mol. Opt. Phys.* **38** R1 (2005)
17. Milošević D B et al. *J. Phys. B At. Mol. Opt. Phys.* **39** R203 (2006)
18. Popruzhenko S V *J. Phys. B At. Mol. Opt. Phys.* **47** 204001 (2014)
19. Agostini P, DiMauro L F *Rep. Prog. Phys.* **67** 813 (2004)
20. Mourou G A, Tajima T, Bulanov S V *Rev. Mod. Phys.* **78** 309 (2006)
21. Schelev M Ya *Phys. Usp.* **55** 607 (2012); *Usp. Fiz. Nauk* **182** 649 (2012)
22. Agostini P, DiMauro L F *Adv. At. Mol. Opt. Phys.* **61** 117 (2012)
23. Krausz F, Ivanov M *Rev. Mod. Phys.* **81** 163 (2009)
24. Andruszkow J et al. *Phys. Rev. Lett.* **85** 3825 (2000)
25. Shintake T et al. *Nature Photon.* **2** 555 (2008)
26. Emma P et al. *Nature Photon.* **4** 641 (2010)
27. Young L et al. *Nature* **466** 56 (2010)
28. Ionin A A *Phys. Usp.* **55** 721 (2012); *Usp. Fiz. Nauk* **182** 773 (2012)
29. Free-electron laser FLASH, http://flash.desy.de
30. Yanovsky V et al. *Opt. Express* **16** 2109 (2008)
31. http://www.extreme-light-infrastructure.eu
32. XCELS, http://www.xcels.iapras.ru
33. IZEST Project, http://www.izest.polytechnique.edu
34. Dunne G V *Eur. Phys. J. Special Topics* **223** 1055 (2014)
35. Sauter F *Z. Phys.* **69** 742 (1931); *Z. Phys.* **73** 547 (1932)
36. Heisenberg W, Euler H *Z. Phys.* **98** 714 (1936)
37. Schwinger J *Phys. Rev.* **82** 664 (1951)
38. Di Piazza A et al. *Rev. Mod. Phys.* **84** 1177 (2012)
39. Narozhny N B, Fedotov A M *Eur. Phys. J. Special Topics* **223** 1083 (2014)
40. Paulus G G et al. *Nature* **414** 182 (2001)
41. Karnakov B M, Mur V D, Popov V S *JETP Lett.* **88** 423 (2008); *Pis'ma Zh. Eksp. Teor. Fiz.* **88** 495 (2008)
42. Karnakov B M, Mur V D, Popov V S, Popruzhenko S V *Phys. Lett. A* **374** 386 (2009)
43. Alekseev A I *Sbornik Zadach po Klassicheskoi Elektrodinamike* (Collection of Problems on Classical Electrodynamics) (Moscow: Nauka, 1977) Problem No. 409
44. Fuji T, Nomura Y *Appl. Sci.* **3** 122 (2013)
45. Wolkow D M *Z. Phys.* **94** 250 (1935)
46. Volkov D M *Zh. Eksp. Teor. Fiz.* **7** 1286 (1937)
47. Berestetskii V B, Lifshitz E M, Pitaevskii L P *Quantum Electrodynamics* (Oxford: Pergamon Press, 1982); Translated from Russian: *Kvantovaya Elektrodinamika* (Moscow: Nauka, 1989)
48. Landau L D, Lifshitz E M *Quantum Mechanics*: *Non-Relativistic Theory* (Oxford: Pergamon Press, 1977); Translated from Russian: *Kvantovaya Mekhanika. Nerelyativistskaya Teoriya* (Moscow: Nauka, 1989)
49. Rastunkov V S, Krainov V P *J. Phys. B At. Mol. Opt. Phys.* **40** 2277 (2007)
50. Krainov V P, Sofronov V S *Phys. Rev. A* **77** 063418 (2008)
51. Dykhne A M *Sov. Phys. JETP* **14** 941 (1962); *Zh. Eksp. Teor. Fiz.* **41** 1324 (1961)
52. Dykhne A M, Yudin G L *Sov. Phys. Usp.* **21** 549 (1978); *Usp. Fiz. Nauk* **125** 377 (1978)
53. Landau L D, Lifshitz E M *Mechanics* (Oxford: Pergamon Press, 1976); Translated from Russian: *Mekhanika* (Moscow: Nauka, 1988)
54. Goldstein H *Classical Mechanics* (Cambridge, Mass.: Addison-Wesley Press, 1950); Translated into Russian: *Klassicheskaya Mekhanika* (Moscow: Gostekhizdat, 1957)
55. Popov V S *Phys. Atom. Nucl.* **68** 686 (2005); *Yad. Fiz.* **68** 717 (2005)
56. Popov V S, Mur V D, Karnakov B M *JETP Lett.* **66** 229 (1997); *Pis'ma Zh. Eksp. Teor. Fiz.* **66** 213 (1997)
57. Popov V S, Karnakov B M, Mur V D *JETP Lett.* **79** 262 (2004); *Pis'ma Zh. Eksp. Teor. Fiz.* **79** 320 (2004)
58. Popov V S, Karnakov B M, Mur V D, Pozdnyakov S G *JETP* **102** 760 (2006); *Zh. Eksp. Teor. Fiz.* **129** 871 (2006); Preprint No. 22-05 (Moscow: ITEF, 2005)
59. Popov V S *Laser Phys.* **10** 1033 (2000)
60. Popov V S *JETP Lett.* **73** 1 (2001); *Pis'ma Zh. Eksp. Teor. Fiz.* **73** 3 (2001)
61. Popov V S *JETP* **93** 278 (2001); *Zh. Eksp. Teor. Fiz.* **120** 315 (2001)
62. Migdal A B *Qualitative Methods in Quantum Theory* (Reading, Mass.: W.A. Benjamin, 1977); Translated from Russian: *Kac=hestvennye Metody v Kvantovoi Teorii* (Moscow: Nauka, 1975) Ch. 1
63. Keldysh L V, Private communication (2001)
64. Lindner F et al. *Phys. Rev. Lett.* **95** 040401 (2005)
65. Gopal R et al. *Phys. Rev. Lett.* **103** 053001 (2009)
66. Demkov Yu N, Drukarev G F *Sov. Phys. JETP* **20** 614 (1965); *Zh. Eksp. Teor. Fiz.* **47** 918 (1964)
67. Paulus G G et al. *Phys. Rev. Lett.* **91** 253004 (2003)
68. Reichle R, Helm H, Kiyan I Yu *Phys. Rev. Lett.* **87** 243001 (2001); *Phys. Rev. A* **68** 063404 (2003)
69. Kiyan I Yu, Helm H *Phys. Rev. Lett.* **90** 183001 (2003)
70. Bergues B et al. *Phys. Rev. Lett.* **95** 263002 (2005)
71. Bergues B et al. *Phys. Rev. A* **75** 063415 (2007)
72. Gazibegović-Busuladžić A, Milošević D B, Becker W *Opt. Commun.* **275** 116 (2007)
73. Gazibegović-Busuladžić A et al. *Phys. Rev. Lett.* **104** 103004 (2010)
74. Manakov N L et al. *J. Phys. B At. Mol. Opt. Phys.* **36** R49 (2003)
75. Frolov M V et al. *Phys. Rev. Lett.* **91** 053003 (2003)
76. Bauer D, Milošević D B, Becker W *Phys. Rev. A* **72** 023415 (2005)
77. Korneev Ph A et al. *New J. Phys.* **14** 055019 (2012)
78. Chin S L et al. *Phys. Rev. Lett.* **61** 153 (1988)
79. Ammosov M V, Delone N B, Krainov V P *Sov. Phys. JETP* **64** 11918 (1986); *Zh. Eksp. Teor. Fiz.* **91** 2008 (1986)
80. Delone N B, Krainov V P *Phys. Usp.* **41** 469 (1998); *Usp. Fiz. Nauk* **168** 531 (1998)
81. Popov V S *Phys. Usp.* **42** 733 (1999); *Usp. Fiz. Nauk* **169** 819 (1999)
82. Goreslavski S P, Paulus G G, Popruzhenko S V, Shvetsov-Shilovskii N I *Phys. Rev. Lett.* **93** 233002 (2004)
83. Popov V S, Mur V D, Popruzhenko S V *JETP Lett.* **85** 223 (2007); *Pis'ma Zh. Eksp. Teor. Fiz.* **85** 275 (2007)
84. Popruzhenko S V, Paulus G G, Bauer D *Phys. Rev. A* **77** 053409 (2008)
85. Popruzhenko S V, Bauer D *J. Mod. Opt.* **55** 2573 (2008)
86. Smirnova O, Spanner M, Ivanov M *Phys. Rev. A* **77** 033407 (2008)
87. Torlina L, Smirnova O *Phys. Rev. A* **86** 043408 (2012)
88. Potvliege R M *Comp. Phys. Commun.* **114** 42 (1998)
89. Bauer D, Koval P *Comp. Phys. Commun.* **174** 396 (2006)
90. Bashkansky M, Bucksbaum P H, Schumacher D W *Phys. Rev. Lett.* **60** 2458 (1988)
91. Paulus G G et al. *Phys. Rev. Lett.* **84** 3791 (2000)
92. Yan T-M, Popruzhenko S V, Vrakking M J J, Bauer D *Phys. Rev. Lett.* **105** 253002 (2010)
93. Sorokin A A et al. *Phys. Rev. Lett.* **99** 213002 (2007)
94. Torlina L et al., arXiv:1402.5620
95. Torlina L et al. *J. Phys. B At. Mol. Opt. Phys.* **47** 204021 (2014)
96. Torlina L et al. *Phys. Rev. A* **86** 043409 (2012)
97. Huismans Y et al. *Science* **331** 61 (2011)
98. Marchenko T et al. *Phys. Rev. A* **84** 053427 (2011)
99. Castañeda Cortés H M, Popruzhenko S V, Bauer D, Pálffy A *New J. Phys.* **13** 063007 (2011)
100. Fedotov A M et al. *Phys. Rev. Lett.* **105** 080402 (2010)
101. Schenk M, Küger M, Hommelhoff P *Phys. Rev. Lett.* **105** 257601 (2010)
102. Popov V S, Karnakov B M, Mur V D *Phys. Lett. A* **229** 306 (1997)
103. Popov V S, Karnakov B M, Mur V D *JETP* **86** 860 (1998); *Zh. Eksp. Teor. Fiz.* **113** 1579 (1998)
104. Popov V S, Sergeev A V *JETP Lett.* **63** 417 (1996); *Pis'ma Zh. Eksp. Teor. Fiz.* **63** 398 (1996)
105. Karnakov B M, Mur V D, Popov V S *JETP Lett.* **65** 405 (1997); *Pis'ma Zh. Eksp. Teor. Fiz.* **65** 391 (1997)
106. Popov V S, Karnakov B M, Mur V D *JETP* **88** 902 (1999); *Zh. Eksp. Teor. Fiz.* **115** 1642 (1999)
107. Davydov A S *Teoriya Tverdogo Tela* (Theory of the Solid State) (Moscow: Nauka, 1976)
108. Sakharov A D *Sov. Phys. Dokl.* **10** 1045 (1966); *Dokl. Akad. Nauk* **165** 65 (1965)
109. Sakharov A D *Sov. Phys. Usp.* **9** 294 (1966); *Usp. Fiz. Nauk* **88** 725 (1966)
110. Sakharov A D *Nauchnye Trudy* (Scientific Works) (Moscow: OTF FIAN. Tsentrkom, 1995)
111. Pavlovskii A I, in Sakharov A D *Nauchnye Trudy* (Scientific Works) (Moscow: OTF FIAN. Tsentrkom, 1995) p. 85
112. Terent'ev M V *Istoriya Efira* (The History of Ether) (Moscow: FAZIS, 1982)
113. Dirac P A M *Priroda* (3) 68 (1972)

114. Landau L D, Lifshitz E M *Electrodynamics of Continuous Media* (Oxford: Pergamon Press, 1984); Translated from Russian: *Elektrodinamika Sploshnykh Sred* (Moscow: Nauka, 1982)
115. Sarri G et al. *Phys. Rev. Lett.* **109** 205002 (2012)
116. Wagner U et al. *Phys. Rev. E* **70** 026401 (2004)
117. Popov V S, Karnakov B M *Phys. Usp.* **57** 257 (2014); *Usp. Fiz. Nauk* **184** 273 (2014)
118. Popov V S, Mur V D, Karnakov B M *JETP Lett.* **66** 229 (1997); *Pis'ma Zh. Eksp. Teor. Fiz.* **66** 213 (1997)
119. Popov V S, Mur V D, Karnakov B M *Phys. Lett. A* **250** 20 (1998)
120. Mur V D, Karnakov B M, Popov V S *JETP* **87** 433 (1998); *Zh. Eksp. Teor. Fiz.* **114** 798 (1998)
121. Karnakov B M, Mur V D, Popov V S *Phys. Atom. Nucl.* **62** 1363 (1999); *Yad. Fiz.* **62** 1444 (1999)
122. Karnakov B M, Mur V D, Popov V S *JETP* **105** 292 (2007); *Zh. Eksp. Teor. Fiz.* **132** 331 (2007)
123. Fock V A *Phys. Z. Sowjetunion* **12** 404 (1937); *Izv. Akad. Nauk SSSR* (4 – 5) 551 (1937)
124. Fock V A *Raboty po Kvantovoi Teorii Polya* (Works on the Quantum Field Theory) (Leningrad: Izd. Leningr. Univ., 1957) p. 141
125. Popov V S, Doctoral Thesis (Moscow: ITEF, 1974) p. 219
126. Klein O *Z. Phys.* **37** 895 (1926)
127. Fock V *Z. Phys.* **38** 242 (1926); *Z. Phys.* **39** 226 (1926)
128. Gordon W *Z. Phys.* **40** 117 (1926)
129. Zel'dovich Ya B *Sov. Phys. JETP* **24** 1006 (1967); *Zh. Eksp. Teor. Fiz.* **51** 1492 (1966); *Sov. Phys. Usp.* **16** 427 (1973); *Usp. Fiz. Nauk* **110** 139 (1973)
130. Ritus V I *Sov. Phys. JETP* **24** 1041 (1967); *Zh. Eksp. Teor. Fiz.* **51** 1544 (1966)
131. Manakov N L, Rapoport L P *Sov. Phys. JETP* **42** 430 (1975); *Zh. Eksp. Teor. Fiz.* **69** 842 (1975)
132. Berson I J *J. Phys. B At. Mol. Opt. Phys.* **8** 3078 (1975)
133. Manakov N L, Ovsiannikov V D, Rapoport L P *Phys. Rep.* **141** 320 (1986)
134. Okun L B *Phys. Usp.* **53** 835 (2010); *Usp. Fiz. Nauk* **180** 871 (2010)
135. Mur V D, Popov V S *Theor. Math. Phys.* **27** 429 (1976); *Teor. Mat. Fiz.* **27** 204 (1976)
136. Popov V S, Eletskii V L, Mur V D *Sov. Phys. JETP* **44** 451 (1976); *Zh. Eksp. Teor. Fiz.* **71** 856 (1976)
137. Karnakov B M, Mur V D, Popov V S *Laser Phys.* **15** 1556 (2005)
138. Dirac P A M *The Principles of Quantum Mechanics* (Oxford: Clarendon Press, 1958); Translated into Russian: *Printsipy Kvantovoi Mekhaniki* (Moscow: Nauka, 1979) p. 71
139. Wightman A S *Introduction to Some Aspects of Relativistic Dynamics of Quantized Fields* (Princeton: Princeton Univ. Press, 1964)
140. Zeldovich Ya B, Popov V S *Sov. Phys. Usp.* **14** 673 (1972); *Usp. Fiz. Nauk* **105** 403 (1971)
141. Richtmyer R D *Principles of Advanced Mathematical Physics* (New York: Springer-Verlag, 1978); Translated into Russian: *Printsipy Sovremennoi Matematicheskoi Fiziki* (Moscow: Mir, 1982) Ch. 5
142. Voronov B L, Gitman D M, Tyutin I V *Theor. Math. Phys.* **150** 34 (2007); *Teor. Mat. Fiz.* **150** 41 (2007)
143. Pomeranchuk I Ya, Smorodinsky Ya A *J. Phys. USSR* **9** 97 (1945)
144. Sommerfeld A *Puti Poznaniya v Fizike* (The Paths of Knowledge in Physics) (Moscow: Nauka, 1973) p. 191
145. Gershtein S S, Zel'dovich Ya B *Sov. Phys. JETP* **30** 358 (1970); *Zh. Eksp. Teor. Fiz.* **57** 654 (1969)
146. Zel'dovich Ya B et al. *Sov. Phys. Usp.* **14** 811 (1972); *Usp. Fiz. Nauk* **105** 780 (1971)
147. Brodsky S *Comm. At. Mol. Phys.* **4** 109 (1973)
148. Okun L B *Comm. Nucl. Part. Phys.* **6** 25 (1974)
149. Bandrauk A *Molecules in Laser Fields* (New York: Dekker, 1994)
150. Posthumus J H *Rep. Prog. Phys.* **67** 623 (2004)
151. Stapelfeldt H, Seideman T *Rev. Mod. Phys.* **75** 543 (2003)
152. Becker W et al. *Phys. Rev. A* **76** 033403 (2007)
153. Busuladžić M, Milošević D B *Phys. Rev. A* **82** 015401 (2010)
154. Borzunov S V et al. *Phys. Rev. A* **88** 033410 (2013)
155. Gertsvolf M et al. *Phys. Rev. Lett.* **101** 243001 (2008)
156. Rajeev P P et al. *Phys. Rev. Lett.* **102** 083001 (2009)
157. Ghimire S et al *J. Phys. B At. Mol. Opt. Phys.* **47** 204030 (2014)
158. Eckle P et al. *Science* **322** 1525 (2008)
159. Eckle P et al. *Nature Phys.* **4** 565 (2008)
160. Pfeiffer A N et al. *Nature Phys.* **8** 76 (2011)
161. Pfeiffer A N et al. *Phys. Rev. Lett.* **109** 083002 (2012)
162. Pfeiffer A N et al. *Chem. Phys.* **414** 84 (2013)
163. McDonald C R et al. *Phys. Rev. Lett.* **111** 090405 (2013)
164. Kheifets A S, Ivanov I A *Phys. Rev. Lett.* **105** 233002 (2010)
165. Dahlström J M, L'Huillier A, Maquet A *J. Phys. B At. Mol. Opt. Phys.* **45** 183001 (2012)
166. Nubbemeyer T et al. *Phys. Rev. Lett.* **101** 233001 (2008)
167. Blaga C I et al. *Nature Phys.* **5** 335 (2009)
168. Quan W et al. *Phys. Rev. Lett.* **103** 093001 (2009)
169. Wu C Y et al. *Phys. Rev. Lett.* **109** 043001 (2012)
170. Dura J, Camus N, Thai A *Sci. Rep.* **3** 2675 (2013)
171. Faisal F H M *Nature Phys.* **5** 319 (2009)
172. Liu C, Hatsagortsyan K Z *Phys. Rev. Lett.* **105** 113003 (2010)
173. Kästner A, Saalmann U, Rost J M *Phys. Rev. Lett.* **108** 033201 (2012)
174. Becker W et al. *J. Phys. B At. Mol. Opt. Phys.* **47** 204022 (2014)
175. Dimitrovski D et al. *Phys. Rev. Lett.* **113** 103005 (2014)
176. "Special issue on 50 years of optical tunneling" *J. Phys. B At. Mol. Opt. Phys.* **47** (20) (2014)
177. Baz' A I, Zel'dovich Ya B, Perelomov A M *Scattering, Reactions and Decay in Nonrelativistic Quantum Mechanics* (Jerusalem: Israel Program for Scientific Translations, 1969); Translated from Russian: *Rasseyanie, Reaktsii i Raspady v Nerelyativistskoi Kvantovoi Mekhanike* (Moscow: Nauka, 1971) Ch. IX